In the reply, the referee's comments are in *italics*, our response is in normal text, and quotes from the manuscript are in blue.

Anonymous Referee #1

Major Comments

1. I found the abstract to be long and confusing, it should grab the reader with the most significant results. There's lots of irrelevant detail such as "vertical wind shear and vorticity is insignificant" which does not need to be here. The last sentence (Line 52) adds nothing to the abstract and does not follow from the results of the study

Reply: revised as requested

2. Restructure the introduction (Lines 83-121). It currently bounces between the various ways of measuring TC activity, when it only needs to say that there are implicit (e.g. GPI), semi-explicit (e.g. dynamical downscaling) and explicit (e.g. feature tracking) methods for measuring storm activity (with references). Then go on to describe GPI and VI theory.

Reply: revised as requested

3. I think you need more justification in the text as to why Section 3.4 belongs in the manuscript – it seems to me to be a rather unnecessary accessory that detracts from your GPI and VI results. Also, are there any references that have identified a clear physical relationship between ENSO and storms outside the WNP and NA basins?

Reply: we deleted section 3.4 as suggested

4. Remove Section 3.5 which is confusing and does not anything to the study

Reply: we deleted section 3.5 as suggested

5. Please establish that the GPI and VI differences between G4 and RCP4.5 are significant as Table 3 and Figure 1 do not currently support this argument

Reply: We have done this, making several new tables and figures that show significant changes as tested using Wilcoxon signed rank test and Student's t-test. Fig. 1 has also been revised and the whole results re-evaluated using longer TC seasons.

6. There are many grammatical and spelling issues that need addressing. Please have the study checked for grammar.

Reply: Done

General Comments

1. *Use acronyms throughout the manuscript – please stop jumping between using acronyms and full terminology (e.g. potential intensity and PI are used interchangeably) which is confusing. Define acronyms on first usage (e.g. Greenhouse Gas GHG) and revert to using them exclusively*

Reply: In general we have but in some cases such as with the example the referee gives, Potential Intensity, this can lead to confusion. We use *PI* to define a term in equation 5, while potential intensity is defined as V_{pot} in equation 2. This is deliberately done since the equations define different quantities that may be considered as potential intensity in different formulations.

Use either Stratospheric Sulphate Geoengineering (SSG) or Stratospheric Aerosol Injection (SAI) throughout instead of generic terms such as 'geoengineering' or 'SRM' which comprise a variety of other methods that may have completely different impacts on storms.

Reply: Done.

2. *I'd suggest either using Tropical Storms (TS) or Tropical Cyclones (TC) as the terminology throughout. I see you use typhoon or hurricane at some points, which are basin-exclusive terms and I think not be used*

Reply: Done.

Occasionally you refer to the use of climate indices such as GPI or VI as the 'direct' way of measuring TC activity (e.g. L85) or you say storm tracking is 'indirect' (L489). I disagree completely! Rather, tracking storms is more direct or explicit, whereas indices are implicit or as you say empirical. Please change this throughout the manuscript.

Reply: Done.

3. *You often give p-values – note within the text which tests were used to derive these p-values (I assume 2-sided t-test but this should be specified)*

Reply: Done, we use Student's t-tests but usually the Wilcoxon signed rank test.

5. *Please check references throughout. My particular gripes are that all papers with 2 authors should be labelled as such, for instance 'Tang and Emanuel (2012)' not 'Tang et al. (2012)' (see L100). I found many such instances. Some references are misused and do not contain pertinent detail to the text (see specific comments for details), while the Thomas et al. (2015) reference (Line 120) is missing.*

Reply: Done.

6. If you do keep Section 3.5 in the manuscript, please acknowledge the Hadley Centre for providing you with the 6 hourly data. Please also acknowledge Kevin Hodges if he assisted you in running TRACK.

Reply： Section 3.5 is deleted.

Specific Comments

1. *L33 – 'a complete description of TC variability requires much more dynamical data than models can provide at present' – I don't think this is true, I think the issue is the coarse spatiotemporal resolutions, the models have sufficient dynamics. Please rephrase.*

Reply： rewritten as: an accurate description of TC variability requires much higher spatial and temporal resolution than the models used in the GeoMIP experiments provide

2. *L35 – do you need to list all the individual components of the GPI and VI in the abstract? Surely this is more for the Introduction or Methods section*

Reply： rewritten as Genesis potential index (GPI) and ventilation index (VI) are combinations of dynamic and thermodynamic variables that provide proxies for TC activity under different climate states.

3. *L41 – 'Globally, GPI under G4 is lower than under RCP4.5, though both have a slight decreasing trend'. I am concerned that people might read from this that SAI is not able to counteract GPI changes under global-warming. Rather, the slight decreasing trend in G4 simply relates to the experimental design (i.e. a constant forcing). I would remove the 'slight decreasing trend' line and add a caveat in the conclusions saying if a different SAI approach were taken (e.g. Jones et al (2018) stabilizing global warming at 1.5K) then the GPI trends may be different*

Reply: Yes, rewritten as GPI is consistently and significantly lower under G4 than RCP4.5 in 5 out of 6 ocean basins, but it increases under G4 in the South Pacific.

4. *L42 – 'spatial patterns in the effectiveness of geoengineering show reductions in TC' – I'm not sure what this means, please clarify*

Reply: Yes, rewritten as reply to #3

5. L47 – 'genesis potential' -> 'GPI'

Reply： Changed.

5. *L52 – final line – again I'm not sure what you mean by this final sentence. Do you mean that simple statistical models based on surface temperature or relative humidity changes are appropriate for examining TC changes? I don't think you*

really show this though as you don't explicitly link GPI or VI to modelled TCs in this study

Reply: Agreed, we delete the sentence.

6. *L58-L62 – numerous grammatical issues*

Reply: rewritten as: Anthropogenic greenhouse gas (GHG) emissions are changing climate (IPCC, 2007). The best solution for limiting climate change is to reverse the growth in net GHG emissions. It is doubtful that reductions in emissions can be done fast enough to limit global mean temperatures rises to targets such as the 1.5° or 2°C pledged at the Paris climate meeting (Rogelj et al., 2015).

8. L63 – replace 'retard' with suitable word such as 'counteract'

Reply: Done, replaced with counteract.

9. L67 – consider replacing 'facilitate' with 'homogenize'

Reply: Done.

10. L68 – 'and is supported by about 12 model groups' replace with 'and is currently supported by 12 model groups' – be specific on the number

Reply: Done. supported by 15 model groups

11. L69 – 'Climate system thermodynamics will certainly change under SRM' – this is a strong statement, change compared to what by the way? If you mean compared to business-as-usual then change (of a kind) may welcome! Please reword

Reply: We are not making a value-judgement merely reporting what is well-established, we added a few more references to illustrate the point. Rewritten Climate system thermodynamics will change under SRM geoengineering because the reduction in short wave radiation is designed to offset increases in long wave absorption (Huneeus et al., 2014; Kashimura, H., M. Abe, S. Watanabe, T. Sekiya, D. Ji, J. C. Moore, J.N.S. Cole and B. Kravitz 2017 Shortwave radiative forcing, rapid adjustment, and feedback to the surface by sulfate geoengineering: analysis of the Geoengineering Model Intercomparison Project G4 scenario, *Atmospheric Chemistry and Physics* 17, 3339-3356, doi:10.5194/acp-17-3339-2017, 2017; Visioni, D., Pitari, G., and Aquila, V.: Sulfate geoengineering: a review of the factors controlling the needed injection of sulfur dioxide, Atmos. Chem. Phys., 17, 3879-3889, https://doi.org/10.5194/acp-17-3879-2017, 2017; Russotto, R. D. and Ackerman, T. P.: Energy transport, polar amplification, and ITCZ shifts in the GeoMIP G1 ensemble, Atmospheric Chemistry and Physics, 18, 2287–2305, doi:10.5194/acp-18-2287-2018, 2018.).

12. L82 – 'methods that rely on the statistical links between the thermodynamics of the ocean and atmosphere with cyclone dynamics have been the topic of studies'. This is *not entirely true, Jones et al (2017) do explicitly model storms. Add predominantly between have and been*

Reply: Done.

13. L83 – as mentioned, replace typhoons with TCs

Reply: Done.

14. L83 – as mentioned in the major comments, this paragraph is very confusing, please revise.

Many methods have used to study the changes in TCs under climate warming. These can be divided into implicit methods, such as the GPI and VI which we focus on here, semi-explicit, such as downscaling (Emanuel, 2006; 2013), and explicit such as feature tracking storm systems (Hodges, 1995; Jones et al., 2017). Implicit methods rely on using historical climate and storm records to quantitative relationships between TC and key variables such as local, tropical and global sea surface temperatures, and various teleconnection patterns (Grinsted et al., 2012; Emanuel, 2008; Landsea, 2005; Gray, 1979). Potential intensity theory (Bister et al., 1998; Emanuel et al., 2004) predicts the dependence of TC wind speed on the air-sea thermodynamic imbalance and the temperature of the lower stratosphere. For example, many studies suggest that wind shear has inhibitory effect on the TC activity (Vecchi et al., 2007). Others have also identified changes in the large-scale environmental factors influencing tropical storm activity to assess TC changes in future (Tippett et al., 2011; Grinsted et al., 2013).

15. L96 – 'factors influence genesis' -> 'factors influence TC genesis' or cyclogenesis

Reply: Changed to factors influence TC cyclogenesis.

16. L96 – 'a quantitative theory is lacking' – please add a suitable reference

Reply: rewritten as a quantitative theory is lacking (Emanuel, 2013)

17. L99 – What is the definition of potential intensity, which is rather an abstract concept? Define on first use

Reply: rewritten as The GPI uses four environmental variables: potential intensity, low-level absolute vorticity, vertical wind shear, and relative humidity. Potential intensity is the maximum sustainable intensity of tropical cyclones based on the thermodynamic state of the atmosphere and sea surface, that is the difference between the saturation enthalpy of the sea surface and the moist static energy of the subcloud layer (Riehl H (1950) A model for hurricane formation. J Appl Phys 21:917–925).

18. L108 – Dynamical potential intensity is more about ocean feedbacks (i.e. storms stir up cold water, which in turn reduces the potential intensity) than general ocean impacts

Reply: rewritten as: Dynamic potential intensity is yet another index designed to describe ocean feedbacks on tropical cyclones, that is storms bring cold deeper water to the surface, which reduces the potential intensity.

19. L109 – 'These indices represent the climatological thermodynamic spatial and seasonal control -> please simplify, superfluous language

Reply: rewritten as: These indices represent the thermodynamic and hence seasonal control of TC genesis.

20. L111 – 'more or less beyond the abilities of contemporary climate models'. What about the high-resolution models though, which are able to model storm intensities capably (see Murakami et al (2016) and Roberts et al (2015))

Reply: Yes, a few models can do this, but that's what we meant by "more or less". Rewritten as: which is beyond the abilities of most contemporary climate models, in particular those we use here.

21. L112 – Wang et al (2012) only consider one basin – please replace with a suitable reference comparing different basins

Reply: We use Emanuel (2010) and Wing et al., (2015) to replace Wang et.al (2012).

22. L119 – What do you mean by severe TCs? Perhaps give windspeed constraints

Reply: Done, we Rewritten as: the frequency of intense TC (those having windspeeds larger than 55 ms-1)

23. L120 – Thomas et al (2015) reference missing from bibliography

Reply: Sorry, it should be Knutson et al (2015), and we revised it now.

24. L120 - Kang et al (2012) reference makes no predictions about future changes in TC activity, please change to a relevant reference

Reply: we delete Kang as 2 other references are already cited here.

25. L126 – The sentence describing Jones et al (2017)'s results is confusing. All you need to say is the SAI in the north reduces North Atlantic TC frequency, while SAI in the south enhances NA TC frequency. Their results were inconclusive for the G4 scenario, as investigated here

Reply: rewritten as: Jones et al. (2017) showed SAI in the northern hemisphere reduced the numbers of TC in the North Atlantic while SAI in the southern hemisphere increased numbers in the basin.

26. L131 – Please sell the merits of your study. No other study has looked at GPI and VI in the context of SAI. No other study has investigated storm changes under SAI in *basins outside the North Atlantic! No other study has attempted to attribute changes to storms under SAI to thermodynamic changes. This is good work, an important scientific development, and should be highlighted.*

Reply: Thanks for this, we rewrite the paragraph as: In contrast with earlier work that has focused only on the impacts of SAI on North Atlantic hurricanes (Moore et al., 2015; Jones et al., 2017), we examine ESM simulations of global TC evolution in 6 ocean basins using the GPI and VI indices. We then evaluate how far TC changes under SAI and GHG forcing can be attributed to thermodynamic changes, and hence be forecast in statistical terms.

27. L138 – 'We quantify the contribution of each variable to TC genesis using two statistical methods'. This is a rather weak statement, which variables do you study and which statistical methods do you utilize?

Reply: We rewrite as: We quantify the contribution of SST, relative humidity and wind shear to TC genesis based on attribution of monthly variance in GPI and VI in each basin's time series using multiple linear regression methods.

28. L139 – 'Finally we study the effect of ENSO on TC and TC track of HadGEM2-ES', what justification have you for including these studies here, they don't fit with the GPI and VI work that you have set up to assess

Reply: OK, We delete these sections.

29. L150-L156 – You present the results from Yu et al (2015) and Moore et al (2015), but these will necessarily differ to your results as you use 6 models (you include NorESM-1) and they use 7 models (CSIRO-MK3L and GISS-E2-R). Please state the temperature changes in your ensemble of models, and preferably include ranges. Consider also moving this to the results section of the manuscript

Yes, we delete this text and use revised numbers in the results section

The climate response to G4 forcing has been discussed by Yu et al. (2015). The general pattern of temperature change under GHG forcing includes accentuated Arctic warming, and least warming in the tropics. G4 largely reverses these changes, but leaves some residual warming in the polar regions and under-cools the tropics. SAI also reduces temperatures over land more than over oceans relative to GHG, and hence reduces the temperature difference between land and oceans. Between 2020 and 2069, SSTs in the 6 basins during their TC seasons are 0.4°C (with a model range of 0.2 to 0.6°C) warmer in RCP4.5 than under G4.

30. L162 – Sentence beginning 'It is, however,' should have a suitable reference

Reply: Rewritten as It is, however, more interesting for TC studies because the sulphate aerosol injected into the stratosphere causes radiative heating (Pitari et al., 2014), and other indirect effects on the upper troposphere (Visioni et al., 2018)…

31. L170 – replace 'vector' with 'wind'

Reply: Done.

32. L172 – define Cp in Equation (2)

Reply: Cp is the heat capacity of dry air at constant pressure

33. L174 – why do you use the 100 hPa level for the outflow temperature? Do you have a suitable reference?

Reply: We use Wing, A. A., K. Emanuel, and S. Solomon (2015), On the factors affecting trends and variability in tropical cyclone potential intensity, *Geophys. Res. Lett.*, *42*, 8669–8677, doi:10.1002/2015GL066145 and add some sentences in Section 3.3 on this choice. Wing et al. (2015.) use the trends in reanalysis and radiosonde products at 70 and 100 hPa in TC seasons to represent change in outflow temperature across various TC basins and assign its contribution to trends in V_{pot}. For convenience we choose the tropical tropopause (100 hPa) temperature from the ESM output to represent T_O

34. L177 – please define what the GPI is, i.e. the theoretical maximum intensity, and what increases/decreases to GPI signify (with a suitable reference)

Reply: We define exactly what GPI is by equation later in the text, and it was discussed during the introduction along with other TC proxies. We are not sure exactly what should be added here. We do rewrite the introductory sentences to the section slightly: The GPI has been widely employed to represent TC activity (e.g., Song et al., 2015), and several different formulations have been described (e.g., Emanuel, 2004; 2010). Here, we chose to use perhaps the most commonly-used method

We assess the large-scale environmental conditions for TC generation primarily using the GPI, but make use of the VI for comparison purposes.

35. L188 - please define what the VI is and what increases/decreases to VI signify (with a suitable reference)

Reply: As with point #34 we define VI later by equation later in the text, and it was discussed during the introduction along with other TC proxies. We are not sure exactly what should be added here. We add: In contrast with GPI where increases correspond to heightened TCs, increases in VI mean fewer TCs are likely.

36. L190 – 'greenhouse gas' - > RCP4.5

Reply: Done.

37. L193 – 'air temperature' on levels or near surface air temperature?

Reply: Air temperature on different vertical levels .

38. L200 – 'researchers' -> 'studies'

Reply: Done.

39. L200 – Emanuel 2010 is not a suitable reference as it makes no predictions for the future, only studying observations from 1908-1958

Reply: Actually what we discussing is observations, the reference for Emanuel is correct, but the Knutson reference should be 2010. Rewritten as Some studies (Emanuel, 2010; Knutson et al., 2010) find robust or significant declines in the frequency of events in the Southern Hemisphere, while the Northern Hemisphere is relatively constant in the observational record.

40. L200 – 'find' -> 'predict'

Reply: Actually what we discussing is observations, see #39 and changed reference to Knutson et al., 2010

41. L201 – 'in the Southern Hemisphere' … under global warming

Reply: Actually what we discussing is observations, see #39 and changed reference to Knutson et al., 2010, Southern Hemisphere, while the Northern Hemisphere is relatively constant the observational record.

42. L201 – 'but increasing frequency in the northern hemisphere' – Knutson et al (2015) find no such thing! Sure, they find an increase in the East North Pacific and North Indian basins, but they also predict a decrease in the North Atlantic and West North Pacific basins!

Reply: Actually what we discussing is observations, the Knutson reference should be 2010. Rewritten as Some studies (Emanuel, 2010; Knutson et al., 2010) find robust or significant declines in the frequency of events in the Southern Hemisphere, while the Northern Hemisphere is relatively constant in the observational record.

43. L203 – 'The observed TC annual-mean numbers for the period 1980-2008 for each basin are also listed in Table 2' – where did these numbers come from? I can only find the basin boundaries in Emanuel 2010. Are these numbers consistent with your basin boundaries? Please provide a suitable reference

Reply: These numbers are from the Figure 3 in Emanuel, (2010). And our basin boundaries are consistent with the basin boundaries in Emanuel, (2010).

44. L209 – 'annual' -> 'annual-mean'

Reply: Done.

45. L210 – you use August to October for the Northern Hemisphere, but the North Indian basin has two peaks in activity (one in May) (Li et al., 2013). How does GPI and VI change in this second peak in the Indian basin. Please comment on this.

Reply: We list the model, month and basin GPI and VI in Table S1. Between 2020 and 2069 the GPI under RCP4.5 in May in the North Indian basin is 44, while under G4 it is 55. BNU-ESM, HadGEM2-ES, MIROC–ESM and NorESM1-M both show clear secondary peaks in GPI in April, May, June, the other models do not. Significant differences ($p<0.05$ t-test and Wilcoxon signed rank test) are found for MIROC-ESM, MIROC-ESM-CHEM and NorESM1-M. The secondary may peak is much smaller than the general northern hemisphere peak and we redefine our TC season in any case – see point #46. We add: Li et al. (2013) note that the Northern India TC basin has a secondary peak in TC around May. This peak is reproduced by the BNU-ESM, HadGEM2-ES, MIROC–ESM and NorESM1-M models where it about half the size of the peak months later in the year (Table S1). This does not affect the statistical choice of TC months (Table S2), although it causes the fraction of GPI accounted for in our TC season to be the lowest for the Northern Indian basin (Table S3).

46. L210 – what percentage of total annual storms in each basin occur during your chosen timeframes? These 3 month timeframes seem very narrow to me

Reply: After reading your points and the major point #5 we reassessed our choices. We list the basin GPI and VI by model and month in Table S1.The individual monthly GPI as a fraction of the annual totals are shown in Table S2. We select northern and southern TC season on the basis of the each model's monthly fractions of GPI. We use a threshold of 10% for above uniformly distributed GPI for RCP4.5 and G4 averaged GPI and find that for the northern basins June-November are above the threshold, while for the southern basins it is January-June. Thus there are 6 months in each hemisphere and they account for 68% under RCP4.5 and 69% under G4 of the yearly total GPI (Table S3). We also notice from Table S2 that under G4 the TC season occurs about 1 month earlier than under RCP4.5 in both hemispheres, although our choice of threshold for the TC season means that we can use the same 6 months for each experiment. While peak TC season. The same analysis for VI shows similar results, although the season is less well-defined than for GPI, for instance VI in August is higher than December in northern basins as is January in the southern ones, but the general results do not require separate definitions of season from those for GPI. The Northern Hemisphere peak TC season is August through October and January through March in the Southern Hemisphere season, various authors have used longer periods in analyzing model data, e.g. Emanuel (2013) used all 12 months, while Jones et al., (2017) used June-November for the North Atlantic hurricane season. Li et al. (2013) note that the Northern Indian TC basin has a secondary peak in TC around May. This peak is reproduced by the BNU-ESM, HadGEM2-ES, MIROC–ESM and NorESM1-M models where it about half the size of the peak months later in the year (Table S1). This does not affect the statistical choice of TC months (Table S2), although it causes the fraction of GPI accounted for in our TC season to be the lowest for the Northern Indian basin (Table S3).

47. L217 – 'Furthermore, the G4 means for all models were significantly lower than their RCP4.5 values' – Table 3 seems to say the opposite, that none of the changes to GPI are significant! Please give annual-mean values, standard deviations and p-values for G4 and RCP4.5, perhaps in Table 1?

Reply: There was some confusion what trends were significant, and what was different under G4 and RCP4.5 that we have now resolved. The revised Table 3, new Table 4 and Fig. 1 taking account of the new TC seasons (#46) shows clearer differences. We also produce 3 new tables in the SI that show monthly and basin model results, we prefer this solution than adding results to our Table 1 as the referee suggests. We write: The models we use have considerable range in their absolute values of GPI, which is also a generally observed feature of climate models (Emanuel, 2013). The GPI has a rising trend under RCP4.5 and G4 (Fig. 1). Table 3 shows that there are significantly ($p<0.05$ when tested using the Wilcoxon signed rank test) lower values of GPI under G4 than RCP4.5 for Northern Hemisphere basins in all models, but only MIROC-ESM-CHEM has significantly lower GPI for the Southern Hemisphere basins. The time series indicate that tropical storms will become more frequent with time and that G4 significantly reduces the numbers.

48. L221 – 'The time series indicate that tropical storms will become more frequent with time and that G4 significantly reduces numbers' – Fig. 1 does not indicate this at all to me! There are many years, for each model, where the GPI is higher for G4 than for RCP4.5. Figure 1 will need rethinking as it does not support the central tenet of your paper. How for instance, can a difference of -0.3 % in CanESM2 be significant?

Reply: See reply to #47. Revised TC season numbers in Table 3: Table 3 shows that there are significantly ($p<0.05$ when tested using the Wilcoxon signed rank test) lower values of GPI under G4 than RCP4.5 for Northern Hemisphere basins in all models except for NorESM1-M, but only MIROC-ESM-CHEM has significantly lower GPI for the Southern Hemisphere basins.

49. L226 – Sentence starting 'During most years from 2020 to 2069…' – this is hardly a sufficient statistical test for significance, simply saying VI looks higher for G4 than RCP4.5! Please perform significance tests and identify which models show significant

VI changes and which ones don't. Table 3 suggests that no VI changes are significant!

Reply: Yes, we explicitly now state that we test significance using both Student's t-test (Table S1) and Wilcoxon signed rank test (Tables S1 and 3). We rewrite: Fig. 1 also shows the evolution of VI in the TC seasons during 2020 to 2069 among the five models. Note that following the definition of VI in Tang et al. (2014) we use the median value not its mean. All models show decreasing trends over time, indicating a tendency for more TCs, consistent with trends in GPI. Table 3 shows that G4-RCP4.5 differences in Northern Hemisphere basins are significantly positive except for NorESM1-M, Southern Hemisphere basins show less consistent results, which is also consistent with GPI which indicates that G4 reduces TC occurrence, and is more effective in the Northern Hemisphere.

Models	*Ts* (°C)	*To* (°C)	*Ts-To* (°C)	GPI (%)	V_{pot} (ms^{-1})	*H* (%)	V_{shear} (ms^{-1})	η (×10^{-8} s^{-1})	VI (%)	χ_m (×10^{-3})
BNU-ESM	**-0.50**	**0.12**	**-0.62**	**-3.8**	**-0.45**	-0.071	0.014	-0.63	**2.2**	**16**
	-0.42	0.11	**-0.53**	0.37	0.070	0.20	**-0.27**	-1.0	**-1.5**	**15**
MIROC-ESM	**-0.34**	**-0.58**	**0.24**	**-6.7**	**-0.94**	**-0.36**	0.13	1.3	**2.5**	-3.7
	-0.30	**-0.56**	**0.26**	-0.86	**-0.50**	-0.19	0.13	-2.3	**2.3**	6.8
MIROC-ESM-CHEM	**-0.25**	**-0.45**	**0.21**	**-4.8**	**6.9**	**4.8**	**1.8**	-0.054	**1.9**	**-7.9**
	-0.21	**-0.43**	**0.22**	**-11**	**6.5**	**3.6**	**2.2**	-0.027	**1.3**	3.6
NorESM1-M	**-0.23**	**-0.087**	**-0.15**	**4.8**	**-0.52**	**-0.51**	0.029	**-3.4**	**-2.0**	-4.8
	-0.21	-0.071	**-0.14**	-0.73	**-0.62**	-0.10	-0.12	-0.83	**2.5**	3.3
HadGEM2-ES	**-0.65**	**0.16**	**-0.80**	**-3.1**	**-1.0**	0.17	0.041	**1.9**	**3.8**	**35**
	-0.61	**0.15**	**-0.76**	0.39	**-0.71**	-0.088	-0.079	1.0	**1.1**	**30**
Ensemble	**-0.40**	**-0.14**	**-0.26**	**-2.7**	**0.80**	**0.80**	**0.40**	-0.2	**1.9**	**7.0**
	-0.35	**-0.13**	**-0.23**	**-2.5**	**0.95**	**0.68**	**0.37**	-0.7	**1.0**	**11.8**

Table 3. Differences (G4-RCP4.5) in TC basins and season during 2020-2069 year calculated point-by-point. Northern Hemisphere numbers are above and Southern Hemisphere below Bold fonts are significant at 95% level using the Wilcoxon signed rank test. The ensemble means are not normalized.

50. L231 – 'As with GPI, there is about a factor of 2-3 range in absolute values between the models' – perhaps plot normalised anomalies relative to 2020-2030 in Figure 1 instead?

Reply: We experimented with many different ways of plotting, and now use the methods shown, with a different method for VI than GPI because of the separation of the model results.

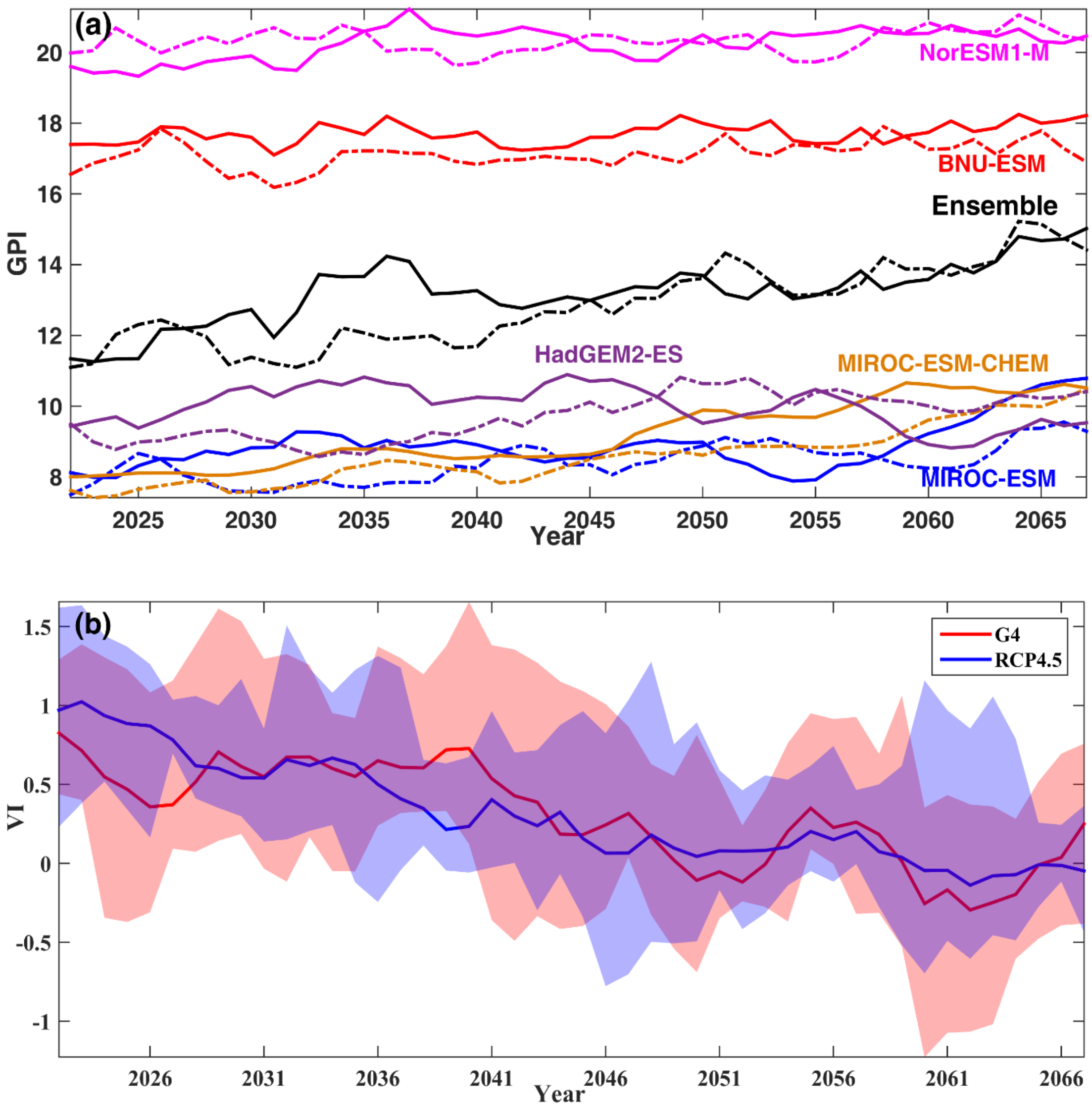

Figure 1. Five yearly moving annual averages across the 6 TC basins and TC season, of (a) GPI, solid lines denote forcing under RCP4.5 and dotted lines values under G4. Ensemble mean series were calculate using normalized time series, shifted by the ensemble mean. (b) VI with solid lines denoting model ensemble means and shading indicating the range across the five models.

Since we recalculate with new TC season all figures in the paper have been revised, and their associated text. We rewrite: Fig. 2 shows the correlations between model differences G4-RCP4.5 for annual mean GPI and VI. Most models, and the ensemble show significant anti-correlation across all TC basins, except the South Pacific where half the models have significant correlation. The ensemble mean correlation is only around -0.3, indicating that GPI and VI are addressing sufficiently different aspects of TC to warrant independent analysis.

51. L245 – 'All models except NorESM1-M show negative differences in the North Indian basin' – this may be true on a basin-wide basis, but BNU-ESM shows GPI increases in the Bay of Bengal. This might indicate a change in the spatial distribution of storms in the North Indian basin. This is also apparent in the ensemble-mean

Reply: Actually with the new TC season BNU-ESM has no clear sign of response in NI basin, so our statement is better than the referee's suggestion.

52. L269 – consider changing 'item' to 'component' or 'term' throughout this paragraph

Reply: Done.

53. L274 – has this decomposition (Eq. 5) been used before? If so, provide a relevant reference

Reply: Yes, it is from Li et al., 2013. We rewrite as : Li et al. (2013) expressed Equation (1) for GPI as the product of four terms, respectively representing an atmospheric absolute vorticity term (*AV*), a vertical wind shear term (*WS*), a relative humidity term (*RH*), and an atmospheric potential intensity term (*PI*).

54. L301 – 'Hence, these are the factors that primarily enable solar geoengineering'

Reply: Done.

55. L304 – do you have any idea as to why MIROC-ESM-CHEM is so different?

Reply: Yes. Firstly there was error in analyzing the MIROC-ESM-CHEM ensemble. Second, the 9 members divide into 2 separate groups in terms of how much variance the explanatory variables make to linearized GPI and VI. On this basis we exclude CanESM2 from the analysis completely, and add new supplementary figures to show how MIROC-ESM-CHEM members differ from each other. In section 2 we write Although to date 8 ESM have performed the RCP4.5 and G4 simulations, a subset of 6 models have access to all required model data fields, but one of those, CanESM2, was not used because all three of the realizations available it failed to pass statistical tests leaving 5 models (Table 1). The particular tests we did to exclude some data and models from the analysis are discussed in detail in section 3.2. The rejected simulations all produced statistically weak and insignificant regression fits to linearized forms of GPI and VI with all combinations of the thermodynamic and dynamic terms used to compute them. Hence, it is unlikely that VI or GPI can meaningfully represent TC activity in these cases. In comparison, the ESM simulations we do use have regression models that are significant at least at the 5% level, and in many cases, achieve far higher significance.

In section 3.2.2 Fig. S1 shows the same analysis as Fig. 5, but for all 9 realizations of MIROC-ESM-CHEM. The first four realizations behave similarly as the BNU-ESM, HadGEM2-ES and MIROC-ESM models in Fig. 5, with variance accounted for around 80% of total and the *RH* terms being about twice as important as *WS* and *PI* terms. The remaining 5 realizations have far lower variance explained, similar as for NorESM1-M, with *RH* still the dominant term…. Fig. S3 shows the VI components for all 9 realizations of MIROC-ESM-CHEM, which appears similarly divided into two groups as they were for GPI in Fig. S1…. When we analyzed the realizations 5-9 of MIROC-ESM-CHEM we found much lower F-statistics than for realizations 1-4 (Fig. S4), with values similar as for NorESM1-M of 50-100. In general, the models show *RH* has the largest F-statistic for single parameter models, consistent with Figs. 4 and 5. Fig. S4 also shows that all three realizations of CanESM2, which we do not use for TC analysis in this paper, have even lower F values, particularly r2 and r3, which are around 2.

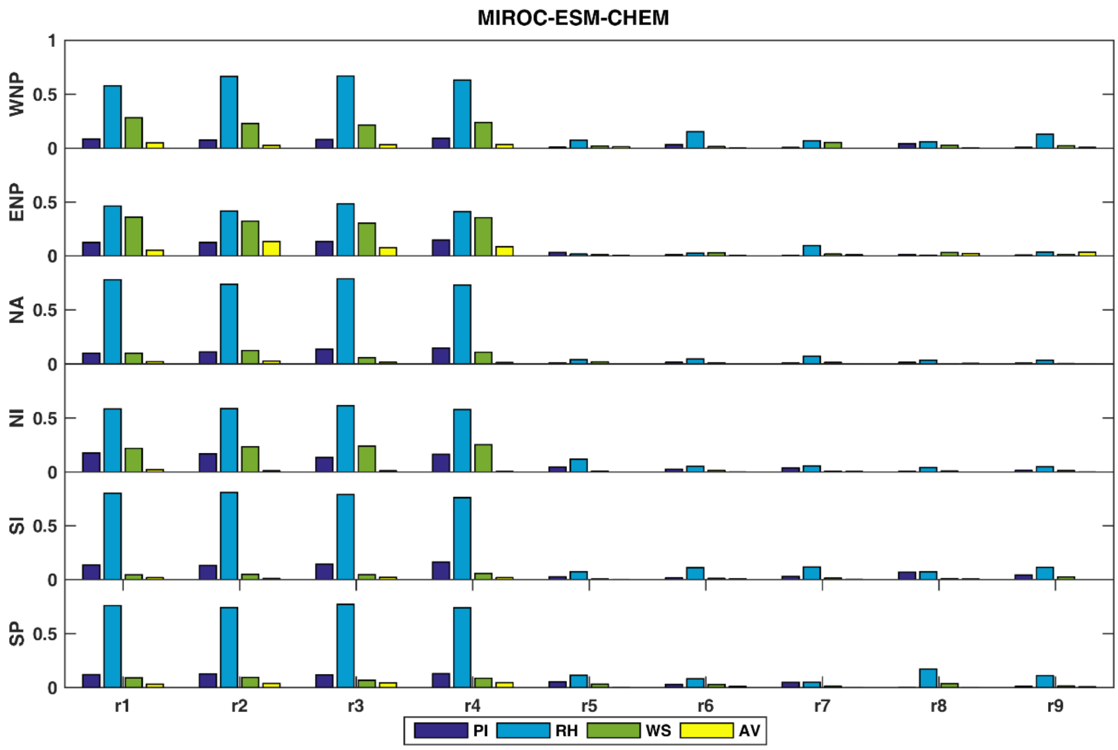

Figure S1. As Fig. 5 but for the 9 realizations of MIROC-ESM-CHEM: The fractional variance contribution of components of GPI during the TC season and within the six TC basins during 2020-2069.

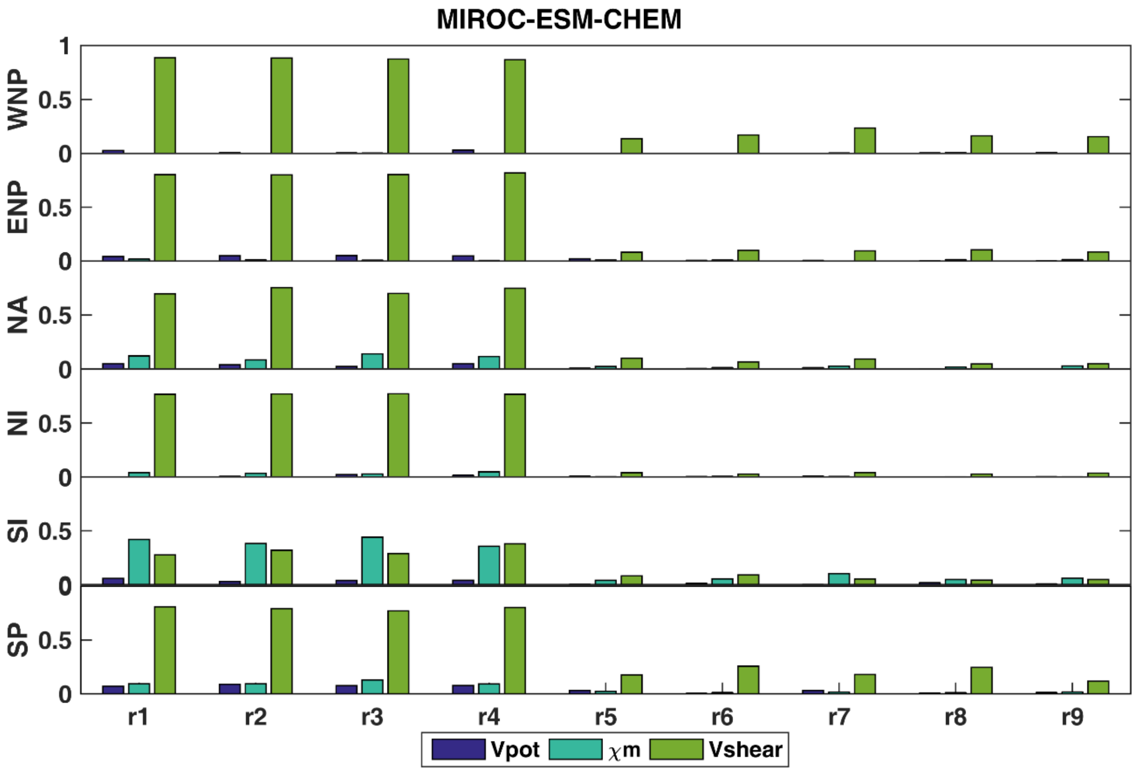

Figure S3. As S2 but for the 9 realizations of MIROC-ESM-CHEM: The fractional variance contribution of components of VI during the TC season and within the six TC basins during 2020-2069.

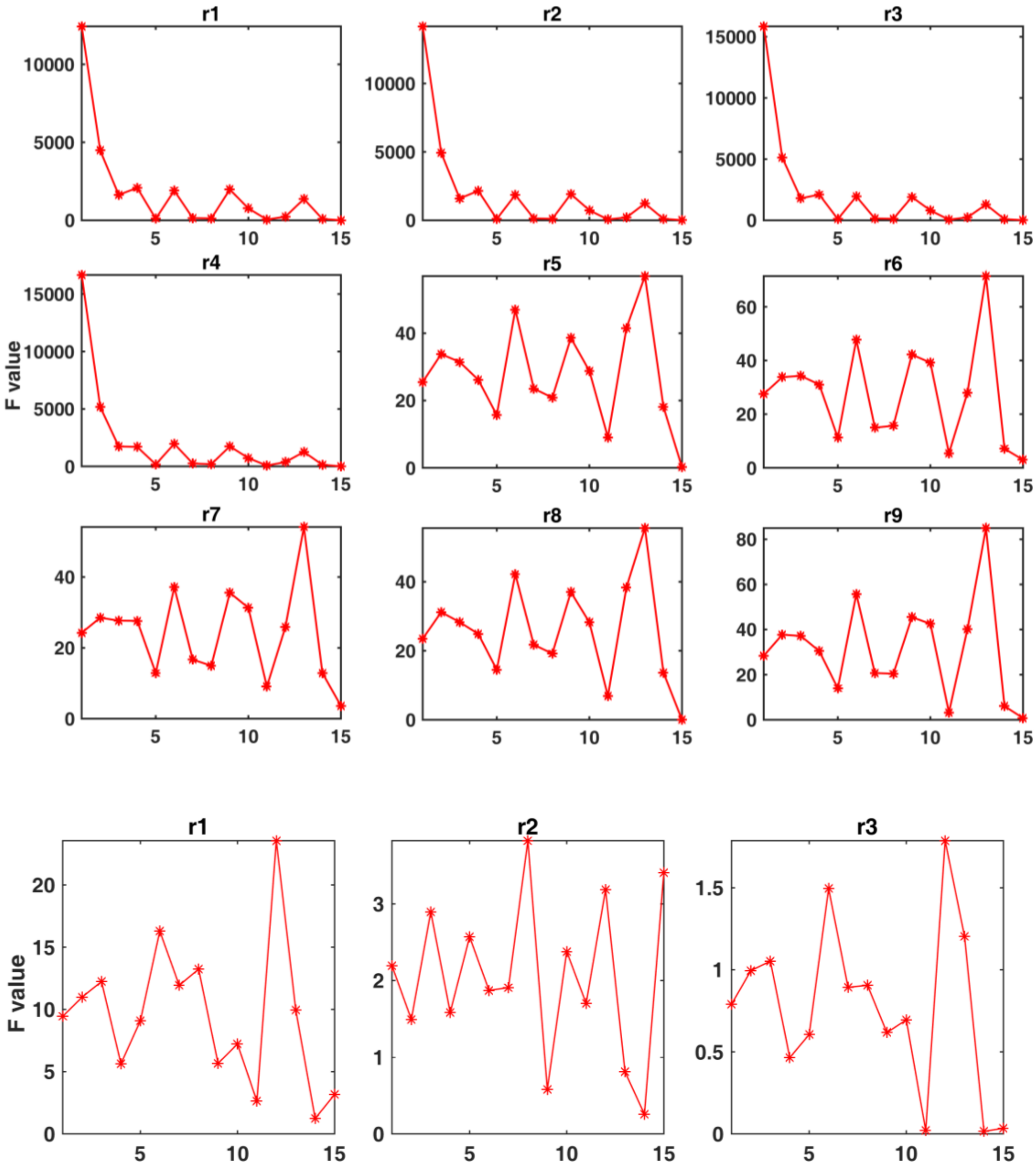

Fig. S4 As Fig6: The F-statistic of the 15 different combinations of regression variables for GPI differences between G4 and RCP4.5**,** but for each realizations 1-9 of MIROC-ESM-CHEM, (top 3 rows, and for the 3 realizations of CanESM2 (bottom row). The x-axis on each panel represents the combination of components used as predictors in each regression equation: 1:*(PI,RH,WS,AV)*, 2:*(PI,RH,WS)*, 3:*(PI,RH,AV)*, 4:*(AV,RH,WS)*, 5:*(PI,AV,WS)*, 6:*(PI,RH)*, 7:*(PI,WS)*, 8:*(PI,AV)*, 9:*(RH,WS)*, 10:*(RH,AV)*, 11:*(AV,WS)*, 12:*(PI)*, 13:*(RH)*, 14:*(WS)*, 15:*(AV)*.

56. L312 – Sentence starting 'Fig. 4 shows that the HadGEM2 values tend to be smaller' – CanESM2 is similarly muted and seems to have the same signs as HadGEM2

Reply: In fact the new Fig. 3 and 4 shows that HadGEM2 results are not strikingly muted or different form the other models. So we delete that part of the sentence.

57. L356 – 'The key factors affecting TCs' – consider adding a more informative title, possibly, 'Primary factors that control GPI and VI changes'?

Reply: Changed as suggested.

58. L357 – You seem to have found in Section 3.2 that relative humidity is the most important factor for GPI, and then ignore this finding in Section 3.3, which I found curious

Reply: Actually we discuss *RH* later but we move that paragraph up and introduce the main ideas before discussing *PI*.

The analysis above shows that the common factors across models and basins that affect TCs are potential intensity (V_{pot}), relative humidity (H), and vertical wind shear (V_{shear}). We now discuss these factors separately, beginning with V_{pot} as this is function of several different ESM variables.

59. L368 – 'The model ensemble' -> 'The ensemble-mean'

Reply: Done.

60. L370 – 'Fig S3 shows that correlations for both models under RCP4.5 and G4 separately are not atypical, simply that their G4-RCP4.5 differences are small' – I'm not sure what you mean by this sentence, please rephrase

Reply: With the new TC seasons this sentence is no longer needed and deleted. Fig. 7a shows the dependence of V_{pot} differences (G4-RCP4.5) on (T_S - T_O) differences for the models. All models have significant correlation for all TC basins except BNU-ESM in the SI and SP basins and HadGEM2-ES in the SP basin. However, there is an even stronger dependence for V_{pot} on T_S anomalies (Figs. 7b, S3). The ensemble mean V_{pot} is better correlated with T_s rather than (T_S - T_O) due to better correlations of all models in all basins except HadGEM2-ES.

61. L373 – Similarly the last sentence is unclear. Do you mean that all models excepts CanEMS2 and NorESM1 exhibit significant correlation between Ts and Vpot in all basins?

Reply: This sentence is deleted and replace with All models show significant correlation between GPI and T_S anomalies shown as Fig. 7c. Some models have insignificant correlations in particular basins, e.g., BNU-ESM is slightly anti-correlated in NA, as is HadGEM2-ES in WNP. GPI is not significantly correlated with T_s for half the ESM in the NI and SP basins. Fig. S3 shows that there are fewer significant correlations under G4 than under RCP4.5.

62. L376 – Change 'variability' to 'cycle' throughout this paragraph

Reply: Done.

63. L384 – Remove 'Comparing'

Reply: Done.

64. L388 – The last sentence – can you also plot the seasonal cycle of Ts in ERA-interim just to confirm that all the models are doing reasonably well here?

Reply: Added to renumbered Fig. S9.

65. L390 – Consider splitting this paragraph into two. It is too long and unwieldy as it is

Reply: Done.

66. L391 – Sentence beginning 'In Figs 7d and 7e we plot' – please reword this sentence to something like 'we plot correlations between H / Vshear and Ts.

Reply: We plot H differences between G4 and RCP4.5 as a function of sea surface temperature differences in Fig. 7d.

67. L399 – 'there is generally an anti-correlation between Vshear and Ts'

Reply: rewritten as: Fig 7e shows how RCP4.5-G4 differences in V_{shear} and T_s are generally anti-correlated. The across-model spread for correlations of V_{shear} and T_s under both G4 and RCP4.5 (Fig. S3) are similar as for the other key variables. Anti-correlation with T_s is weakest in the SP and NA basins, but still significant. In terms of the differences in Fig. 7e, all models show clear significant anti-correlations, with the NI and NA basins having weakest correlations.

68. L402 – Vecchi and Soden (2007) found that wind shear increases in both the North

Atlantic and the East Pacific under global warming.

Reply: Rewritten as Vecchi and Soden (2007) found the North Atlantic and East North Pacific wind shear increases in model projections under global warming. If the models assessed here capture the effect under G4 and RCP45, we would expect positive correlations between V_{shear} and T_s over these two basins for G4 and RCP4.5 in Fig. S3.

69. L404 – 'If the models assessed here'

Reply: Done.

70. L407 to L415 – I'm not sure what you are trying to prove here, it seems peripheral and needs to be reworded

Reply: We delete this section and Fig. S7, though we use the reference in the discussion where it may make our point clearer than it was: The final variable, V_{shear} , shows large scatter across the models, but consistent anti-correlation with T_s. However, there are also good but different relations between H and V_{shear} in every basin suggesting that the state of this dynamic variable can be explained to a significant degree by the thermodynamic state driving H and T_s. This is consistent with analysis (Li et al., 2010), showing that prescribed sea surface temperatures can account for some changes in TC in the Pacific basins as surface temperature gradients drive trade winds, which changes the wind shear

We deleted sections 3.4 and 3.5 so points #71 - 75 are moot

71. L441 – 'The analysis for individual basins indicates most models have significant correlations with ENSO in the WNP' – This is not true! Only 4/7 of the models have significant correlation in the WNP in RCP4.5

72. L448 – is there any previous studies that suggest a link between ENSO and tropical cyclone activity in basins outside the North Atlantic and the Pacific. If so, please cite

73. L449 – 'is most consistently felt in the Pacific Ocean'–particularly the South Pacific

74. L473 – why are the TRACK results so much lower in your Table 4 than in Jones et al. (2017)? For instance, you get 1.2 storms per year in the North Atlantic basin in G4 compared to ~11 per year in their work (their Fig. 4). Their reasoning behind the use of the (4.5,3.5,4) configuration was to attain ~10 storms per year on average in the historical period. Please check these numbers, they seem wrong.

75. L487 – Change 'typical' to 'current'

We delete sections 3.4 and 3.5 so points #71 - 75 are moot

76. L489 – 'The storms that may be counted using indirect methods such as the TRACK algorithm include the whole climate condition' – This doesn't make sense to me.

Consider replacing with 'Simulated storms that may be counted using methods such as the TRACK algorithm allow for feedbacks with the climate system'

Reply: Simulated storms that may be counted using methods such as the TRACK algorithm (Hodges, 1995; Jones et al. 2017) that allow for feedbacks with the climate system.

77. L490 – 'Statistical methods (Moore et al., 2015) also implicitly include feedbacks between storm and climate conditions' – in what way do they include feedbacks? I don't understand this. They are simply diagnostics

Reply: They do include feedbacks in their maps of teleconnections because they consider the non-local changes in e.g. the surface temperature that are both caused by, and that cause Atlantic hurricanes. Thus cooling over the USA related to extreme hurricanes is because of the cooling they produce, while heating over deserts is related to factors that lead to Atlantic hurricanes. We expand slightly the sentence: Statistical methods (Moore et al., 2015) may also implicitly include feedbacks between regional storm and background global climate conditions

78. L492 – 'but dynamical downscaling methods (Emanuel, 2013) cannot include them' – I disagree, Emanuel employs a simple ocean model which can be adjusted to provide climate feedback. In fact, I think the semi-explicit scheme offers more opportunity to incorporate feedbacks than the statistical methods

Reply: But that means it has to be manually adjusted rather than automatically occurring because of TC events. In that sense it does not include a feedback as the statistical methods do. We slightly rewrite to say but dynamical downscaling methods (Emanuel, 2013) do not include them

79. L493 – change 'apply' to 'utilize'

Reply: Done.

80. L495 – change 'relatively little data' to 'coarse temporal-resolution data'

Reply: Done.

81. L502 – Change 'diagnose tropical storms in climate models' to 'relate tropical storm activity to ambient meteorology'

Reply: Done.

82. L507 – 'Thus stratospheric sulphate aerosol injection could lead to fewer TCs in the North Atlantic …' – note that this is one solar geoengineering scenario (a uniform one). Injecting aerosol preferentially into one hemisphere may increase the amount of storms in the North Atlantic (Jones et al (2017)) with unknown effects in other basins

Reply： Rewritten as: Thus the G4 scenario of SAI based on equatorial lower stratosphere injection of SO_2 could lead to fewer TCs in the North Atlantic and Indian Ocean but more TCs in the South Pacific region than under GHG induced global warming

83. L510 – 'The impact of ENSO on TCs can be detected in the GPI' – this is poorly worded, you have not explicitly looked at ENSO and TCs, only at ENSO and GPI. Rephrase in such a way: 'ENSO is found to be correlated with GPI'. Are there any implications specifically in terms of solar geoengineering from your results? I mean, is there a decrease in El Nino years in the G4 simulations?

Reply： We delete discussion of ENSO and this sentence.

84. L515 – remove 'such as'

Reply： Done.

85. L521 – 'a simplified representation of TCs depending on fewer variables is possible'> 'a simplified representation of the GPI depending on fewer variables may be possible'

Reply： Done.

86. L523 – sentence running from 'it is encouraging that the thermodynamic state …' I don't understand what you mean here?

Reply： Rewritten to clarify that local factors are also important: Although wind shear is important and a dynamic variable, it in encouraging that the thermodynamic state of the system is of prime importance for the GPI. This suggests that statistical methods of predicting changes in TC behavior are plausible, although individual basin behavior depends on particular local forcing factors in addition the accessible thermodynamic variables used in the GPI and VI.

87. L529 – '(the 100hPa level)' -> (evaluated at 100 hPa)'

Reply： Done.

88. L529 – Replace 'note that' with 'find that changes to' and add 'changes' after GPI

Reply： Done.

89. L542 – rather than using temperature changes from Pitari et al (2014), can you give the ensemble mean upper-tropospheric temperature changes from your 6-member ensemble please

Reply： We do give this in Table 3, as we say in the text, assuming that 100 hPa temperatures represent the upper tropospehere values. Pitari et al., (2014) note a warming of the 100 hPa layer under G4 relative to RCP4.5 for the MIROC-ESM-CHEM model in the 2040s for the tropics. Most models (Table 3) in the TC basins and seasons show a cooling of (ensemble mean of 0.14°C) with only HadGEM2-ES and BNU-ESM having warming at 100 hPa. Given the complexities of changes in the upper troposphere due to the process outlined in the previous paragraph the range in static stabilities represented by the model range in T_s-T_o differences relative to RCP4.5 is probably not surprising. Therefore, although we might expect to see an improvement in correlation of potential intensity and GPI by using 100 hPa temperatures in addition to SSTs, the ability of the models to capture all the processes varies. The result is that the models used here have a better relationship with sea surface temperatures than static stability, and suggests that the aerosol effects are not being properly simulated to allow their impacts on TC genesis to be fully estimated.

90. L542 – 'This is about half the range of the G4-RCP4.5 difference in static stability (Fig. 7)' – Figure 7 does not show that changes to static stability…

Reply: We rewrite this section : In contrast with the solar dimming G1 experiments analyzed by Davis et al., (2016), here we analyse G4 which is an aerosol injection protocol. The aerosol is prescribed in the GeoMIP G4 protocol (Kravitz et al., 2011a) as injected into the equatorial stratosphere at 16-25 km altitude, where most of the direct radiative heating takes place (Pitari et al., 2014). However, due to the large size of the geoengineering aerosol particles (effective radius of the order of 0.6 μm or more), a significant fraction of the stratospheric particles settle below the tropical tropopause (Niemeier et al., 2011; English et al., 2012; Cirisan et al, 2013), thus producing some diabatic heating a few kilometres immediately below the tropical tropopause. This is superimposed on the convectively-driven upper tropospheric cooling caused by surface cooling due to the SAI and reduced convection and weakened hydrological cycle (Bala et al., 2008). This may be expected to be the dominant process controlling the SAI-induced changes in atmospheric static stability. Furthermore, recent work (Visioni et al., 2018 ACP in discussion) explores the secondary of surface cooling on the upper troposphere with the impact on cirrus clouds, and the concomitant impact on static stability. Surface cooling and lower stratospheric warming, together, tend to stabilize the atmosphere, thus decreasing turbulence and water vapor updraft velocities. The net effect is an induced cirrus thinning, which serves to increase net global cooling due to the SAI.

91. L544 – remove 'significant'

Reply: Done.

92. L545 – why does T0 not warm with most models under G4? Do you have a reason that you can offer? It is that the aerosol particles are small?

We rewrite this part to try to answer these questions using suggestions from Ref #2. In contrast with the solar dimming G1 experiments analyzed by Davis et al., (2016), here we analyse G4 which is an aerosol injection protocol. The aerosol is prescribed in the GeoMIP G4 protocol (Kravitz et al., 2011a) as injected into the equatorial stratosphere at 16-25 km altitude, where most of the direct radiative heating takes place (Pitari et al., 2014). However, due to the large size of the geoengineering aerosol particles (effective radius of the order of 0.6 μm or more), a significant fraction of the stratospheric particles settle below the tropical tropopause (Niemeier et al., 2010; English et al., 2012; Cirisan et al, 2013), thus producing some diabatic heating a few kilometres immediately below the tropical tropopause. This is superimposed on the convectively-driven upper tropospheric cooling caused by surface cooling due to the SAI and reduced convection and weakened hydrological cycle (Bala et al., 2008). This may be expected to be the dominant process controlling the SAI-induced changes in atmospheric static stability. Furthermore, recent work (Visioni et al., 2018 ACP in discussion) explores the secondary of surface cooling on the upper troposphere with the impact on cirrus clouds, and the concomitant impact on static stability. Surface cooling and lower stratospheric warming, together, tend to stabilize the atmosphere, thus decreasing turbulence and water vapor updraft velocities. The net effect is an induced cirrus thinning, which serves to increase net global cooling due to the SAI.

Pitari et al. (2014) note a warming of the 100 hPa layer under G4 relative to RCP4.5 for the MIROC-ESM-CHEM model in the 2040s for the tropics. Most models (Table 3) in the TC basins and seasons show a cooling of (ensemble mean of 0.14°C) with only HadGEM2-ES and BNU-ESM having warming at 100 hPa. Given the complexities of changes in the upper troposphere due to the process outlined in the previous paragraph the range in static stabilities represented by the model range in T_s-T_o differences relative to RCP4.5 is probably not surprising. Therefore, although we might expect to see an improvement in correlation of potential intensity and GPI by using 100 hPa temperatures in addition to SSTs, the ability of the models to capture all the processes varies. The result is that the models used here have a better relationship with sea surface temperatures than static stability, and suggests that the aerosol effects are not being properly simulated to allow their impacts on TC genesis to be fully estimated.

93. L578 – 'Many models, owing to their low resolutions, produce much weaker and larger TC' – this statement has been repeated a few times (e.g. L487). Please do not repeat statements

Reply: Rewritten as: Considering the coarse spatio-temporal resolution of most ESM models, evaluating the GPI is likely to remain a popular be a good diagnostic of TC variations under different climates.

94. L582 – change 'would be' to 'this is'

Reply: Done.

In the reply, the referee's comments are in *italics*, our response is in normal text, and quotes from the manuscript are in blue.

Anonymous Referee #2

In this numerical work, a statistical approach is described for analysing the effects of sulphate geoengineering on the genesis of tropical storms. The procedure is well designed on the general methodology of the GeoMIP project, with use of data that independent global models have provided in a common database with their G4 simulations. The manuscript is scientifically robust and deserves publication on ACP.

Some of the conclusions are important, mainly the fact that the thermodynamic role of SST changes induced by geoengineering aerosols dominates over the lower stratospheric aerosol heating. However, sometimes the authors compare the SST effects with changes in static stability, as if they were two independent things (see for example in the conclusions, lines 547-549). Actually, SST changes may affect the atmospheric static stability by themselves, even in the absence of a stratospheric warming. I would suggest rephrasing. The authors themselves clearly explain how static stability changes are controlled by both surface and upper tropospheric temperatures (page 18, lines 358-360). This is the main specific point I suggest to better clarify all along the manuscript, before final publication on ACP.

Reply: Yes, this is good point. We fully appreciate the point that static stability is not the same as SST. Apparently our original sentences were not clear enough on this and we have rewritten the entire section discussing impacts on static stability due to SAI, with the helpful suggestions from the referee.

In addition, it is true that the aerosol heating is mostly located in the 16-25 km layer (see page 27, lines 540-542); however, due to the large size of the geoengineering aerosol particles (effective radius of the order of 0.6 μm or more), a significant fraction of the stratospheric particles would settle down below the tropical tropopause (Niemeier et al., 2010; English et al., 2012; Cirisan et al, 2013), thus producing some diabatic heating superimposed to the convectively-driven upper tropospheric cooling. This means that the surface cooling (with associated upper tropospheric tropical cooling, due to lesser efficient convective motions) may be expected as the dominant process controlling the geoengineering induced changes of atmospheric static stability. At the same time, the aerosol heating in a few kilometres layer immediately below the tropical tropopause (due to gravitational sedimentation of large geoengineering sulfate aerosols) should also be considered as a contributing smaller effect.

Reply: Thank you for this insight. We modify the text to take these points into account: In contrast with the solar dimming G1 experiments analyzed by Davis et al., (2016), here we analyze G4 which is an aerosol injection protocol. The aerosol is prescribed in the GeoMIP G4 protocol (Kravitz et al., 2011a) as injected into the equatorial stratosphere at 16-25 km altitude, where most of the direct radiative heating takes place (Pitari et al., 2014). However, due to the large size of the geoengineering aerosol particles (effective radius of the order of 0.6 μm or more), a significant fraction of the stratospheric particles settle below the tropical tropopause (Niemeier et al., 2010; English et al., 2012; Cirisan et al, 2013), thus producing some diabatic heating a few kilometres immediately below the tropical tropopause. This is superimposed on the convectively-driven upper tropospheric cooling caused by surface cooling due to the SAI and reduced convection and weakened hydrological cycle (Bala et al., 2008). This may be expected to be the dominant process controlling the SAI-induced changes in atmospheric static stability

It would be worth to note that another indirect effect of sulfate geoengineering, related to the surface cooling and static stability changes, is discussed in Visioni et al. (2018). Here the sensitivity of upper tropospheric ice formation is studied with inclusion of the aerosol-induced surface cooling, with respect to a reference condition documented in Kuebbeler et al. (2016), where only the stratospheric warming due to the aerosols was taken into account. The conclusions presented in the manuscript of Wang et al. (2018) go in the same direction of what discussed in this other study.

Reply： Yes, thank you we not this now: Furthermore, recent work (Visioni et al., 2018 ACP in discussion) explores the surface cooling impact on upper tropospheric cirrus cloud formation, and the concomitant impact on static stability. Surface cooling and lower stratospheric warming, together, tend to stabilize the atmosphere, thus decreasing turbulence and updraft velocities. The net effect is an induced cirrus thinning, which indirectly increases net global cooling due to the SAI.

Minor points

P. 3, line 66: the Kravitz reference has a wrong comma between the name and et al.

Reply： Done

P. 3, line 72: some more recent articles can be cited here, for example Visioni et al. (2017).

Reply： yes we added Visioni (2017); Kashimura, H., M. Abe, S. Watanabe, T. Sekiya, D. Ji, J. C. Moore, J.N.S. Cole and B. Kravitz 2017 Shortwave radiative forcing, rapid adjustment, and feedback to the surface by sulfate geoengineering: analysis of the Geoengineering Model Intercomparison Project G4 scenario, *Atmospheric Chemistry and Physics* 17, 3339-3356, doi:10.5194/acp-17-3339-2017, 2017; and Russotto, R. D. and Ackerman, T. P.: Energy transport, polar amplification, and ITCZ shifts in the GeoMIP G1 ensemble, Atmospheric Chemistry and Physics, 18, 2287–2305, doi:10.5194/acp-18-2287-2018, 2018)

P. 4, line 83: are used instead of have used.

Reply： Done

P. 6, line 126-130: I would suggest rephrasing this concept, maybe splitting the long sentence in two. In its present form it is hard to follow.

Reply： Rewritten: Jones et al. (2017) showed SAI in the northern hemisphere reduced the numbers of TC in the North Atlantic while SAI in the southern hemisphere increased numbers in the basin.

P. 7, line 149: explain better the altitude at which the injection is simulated, since it has been shown how different injection heights may affect differently the climate response (Tilmes et al., 2017; Kleinschmitt et al., 2018).

Reply： Rewritten . G4 is based on the GHG emissions from the RCP4.5 scenario but short wave radiative forcing is reduced by injection of SO_2 into the equatorial lower stratosphere at altitudes of 16–25 km, at a rate of 5 Tg per year from the year 2020 to 2069.

P. 8, line 162-165: for a recent study analysing the connection between the stratospheric warming due to the sulfur injection and the tropospheric response in term of vertical motions, see Visioni et al. (2018) (now under review in ACPD).

Reply： Rewritten, reference added

P. 14-15: I suggest to the authors to move some of the longer equations derivations to the supplementary material for better readability of the manuscript.

Reply：Several equations are removed and so improve readability.

P. 22, line 433: no comma between models and are.

Reply：This section has been deleted in response to Ref#1.

P. 25, line 510: I would suggest using "variability" instead of "variations".

Reply：Done

P. 27, line 539: analyze instead of analysis. Better rephrase "aerosol injection scheme" into a more appropriate description, such as "protocol".

Reply：Done.

P. 27, line 552: "in the response strength across the ocean basins" sounds probably better than "in strength of response across the ocean basins".

Reply：Done.

P.38, Fig. 1: adding a legend outside the figure, instead of having the names of the models close to the related lines, would make it easier to read.

Reply：We have revised Fig. 1 to separate the lines better which we hope solves this problem.

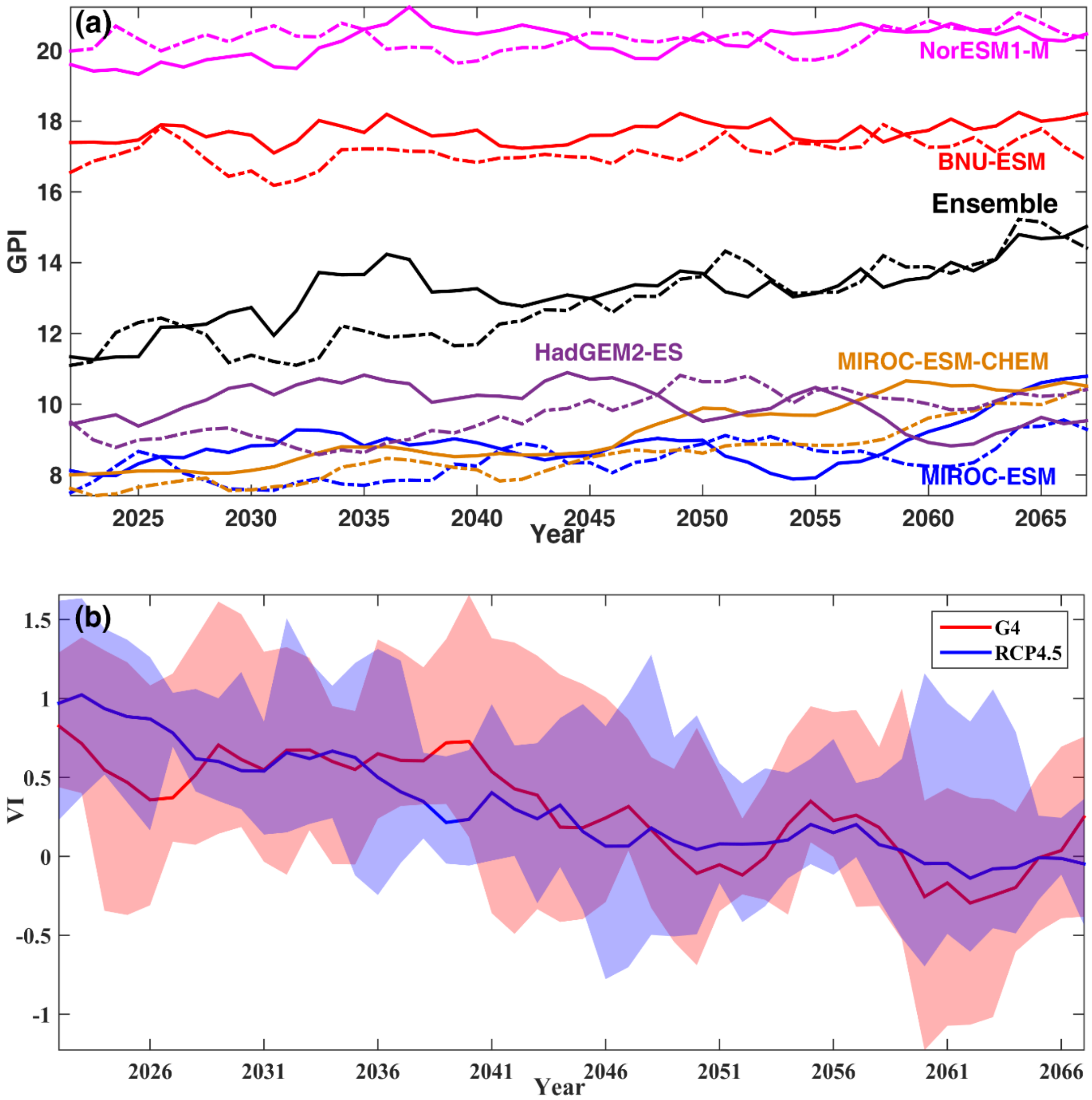

Figure 1. Five yearly moving annual averages across the 6 TC basins and TC season, of (a) GPI, solid lines denote forcing under RCP4.5 and dotted lines values under G4. Ensemble mean series were calculate using normalized time series, shifted by the ensemble mean. (b) VI with solid lines denoting model ensemble means and shading indicating the range across the five models.

A statistical examination of the effects of stratospheric sulphate geoengineering on tropical storm genesis

Qin Wang[1], John C. Moore[1,2,3*], Duoying Ji[1]

[1] College of Global Change and Earth System Science, Beijing Normal University, 19 Xinjiekou Wai St., Beijing, 100875, China

[2] Arctic Centre, University of Lapland, P.O. Box 122, 96101 Rovaniemi, Finland

[3] CAS Center for Excellence in Tibetan Plateau Earth Sciences, Beijing 100101, China

*** *Correspondence to*: John C. Moore. College of Global Change and Earth System Science Beijing Normal University 19 Xinjiekou Wai street, Beijing,China,100875 fax:+86-1058802165 Mobile +86-13521460942 E-mail: john.moore.bnu@gmail.com.**

Abstract

The thermodynamics of the ocean and atmosphere partly determine variability in tropical cyclone (TC) number and intensity and are readily accessible from climate model output, but ~~a complete~~an accurate description of TC variability requires much ~~more dynamical data~~higher spatial and temporal resolution than ~~climate~~the models ~~can~~used in the GeoMIP experiments provide~~ at present~~. Genesis potential index (GPI) and ventilation index (VI) are combinations of ~~potential intensity, vertical wind shear, relative humidity, midlevel entropy deficit, and absolute vorticity that can quantify both~~ dynamic and thermodynamic ~~and dynamic forcing of~~variables that provide proxies for TC activity under different climate states. Here we use ~~six~~five CMIP5 models that have run the RCP4.5 experiment and the Geoengineering Model Intercomparison Project (GeoMIP) stratospheric aerosol injection G4 experiment, to calculate the two TC indices over the 2020 to 2069 period across the 6 ocean basins that generate ~~tropical cyclones. Globally,~~TCs. GPI is consistently and significantly lower under G4 ~~is lower~~ than ~~under~~ RCP4.5~~, though both have a slight increasing trend. Spatial patterns in the effectiveness~~ in 5 out of ~~geoengineering show reductions in TC in the North Atlantic basin, and Northern Indian Ocean in all models except NorESM1-M. In the North Pacific, most models also show relative reductions~~6 ocean basins, but it increases under G4~~. Most~~ in the South Pacific. The models project potential intensity and relative humidity to be the dominant variables affecting ~~genesis potential.~~GPI. Changes in vertical wind shear are significant, but ~~both it and vorticity exhibit relatively small changes~~it is correlated with ~~large variation~~relative humidity though with different relations across both models and ocean basins. We find that tropopause temperature is not a useful addition to sea surface temperature in projecting TC genesis, despite radiative heating of the stratosphere due to the aerosol injection, and heating of the upper troposphere affecting static stability and potential intensity. Thus, simplified statistical methods that quantify the thermodynamic state of the major genesis basins may reasonably be used to examine stratospheric aerosol geoengineering impacts on TC activity.perhaps because the ESM vary in their simulation of the various upper tropospheric changes induced by the aerosol injection.

Key word: tropical cycloneTC, hurricanes, ENSO, statistical methods., Geoengineering.

1 Introduction

Anthropogenic greenhouse gases emissiongas (GHG) emissions are changing climate (IPCC, 2007). The best solution for limiting climate change is to reverse the growth in net greenhouse gasesGHG emissions. It is doubtful that reductions in emissionemissions can be done fast enough to limit global mean temperatures rises to targets such as the 1.5° or 2°C pledged at the Paris climate meeting (Rogelj et al., 2015). Geoengineering is the deliberate and large-scale intervention of Earth's climate system to retardcounteract climate warming (Crutzen, 2006; Wigley, 2006). Geoengineering by solar radiation management (SRMStratospheric Aerosol Injection (SAI) attempts to lessen the incoming sunlight to counteract the effect of global warming. The Geoengineering Model Intercomparison Project (GeoMIP) (Kravitz, et al., 2011) is a standardized set of experiments designed to ~~facilitate~~homogenize earth system model (ESM) simulations of geoengineered climates, and is supported by ~~about 12~~15 model groups globally, with further experiments planned under CMIP6 (Kravitz et al., 2015). Climate system thermodynamics will ~~certainly~~ change under ~~SRM~~SAI geoengineering ~~where~~because the reduction in short wave radiation is designed to offset increases in long wave absorption (Huneeus et al., 2014; Kashimura, et al., 2017; Visioni, et al., 2017; Russotto and Ackerman, 2018).

Tropical cyclones (TCs) are one of the most disastrous weather phenomena influencing agriculture, human life, and property (Chan et al., 2005). The large-scale changes in surface temperatures under ~~greenhouse gas~~GHG forcing will impact cyclogenesis changing both the frequency and intensity of ~~tropical cyclones~~TCs (Grinsted et al., 2012; 2013). Hence, how ~~tropical cyclones~~TCs would change in a geoengineered world is of general as well as scientific interest for its enormous social and economic impact. However, since almost all climate models do not, at present, possess the resolution required to simulate directly the response of ~~tropical cyclones~~TCs to changing patterns of radiative forcing, methods that rely on the statistical links between the thermodynamics of the ocean and atmosphere with cyclone dynamics have predominantly been the topic of studies.

Many methods have used to study the changes in ~~typhoons~~TCs under climate warming. ~~Some~~These can be divided into implicit methods, such as the GPI and VI which we focus on ~~the movement of tropical storm tracks, tropical cyclone intensity~~

~~and frequency by~~here, semi-explicit, such as downscaling (Emanuel, 2006~~). The most direct way is to use~~; 2013), and explicit such as feature tracking storm systems (Hodges, 1995; Jones et al., 2017). Implicit methods rely on using historical climate and storm records to ~~quantitatively study tropical cyclone activity and its relation to~~quantitative relationships between TC and key variables such as local, tropical and global sea surface temperatures, and various teleconnection patterns (Grinsted et al., 2012; Emanuel~~,~~ et al., 2008; Landsea, 2005; Gray, 1979). Potential intensity theory (Bister ~~et al.,~~and Emanuel, 1998; Emanuel ~~et al.,~~and Nolan, 2004) predicts the dependence of ~~typhoon~~TC wind speed on the air-sea thermodynamic imbalance and the temperature of the lower stratosphere. For example, many studies suggest that wind shear has inhibitory effect on the TC activity (Vecchi ~~et al.,~~and Soden, 2007). Others have also identified changes in the large-scale environmental factors influencing ~~the~~ tropical storm activity to assess ~~the~~ TC ~~activities~~changes in~~ the~~ future (Tippett et al., 2011; Grinsted et al., 2013).

While much is known about which factors influence ~~genesis~~TC cyclogenesis, a quantitative theory is lacking~~,~~ (Emanuel, 2013), so empirical methods have been used to define the relationship between large-scale environmental factors and tropical cyclogenesis. The GPI uses four environmental variables: potential intensity, low-level absolute vorticity, vertical wind shear, and relative humidity. ~~Tang et al.~~Potential intensity is the maximum sustainable intensity of TCs based on the thermodynamic state of the atmosphere and sea surface, that is the difference between the saturation enthalpy of the sea surface and the moist static energy of the subcloud layer (Riehl, 1950). Tang and Emanuel (2012) introduced the VI, defined as the flux of low-entropy air into a tropical disturbance or TC, because ventilation disrupts the formation of a deep, moist column that is hypothesized to be necessary for the spin up of the vortex (Bister et al.,and Emanuel, 1997; Nolan, 2007; Rappin et al., 2010). For the Atlantic hurricane region, Tippett et al. (2011) formulated a genesis potential index using the relative sea surface temperature, defined as the tropical Atlantic sea surface temperatures minus the tropical mean sea surface temperatures, and midlevel relative humidity in lieu of the potential intensity and non-dimensional entropy deficit, respectively. Dynamic potential intensity (DPI) is yet another index designed to describe ocean feedbacks on TCs, because storms bring cold, deeper water to the ocean's impact on tropical cyclonessurface, which reduces the potential intensity (Balaguru et al., 2015). These indices represent the climatological thermodynamic spatial and hence seasonal control of TC genesis and not the dynamic development of individual storms, which is more or less beyond the abilities of most contemporary climate models, in particular those we use here. The relative contribution of the individual large-scale environmental factors to TC genesis may be different in different ocean basins (WangEmanuel, 2010; Wing et al., 20122015).

An increase in future global TC frequency has been projected based on statistical-dynamical downscaling CMIP5 models (Emanuel, 2013). However, the same downscaling applied to the CMIP3 models projected a decrease in global TC frequency

(Tory et al., 2013; Emanuel~~ et al.~~, 2006). Some models show that although Atlantic TC frequency will decrease, the frequency of ~~severe TC~~intense TC (~~-~~those having windspeeds larger than 55 ms^{-1}) will increase, and different TC basins are predicted to behave differently (Emanuel et al., 2008; ~~Thomas~~Knutson et al., 2015~~; Kang et al., 2012~~).

There has been little research about TC changes under ~~geoengineering~~SAI. Moore et al. (2015) used statistical relation between Atlantic tropical storm surges and spatial patterns of global surface temperature to deduce that moderate amounts of ~~SRM~~SAI could reduce the frequency of the most intense ~~hurricanes~~TC relative to ~~greenhouse gas~~GHG only climates. Jones et al. (2017) ~~show that applying aerosol injection to northern and southern hemispheres separately~~ showed SAI in the northern hemisphere reduced the numbers of TC in the North Atlantic ~~if the northern hemisphere was cooled,~~ while ~~increasing them if aerosol was released only~~SAI in the southern hemisphere~~, relative to both greenhouse gas forcing both with, and without, global stratospheric aerosol injection.~~ increased numbers in the basin.

~~Here~~In contrast with earlier work that has focused only on the impacts of SAI on North Atlantic hurricanes (Moore et al., 2015; Jones et al., 2017), we examine ESM simulations of global TC evolution ~~under stratospheric sulphate injection geoengineering and greenhouse gas forcing based on the climatological~~ in 6 ocean basins using the GPI and VI indices. We ~~explore the effects of geoengineering on~~ then evaluate how far TC ~~thermodynamics~~changes under SAI and GHG forcing can be attributed to thermodynamic changes, and ~~study regional characteristics of typhoon and hurricane development after implementation of geoengineering~~hence be forecast in statistical terms.

Section 2 introduces the methods and data used in this study. Section 3 describes the temporal and spatial variations of the GPI and ventilation index in ~~six~~five models, in ~~greenhouse gas~~GHG and ~~SRM~~SAI simulations. We quantify the contribution of ~~each variable~~SST, relative humidity and wind shear to TC genesis based on attribution of monthly variance in GPI and VI in each basin's time series using ~~two statistical~~multiple linear regression methods. Finally~~ we study the effect of ENSO on TC. A~~, a discussion and conclusions are provided in section 4.

2 Methods and data

a. Methods

We use climate model output from the GeoMIP G4 experiment (Kravitz et al., 2011) and the control simulation, RCP4.5 experiment of CMIP5 (Taylor et al., 2012) to analysis the characteristic of TC changes in the future in different models. G4 is based on the ~~greenhouse gas~~GHG emissions from the RCP4.5 scenario but short wave radiative forcing is reduced by injection of SO_2 into the equatorial lower stratosphere at altitudes of 16–25 km, at a rate of 5 Tg per year from the year 2020 to 2069. The experiment continues for a further 20 years to 2089 with only ~~greenhouse gas forcing as specified by RCP4.5. The general climate response to G4 forcing has been discussed~~

~~by Yu et al. (2015). Between 2050 and 2069, global surface air temperatures warm by 1.3 °C in RCP4.5, and by 0.79 °C with G4 relative to 2010–2029. Over the same interval, tropical North Atlantic temperatures in the so-called Main Development Region (MDR) of cyclogenesis in the basin warm by 0.8 °C and 0.4 °C with RCP4.5, and G4, respectively (Moore et al., 2015).~~GHG forcing as specified by RCP4.5.

We assess the large-scale environmental conditions for TC generation primarily in reference to the widely used genesis potential and ventilation index (GPI), and use results for the VI for comparison. While other indices also exist as mentioned above, the data fields required to calculate them are presently not all available. The signal to noise ratio of the G4 experiment is not as large as that of G1 (Yu et al., 2015) where solar dimming offsets quadrupled CO_2 concentrations. It is, however, more interesting for TC studies because the sulphate aerosol injected into the stratosphere causes radiative heating (Pitari et al., 2014), and other indirect effects on the upper troposphere (Visioni et al., 2018) that will potentially affect the deep tropospheric convention systems that characterize intense tropical storms.

The GPI has been widely employed to represent TC ~~activities~~activity (e.g., Song et al., 2015~~). We use the~~), and several different formulations have been described (e.g., Emanuel ~~et al., (~~, 2004~~)~~; 2010). Here, we chose to use perhaps the most commonly-used method, (Emanuel, 2004) to calculate the GPI as follows:

$$GPI = \left|10^5 \eta\right|^{3/2} \left(\frac{H}{50}\right)^3 \left(\frac{V_{pot}}{70}\right)^3 \left(1 + 0.1V_{shear}\right)^{-2} \qquad (1)$$

Where η is the absolute vorticity in s^{-1}, H is the relative humidity at 700 hPa in percent, V_{pot} is the Potential intensity in ms^{-1}, and V_{shear} is the magnitude of the ~~vector~~wind shear from 850 to 200 hPa, in ms^{-1}. Potential intensity (Emanuel, 2000) is defined as

$$V_{pot}^2 = C_p\left(T_S - T_O\right)\frac{T_S}{T_O}\frac{C_K}{C_D}\left(\ln\theta_e^* - \ln\theta_e\right) \tag{2}$$

Where T_S is the ocean surface temperature, T_O is the mean outflow temperature, which is taken near the tropopause at the 100 hPa level and spatially averaged (Wing et al., 2015), C_p is the heat capacity of dry air at constant pressure, C_K is the exchange coefficient for enthalpy, and C_D is the drag coefficient. θ_e^* is the saturation equivalent potential temperature at the ocean surface, and θ_e is the boundary layer equivalent potential temperature.

We ~~also~~assess the large-scale environmental conditions for TC generation primarily using the GPI, but make use ~~a second and more recent method to estimate TC called the ventilation index~~of the VI for comparison purposes (Tang~~, et al.,~~ and Camargo, 2014), defined as:

$$VI = \frac{\chi_m V_{shear}}{V_{pot}} \tag{3}$$

Where χ_m is the (nondimensional) entropy deficit, defined as:

$$\chi_m = \frac{s_m^* - s_m}{s_{SST}^* - s_b} \tag{4}$$

where s_m^* is the saturation entropy at 600 hPa in the inner core of the TC, s_m is the environmental entropy at 600 hPa , s_{SST}^* is the saturation entropy at the sea surface temperature, and s_b is the entropy of the boundary layer, which we chose as the 925 hPa layer. The numerator of (4) is the difference in entropy between the TC and the environment at mid-levels, while the denominator is the air-sea disequilibrium, both are calculated following Emanuel (1994). In contrast with GPI where increases correspond to heightened TCs, increases in VI mean fewer TCs are likely.

b. –Data

Although to date 8 ESMs have performed the ~~greenhouse gas~~RCP4.5 and G4 simulations, ~~we selected~~ a subset of 6 models ~~to use here based on~~have access to all required model data fields, but one of those, CanESM2, was not used because all three of the realizations available ~~it~~ failed to pass statistical tests leaving 5 models (Table 1). The particular tests we did to exclude some data and models from the analysis are discussed in detail in section 3.2. The rejected simulations all produced statistically weak and insignificant regression fits to linearized forms of GPI and VI with all combinations of the thermodynamic and dynamic terms used to compute them. Hence, it is unlikely that VI or GPI can meaningfully represent TC activity in these cases. In comparison, the ESM simulations we do use have regression models that are significant at least at the 99.9% level, and in many cases, achieve far higher significance.

We use monthly sea surface temperature (SST), relative humidity, vertical wind shear, sea level pressure, specific humidity, air temperature~~.~~ on different vertical levels.

All the model outputs at different spatial resolutions were interpolated to a common grid (128×64) using the bilinear interpolation method. All the models were weighted equally in the ensemble mean, so the models with more than a single ensemble member were first averaged before taking the overall model ensemble mean.

c. –TC basins

Factors influencing TC change are diverse across different ocean basins. Some ~~researchers~~studies (Emanuel, 2010; Knutson et al., ~~2015~~2010) find ~~a decline~~robust or significant declines in the frequency of events in the Southern Hemisphere, ~~but increasing frequency in~~while the Northern Hemisphere is relatively constant in the observational record. We therefore examine relationships across all the six TC basins listed in Table 2. The observed TC annual mean numbers for the period 1980-2008 for each basin (Emanuel, 2010) are also listed in Table 2. The North Atlantic makes up a relatively small fraction of the total, with the Pacific dominant in the global locations of ~~tropical cyclones~~TCs.

~~3~~ 3. Results

The climate response to G4 forcing has been discussed by Yu et al. (2015). The general pattern of temperature change under GHG forcing includes accentuated Arctic warming, and least warming in the tropics. G4 largely reverses these changes, but leaves some residual warming in the polar regions and under-cools the tropics. SAI also reduces temperatures over land more than over oceans relative to GHG, and hence reduces the temperature difference between land and oceans. Between 2020 and 2069, SSTs in the 6 basins during their TC seasons are 0.4°C (with a model range of 0.2-0.6°C) warmer in RCP4.5 than under G4.

3.1 The temporal and spatial distribution of GPI and VI

We list the basin GPI and VI by model and month in Table S1. The individual monthly GPI as a fraction of the annual totals are shown in Table S2. We select northern and southern TC season on the basis of the each model's monthly fractions of GPI. We use a threshold of 10% for above uniformly distributed GPI for RCP4.5 and G4 averaged GPI and find that for the northern basins June-November are above the threshold, while for the southern basins it is January-June. Thus there are 6 months in each hemisphere and they account for 68% under both RCP4.5 and G4 of the yearly total GPI (Table S3). We also notice from Table S2 that under G4 the TC season occurs about 1 month earlier than under RCP4.5 in both hemispheres, although our choice of threshold for the TC season means that we can use the same 6 months for each experiment. ~~While peak TC season.~~ The same analysis for VI shows similar results, although the season is less well-defined than for GPI, for instance VI in August is higher than December in northern basins as is January in the southern ones, but the general results do not require separate definitions of season from those for GPI. The Northern Hemisphere peak TC season is ~~August~~June through ~~Octo~~November and January through ~~March~~June in the Southern Hemisphere, various authors have used longer periods in analyzing model data, e.g. Emanuel (2013) used all 12 months, while Jones et al., (2017) used June-November for the North Atlantic hurricane season. Li et al. ~~The~~

~~time series of annual GPI over the 6 TC basins and during the appropriate TC season (The Northern Hemisphere peak TC season is defined to be August through October, and the Southern Hemisphere season is defined to be January through March.) are shown in Fig. 1. Hereafter, all analyses are calculated and compared using these monthly periods. The mean differences in the TC indices and their component parts are tabulated in Table 3.~~

~~The GPI has a rising trend, significant at the 95% level, for all models except BNU-ESM and CanESM2 under RCP4.5, and for all models except CanESM2 and NorESM1-M under G4. Furthermore, the G4 means for all models were significantly lower than their RCP4.5 values.~~ (2013) note that the Northern Indian TC basin has a secondary peak in TC around May. This peak is reproduced by the BNU-ESM, HadGEM2-ES, MIROC–ESM and NorESM1-M models where it about half the size of the peak months later in the year (Table S1). This does not affect the statistical choice of TC months (Table S2), although it causes the fraction of GPI accounted for in our TC season to be the lowest for the Northern Indian basin (Table S3).

The models we use have considerable range in their absolute values of GPI, which is also a generally observed feature of climate models (Emanuel, 2013). ~~The MIROC-ESM-CHEM model has the largest difference between G4 and RCP4.5 (-16%) while CanESM2 shows the smallest difference (-0.3%).~~The GPI has a rising trend under RCP4.5 and G4 (Fig. 1). Table 3 shows that there are significantly ($p<0.05$ when tested using the Wilcoxon signed rank test) lower values of GPI under G4 than RCP4.5 for

Northern Hemisphere basins in all models except for NorESM1-M, but only MIROC-ESM-CHEM has significantly lower GPI for the Southern Hemisphere basins. The time series indicate that tropical storms will become more frequent with time and that G4 significantly reduces the numbers.

Fig. 1 also shows the evolution of ~~ventilation index~~VI in the TC seasons during 2020 to 2069 among the ~~six~~five models. Note that following the definition of VI in Tang ~~et al.~~and Camargo (2014) we use the median value not its mean. ~~During most years from 2020 to 2069, CanESM2, HadGEM2-ES, MIROC-ESM-CHEM and NorESM1-M show the VI under G4 lies above that under RCP45. There are no significant trends throughout the period though all~~~~All~~The models ensemble shows ~~slight~~ decreasing trends~~. Ventilation is disadvantageous~~ over time, indicating a tendency for ~~TC genesis. Thus, reducing trends suggest~~ more ~~storms in future~~TCs, consistent with trends in GPI. ~~As~~Table 3 shows that G4-RCP4.5 differences in Northern Hemisphere basins are significantly positive except for NorESM1-M, Southern Hemisphere basins show less consistent results, which is also consistent with GPI ~~there~~which indicates that G4 reduces TC occurrence, and is ~~about a factor of 2-3 range~~more effective in ~~absolute values between the models~~the Northern Hemisphere.

Fig. 2 shows ~~that~~ the correlations between model differences G4-RCP4.5 for annual mean GPI and VI. Most models~~-~~, and the ensemble show significant anti-correlation across all TC basins, ~~with the ensemble having significant anti-correlations for all TC basins~~ except the South Pacific~~. The degree of~~ where more than half the models have significant correlation varies widely across the models, with some having coefficients at great as -0.7 and others as low as 0.1.. The ensemble mean correlation is only around -0.253, indicating that GPI and VI are addressing sufficiently different aspects of TC to warrant independent analysis.

We next examine the spatial pattern of GPI and VI calculated over the 3050-year period: 20402020–2069 in the G4 and RCP4.5 experiments. The relative differences as percentages (GPI_{G4}-$GPI_{RCP4.5}$)/$GPI_{RCP4.5}$ during the peak 3-month season6-months of each hemisphere's TC season are shown in Fig. 3. These geographic patterns can be compared with the values in TableTables 3 and 4.

Fig. 3a shows that the GPI anomaly varies by region and by model. For instance, all models except NorESM1-M show negative differences in the North Indian basin. In the Western North Pacific, allAll models except CanESM2 and HadGEM2-ESMIROC-ESM-CHEM show negativethe South Pacific to be reddish in colour indicating increased GPI under G4 compared with RCP4.5 consistent with Table S1. Similarly, the North East Pacific basin has positive differences. in MIROC-ESM-CHEM and NorESM1-M. Negative differences indicate fewer tropical storms with geoengineeringSAI than under greenhouse gasGHG forcing alone. Despite model differences, the ensemble result shows robustly that the GPI difference generally negative in the northern hemisphereNorthern Hemisphere but insignificantly positive in the southern hemisphere.South Pacific and East Northern Pacific basins (Table 4). At present the vast majority of tropical storms occur in the northern hemisphereNorthern

Hemisphere (Table 2), so the overall global numbers would likely decrease.

The spatial distribution of VI also has large variation (Fig. 3b). All models except NorESM1-M have increases in the North Atlantic. In the ~~West~~ North East Pacific, all models except MIROC-ESM-CHEM and ~~BNU-ESM~~NorESM1-M have increases~~,~~ ~~suggesting~~. Increased VI (G4-RCP4.5) differences suggests fewer cyclones in agreement with the results of GPI. ~~All six models have increases in the North Atlantic.~~ In the North Indian Ocean, all models show ~~increasing ventilation index except~~increased VI difference in the Arabian Sea and all except BNU-ESM and MIROC-ESM~~-CHEM and NorESM1-M models, but~~ in the Bay of Bengal. Only MIROC-ESM shows an increase in the South ~~Indian Ocean, BNU-ESM model shows a decrease, while other models increase.~~Pacific. The ensemble results are ~~similar as~~thus largely simply opposite in sign to GPI~~ except for the North Indian basin~~.

3.2 Accounting for changes in GPI and VI

We use two different methods to examine how the contributing climate variables to GPI and VI account for differences between models and across the TC basins. The objectives are 1) learn which are the key variables in the model simulations of cyclones; 2) find a subset that can be tested against the understanding of how ~~aerosol injection~~SAI affects the atmosphere heat and water balance and 3) examine if variations in TC basin extent or cyclone seasons may be expected under ~~aerosol injection~~SAI.

3.2.1 Monthly differences in GPI and VI components between G4 and RCP4.5

To examine the effects of ~~geoengineering~~SAI on cyclone seasonality, we look at the monthly contributions of the factors that make up GPI and VI. Li et al. ~~We can express~~(2013) expressed Equation (1) for GPI as the product of four ~~items~~terms, respectively representing an atmospheric absolute vorticity ~~item~~term (*AV*), a vertical wind shear ~~item~~term (*WS*), a relative humidity ~~item~~term (*RH*), and an atmospheric potential intensity ~~item~~term (*PI*).

$$GPI = \frac{PI \times RH \times AV}{WS} \quad (5)$$

Where $\mathrm{PI} = \left(\frac{Vpot}{70}\right)^3$, $\mathrm{RH} = \left(\frac{H}{50}\right)^3$, $\mathrm{WS} = (1 + 0.1V_{shear})^2$, $\mathrm{AV} = |10^5\eta|^{\frac{3}{2}}$.

The ~~absolute vorticity~~*AV* and ~~vertical wind shear items can be~~ *WS* are considered ~~to be~~ dynamic components, while the ~~relative humidity~~*RH* and ~~potential intensity items~~*PI* are thermodynamic ones.

_We follow ~~Zhi~~Li et.al. (2013) in identifying the individual monthly contributions from the four large-scale environmental processes. ~~First taking~~Taking the natural logarithm of both sides of Eq. (5), ~~obtains~~differentiating, and substituting back into Eq (5) allows GPI to be expressed as annual means and monthly anomalies:

~~$$\log(GPI) = \log(PI) + \log(RH) - \log(WS) + \log(AV) \quad (6)$$~~

~~And differentiating yields~~

~~$$\frac{dGPI}{GPI} = \frac{dPI}{PI} + \frac{dRH}{RH} - \frac{dWS}{WS} + \frac{dAV}{AV} \quad (7)$$~~

~~Substituting Eq. (5) into Eq. (7), we have~~

$$dGPI = dPI \times \frac{RH \times AV}{WS} + dRH \times \frac{PI \times AV}{WS}$$

$$- dWS \times \frac{PI \times RH \times AV}{WS^2} + dAV \times \frac{PI \times RH}{WS} \qquad (8)$$

~~Eq. (8) can be expressed as annual means and monthly anomalies:~~

$$\delta GPI = \alpha_1 \times \delta PI + \alpha_2 \times \delta RH + \alpha_3 \times \delta WS + \alpha_4 \times \delta AV \qquad (~~9~~6)$$

Where
$$\alpha_1 = \frac{\overline{RH} \times \overline{AV}}{\overline{WS}}$$
$$\alpha_2 = \frac{\overline{PI} \times \overline{AV}}{\overline{WS}}$$
$$\alpha_3 = -\frac{\overline{PI} \times \overline{RH} \times \overline{AV}}{\overline{WS}^2}$$
$$\alpha_4 = \frac{\overline{PI} \times \overline{RH}}{\overline{WS}}$$

And $\delta GPI = GPI - \overline{GPI}$

In Eq. (~~9~~6), a bar denotes an annual mean value, and δ represents the difference between an individual month and the annual mean, assuming constant coefficients for α_1, α_2, α_3, and α_4.

We are interested in detecting changes between ~~greenhouse gas~~GHG forcing alone and under ~~geoengineering~~SAI, so we examine the differences G4-RCP4.5 for each model grouping the TC basins by hemisphere in Fig. 4, and use $\delta GPI_{G4} - \delta GPI_{rcp45}$ to calculate the difference. Fig. 4 clearly shows that *RH* and *WS* make the largest contribution to GPI differences in both hemispheres in all models~~ except MIROC-ESM-CHEM.~~. In the Northern Hemisphere, *RH* and *WS* ~~items~~terms show negative contributions in the cyclone season. Hence, these are the factors that ~~enables geoengineering~~primarily enable SAI to reduce GPI relative to ~~greenhouse gas forcing~~GHG. In the Southern Hemisphere there are no clear difference between GPI under G4 or RCP4.5. Absolute vorticity, *AV* makes almost no contribution to the GPI differences under ~~geoengineering~~SAI in all models.

We also do the same mathematical transform for ~~ventilation index~~VI. We obtain annual means and monthly anomalies:

$$\delta\mathrm{VI} = \alpha_5\delta\left(V_{pot}\right) + \alpha_6\delta(\chi_m) + \alpha_7\delta(V_{shear})$$

(~~10~~7)

Where $\alpha_5 = -\overline{V_{shear}}\frac{\overline{\chi_m}}{\overline{V_{pot}^2}}$ $\alpha_6 = \frac{\overline{V_{shear}}}{\overline{V_{pot}}}$ $\alpha_7 = \frac{\overline{\chi_m}}{\overline{V_{pot}}}$

$$\delta\mathrm{VI} = \mathrm{VI} - \overline{VI}$$

Analogously as for GPI, we show also results for VI in Fig. 4. V_{shear} makes the largest contribution to ventilation index differences between ~~geoengineering and greenhouse gas forcing in both hemispheres.~~ SAI and GHG forcing in both hemispheres. ~~Fig. 4 shows that the HadGEM2 values tend to be smaller than for other models and often differ in sign of difference from the other models, consistent with the muted spatial patterns in Fig. 3.~~

3.2.2 Contributions to GPI and VI across TC basins

The GPI and VI dependencies may be expressed as a regression equation of *X* on *Y* where Y is the GPI or VI anomalies under G4 relative to RCP4.5, and the fractional contribution to variance, S, of each variable i in X to Y can be written, following Moore et al. (2006) as,

$$S_i = M_i C_i \sigma X_i / \sigma Y \qquad (~~11~~8)$$

where the σX are the standard deviations of the predictor terms, σY is the standard deviation of the anomalies, C are the correlation coefficients of the X with Y, M are the regression coefficients of the X with Y. The regression can be expressed as a multiple linear regression in log space, and the coefficients simply transformed after fitting. Fitting in log space also allows for the generally heteroscedastic, fractional, nature of the errors in the variables.

The relative contributions to GPI anomalies from its four variable ~~items~~terms following the regression Eq. (~~11~~8) are shown in Fig. 5. *RH* is the dominant factor for GPI differences in all models ~~except MIROC-ESM-CHEM~~ and all TC basins. ~~A striking feature of Fig. 5~~There is ~~that there are very similar patterns of variability between models across all the basins~~little variance explained for the ~~*PI* and the *RH* terms, but not for the *WS* and *AV* terms~~MIROC-ESM-CHEM and NorESM1-M models compared with the other three models. Fig. 5 also shows that *AV* makes very little contribution to variance explained in the (G4-RCP4.5) differences. ~~For~~In all models ~~except MIROC-ESM-CHEM~~, *WS* makes about ~~half~~ the same contribution ~~to variance explained~~ as ~~*RH*~~*PI*.

Fig. ~~Fig. S1~~S1 shows the same analysis as Fig. 5, but for all 9 realizations of

MIROC-ESM-CHEM. The first four realizations behave similarly as the BNU-ESM, HadGEM2-ES and MIROC-ESM models in Fig. 5, with variance accounted for around 80% of total and the *RH* terms being about twice as important as *WS* and *PI* terms. The remaining 5 realizations have far lower variance explained, similar as for NorESM1-M, with *RH* still the dominant term.

Fig. S2 shows the three variables of the ventilation index in a similar way as Fig. 5. V_{shear} makes the largest contribution to VI for all TC basins and all models especially for the BNU-ESM and MIROC-ESM models. Fig. S3 shows the VI components for all 9 realizations of MIROC-ESM-CHEM, which appears similarly divided into two groups as they were for GPI in Fig. S1. Indeed from Fig. S1S2 it appears that VI may be simply replaced by V_{shear}, for the models where any variance is explained, but viewing the month by month contributions in Fig. 4 shows that other components are relatively important for some models during some months of the TC season. χ_m has no consistent contribution for the models and basins, and it sometimes make negative contributions to the difference (GPI_{G4}-$GPI_{RCP4.5}$)..

The statistical power of a regression equation can be expressed as the F-statistic. Given that the different variables in Figs 5 and S1S2 show notable differences in their contribution to the GPI and VI, we can use the F-statistic to examine if a reduced model with fewer variables is a better statistical model for the differences under G4 and RCP4.5. GPI has four variables, so there are 15 combination to examine as shown in Fig. 6. Only for BNU-ESM and MIROC-ESM do the full set of variables have the highest F-statistic. ~~NorESM1-M and MIROC-ESM-CHEM stand out as different from the other models in their general behavior. MIROC-ESM-CHEM is largely governed by *PI* and NorESM1-M by *RH*. In general~~However, HadGEM2-ES has best model with all factors except the atmospheric vorticity term. This is consistent with results shown in Figs. 4 and 5, and with the analysis by Emanuel (2013). The value of the F-statistic represents the degree that the regression model accounts for the data variability compared with model having no independent variables. The 3 models that the full, or nearly full, set of variables performs best have F-statistics over 1000 (p<0.001) while NorESM1-M has F of around 25-60. This is still significant at the 99.9% level. When we analyzed the realizations 5-9 of MIROC-ESM-CHEM, we found much lower F-statistics than for realizations 1-4 (Fig. S4), with values similar as for NorESM1-M of 50-100. In general, the models show *RH* has the largest F-statistic for single parameter models, consistent with Figs. 4 and 5. Fig. ~~4 and 5. VI has 3 variables, so there are 7 combinations possible.~~ S4 also shows that all three realizations of CanESM2, which we do not use for TC analysis in this paper, have even lower F values, particularly r2 and r3, which are around 2 that are not significant. ~~Fig. S2 shows V_{shear} has largest contribution to VI for most of models, and as for GPI, only BNU-ESM and MIROC-ESM models have largest F-statistic for the full set of model variables.~~

VI has three variables, so there are 7 combinations possible. As with GPI in Fig. 6, are remarkable differences in the values of F amongst the models. BNU-ESM, MIROC-ESM, HadGEM2-ES and the realizations 1-4 of MIROC-ESM-CHEM achieve values over 1000 ($p<0.001$), while for NorESM1-M and realizations 5-9 of MIROC-ESM-CHEM have best F-statistics of 50 – 100 ($p<0.001$). Fig. S5 shows V_{shear} has largest contribution to VI for most of models, and MIROC-ESM is the only models have largest F-statistic for the full set of model variables, as it also had for GPI.

3.3 The keyPrimary factors affecting TCsthat control GPI and VI changes

The analysis above shows that PIthe common factors across models and basins that affect TCs are potential intensity (V_{pot}), relative humidity (H), and vertical wind shear (V_{shear}). We now discuss these factors separately, beginning with V_{pot} as this is an important factor affecting TC genesis. function of several different ESM variables.

According to Eq. (2), V_{pot} is dependent on the static stability of the troposphere, which is related to both sea surface (T_S) and upper tropospheric temperatures (T_O) where rising air flows out of the storm. Wing et al. (2015) use the trends in reanalysis and radiosonde products at 70 and 100 hPa in TC seasons to represent change in outflow temperature across various TC basins and assign its contribution to trends in V_{pot}. For convenience, we choose the tropical tropopause (100 hPa) temperature from the ESM output to represent T_O. Fig. , and which can be represented by tropical tropopause (100 hPa) temperature. Fig. S3S6 show the correlations across TC basins and seasons for the various fields in RCP4.5 and G4, while Fig. 7 shows the correlations in the differences between G4 and RCP4.5 so that difference made by the geoengineeringSAI can be clearly evaluated. Fig. 7a shows the dependence of V_{pot} differences (G4-RCP4.5) on (T_S - T_O) differences for the models. All models have significant correlation for all TC basins except BNU-ESM~~, which is significant~~ in ~~WNP, ENP, NI~~the SI and ~~integrated over all TC~~SP basins and HadGEM2-ES in the SP basin. However, there is an even stronger dependence for V_{pot} on T_S anomalies (Figs. 7b, ~~S3~~S6). The ~~model~~ ensemble mean V_{pot} is better correlated with T_s rather than (T_S - T_O) ~~mostly~~ due to better correlations of ~~NorESM1-M and HadGEM2-ES in Fig. 7b.~~ all ~~Fig. S3 shows that correlations for both~~ models ~~under RCP4.5 and G4 separately are not atypical, simply that their (G4-RCP4.5) differences are small. It is also notable that there are worse correlations for the model ensemble values of (T_S - T_O) with~~ V_{pot} ~~under G4 than RCP4.5 (Fig. S3). All models except CanESM2 and NorESM1~~ in ~~show significant correlation between GPI and~~ T_S ~~anomalies shown as Fig. 7c. And all except these two models have significant correlations for~~ all ~~TC~~ basins except HadGEM2-ES.

All models show significant correlation between GPI and T_S anomalies shown as Fig. 7c. Some models have insignificant correlations in particular basins, e.g., BNU-ESM is slightly anti-correlated in NA, as is HadGEM2-ES in WNP. GPI is not significantly correlated with T_s for half the ESM in the NI and SP basins. Fig. S6 shows that there are fewer significant correlations under G4 than under RCP4.5.

Figs. ~~S4~~S7 and ~~S5~~S8 show the seasonal ~~variability~~cycle of T_s and ~~T_θ~~T_o for all the models. The annual cycle of T_s, is very similar, as expected, for all the models, and with good agreement on the differences in seasonal cycle between the Northern and Southern Hemispheres~~.~~ as observed (Fig. S9). However, for ~~T_θ~~T_o the models show differences in the shapes and phases of the cycles in both hemispheres, for example only the NorESM1-M model shows roughly antiphase seasonality between the hemispheres. Fig.

~~S6~~S9 shows the ERA-interim reanalysis ~~T_0~~T_o data, which has similar seasonality in both hemispheres, with peak temperature anomalies in August (~ 1.5°C) and a sharp decline to a long minimum by November or December of similar magnitude. ~~Comparing~~ Figs~~.~~ ~~S5 and S6~~ S7 shows that the models generally follow similar patterns under both G4 and RCP4.5~~, except~~ for ~~NorESM1-M and~~T_s, but Fig S8 shows that there is much larger variability between the models representations of T_o under G4 and RCP4.5. HadGEM2-ES~~. HadGEM2-ES~~ is ~~also~~ the model with largest amplitude of seasonal cycle, somewhat larger than in ERA-Interim; other models have smaller amplitudes, with many around half that observed at present. This degree of difference in ~~T_0~~T_o simulation likely explains ~~much~~some of the inter-model differences in GPI.

~~The other common factors across models and basins that affect TCs are relative humidity (H) and vertical wind shear (V_{shear}). In Figs 7d and 7e we plot H and V_{shear}~~ We plot H differences between G4 and RCP4.5 as a function of sea surface temperature differences in Fig. 7d. Relative humidity rises with warming temperatures under both G4 and RCP4.5 (Fig. ~~S3~~S6), as expected. But there are obvious differences across the ocean basins with weakest response in ENP, NA and NI and strongest correlations in the Southern Hemisphere basins. Differences G4-RCP4.5 follow a similar spatial pattern, ~~but~~ with ~~a significant anti-correlation~~again largest correlations in ~~North Atlantic. Across-model~~ the southern ocean basins.

Fig 7e shows how RCP4.5-G4 differences in V_{shear} and T_s are ~~larger~~generally anti-correlated. The across-model spread for correlations of V_{shear} and T_s under both G4 and

RCP4.5 (Fig. ~~S3) than~~ S6) are similar as for the other key variables. ~~In contrast~~ Anti-correlation with ~~the other parameters, there~~ T_s is ~~generally an anti-correlation with T_s across all ocean basins, with the NA basin having the~~ weakest ~~correlations.~~in the SP and NA basins, but still significant. In terms of the differences in Fig. 7e, all models show clear significant anti-correlations~~ except CanESM2~~, with the NI and NA basins having weakest correlations. Vecchi ~~et al.~~and Soden (2007) found the ~~tropical~~North Atlantic and East North Pacific wind shear increases in model projections under global warming. If the models assessed here capture the effect under G4 and RCP45, we would expect positive ~~correlation~~correlations between V_{shear} and T_s over ~~the tropical Atlantic~~ these two basins for G4 and RCP4.5 in Fig. ~~S3, but all models show negative correlations, although the Pacific Ocean basins more significantly anti-correlated than NA.~~ S6~~Li et al. (2010) showed that under warming there is relative shift of towards the central Pacific Ocean of TC genesis away from the North West Pacific. When we plot the G4-RCP4.5 GPI difference map over the Pacific Ocean, we also see a clear anomaly in the Central Pacific (Fig. S7). Li et al. (2010) showed the same effect when using prescribed sea surface temperature patterns from a suite of models, and they account for the changes in TC by surface temperature gradients that drive trade winds, which changes the wind shear. Our result is thus consistent with their findings of changes under greenhouse gas forcing in the Pacific Ocean if the G4 simulation reverses the effects of RCP4.5 effectively~~.

~~3.4 The effect of ENSO on GPI~~

~~The El Nino-Southern Oscillation (ENSO) is characterized by interannual sea surface temperature (SST) variations in the eastern and central equatorial Pacific Ocean. The impact of ENSO events on the TC activity over the western North Pacific (WNP) has been studied to provide a better understanding of the large-scale steering flow of TCs and the tendency of TC tracks to shift (Wang et al., 2002). There is also clear evidence of teleconnections between ENSO and North Atlantic hurricane season statistics (Gray, 1984; Grinsted et al., 2013). ENSO may be characterized by measures of atmospheric or oceanic variability. We examined the simulated Niño3.4 index of tropical Pacific SSTs in the box 170°W – 120°W, 5°S – 5°N, and the Southern Oscillation Index (SOI) of standardized sea level pressure differences between Tahiti and Darwin, Australia. Previous analysis of the GeoMIP model ENSO response (Gabriel et al., 2015) preferred SST based estimates than noisier atmospheric representations. They also excluded the BNU-ESM, MIROC-ESM and MIROC-ESM-CHEM models from their analysis because of the model's unrealistic amplitudes of ENSO. However, as in the real world, all models and the ensemble we use, show a significant anti-correlation between Niño3.4 index and SOI, except NorESM1-M under G4, (~~There are similar significant relationships between H and V_{shear} under G4 and RCP4.5 (Fig. S6), and also with their differences (Fig. 7f). This relationship is anti-correlation in all basins for most models, except in the North Atlantic. The strength of the relationship are similar as for those with T_s, and demonstrates that the thermodynamic variables T_s and H can be useful proxies for the dynamic V_{shear} variable.

Fig. 8). This suggests that while many models, are deficient in aspects of their ENSO variability, they all capture at least some important aspects of ENSO. The correlation coefficients are more significant in RCP4.5 than under G4 for most models. We combined Niño3.4 and SOI indices with equal weighting to get a single representative index of ENSO to compare with GPI and VI.

Annual GPI for the TC basins and the ENSO index during the TC seasons are, in general, significantly correlated under both G4 and RCP4.5 (Fig. 9). The exception being CanESM2 which exhibits anti-correlation between GPI and ENSO index under both G4 and RCP4.5. The analysis for individual basins indicates most models have significant correlations with ENSO in the WNP and the SP basin, except CanESM2 under the G4 experiment, where it is significantly anti-correlated for RCP4.5. BNU-ESM, MIROC-ESM and MIROC-ESM-CHEM have significant correlations in ENP, with NorESM1 and CanESM2 having little or no correlations. Only MIROC-ESM-CHEM has significant correlation between GPI and ENSO in the NA basin, but the R^2 is relatively low, around 0.22. Both BNU-ESM and NorESM1 have significant correlations in the SI basin, while CanESM2 has significant anti-correlation there. So the impact of ENSO is most consistently felt in the Pacific Ocean, with perhaps surprisingly low correlation in the North Atlantic considering the well-known teleconnections with hurricane activity there.

3.5 TC from Track with HadGEM2-ES

As a supplemental analysis to the results based on the GPI and VI, we also employ a widely-used feature tracking software (TRACK vn. 1.4.9) to directly track vorticity maxima that characterize cyclones. Hodges (1995) provides a detailed account of TRACK's core functionality. Jones et al. (2017) also used TRACK to assess geoengineering impact on North Atlantic hurricane statistics, and we follow their approach. Firstly, we determine the relative vorticity (ξ) on the 850, 500, and 250 hPa vertical pressure levels from the zonal (U) and meridional (V) wind using the definition: $\xi = (1/a \times \cos(\theta)) \times (dV/d\lambda - dU\cos(\theta)/d\theta)$, where a is Earth's radius, and θ and λ are the latitude and longitude in radians respectively. U and V are required on 6 hour time steps, but are only available for the HadGEM2-ES model in our ensemble, and limited to the Northern Hemisphere TC season. TRACK detects storms lasting at least 2 days and additionally requires values setting for three parameters. We follow Jones et al. (2017) in selecting: $\xi_I \geq 4.5$ to express the minimum vorticity intensity required; $\xi_V \geq 3.5$ for the warmth of cyclone core; ξ_I and ξ_V thresholds must be met for at least 4 consecutive time steps. These criteria represent a relaxation of standard parameters (6, 6, 4) but were tuned to produce a match in the statistics of Atlantic hurricanes contained in the HURDAT2 database (Landsea,et al., 2013) from the HADGEM2-ES historical simulation.

In contrast with Jones et al. (2017) which used data from June through November, we confine the analysis to the Northern Hemisphere TC season (August, September, October). The TRACK results suggest that there are significantly more TC under G4 than with RCP4.5 (Table 4) in all basins except the Eastern North Pacific. This

~~surprising result is not consistent with the changes in GPI and VI for the Northern Hemisphere (Table 3). Table 3 shows that the G4 cools relative to RCP4.5 and that wind shear increases. Furthermore, the TRACK result is not consistent with i) the findings of the statistical model based on surface temperatures (Moore et al., 2015), ii) the proxies (including wind shear) for TC examined by Jones et al. (2017), iii) the statistical-dynamical downscaling CHIPS model of Emanuel (2013). Jones et al. (2017) show that TCs numbers evaluated using the direct counting of storms using the TRACK scheme (Bengtsson et al., 2007) produce much smaller differences between G4 and RCP4.5 than those using statistical downscaling based on either statistical-dynamical downscaling using CHIPS (Emanuel et al., 2004) or simply surface temperatures (Moore et al., 2015).~~

4 Discussion and Conclusion

~~Typical~~Storms simulated by ESM ~~are run in coarse resolution that cannot resolve tropical cyclones and hence do not directly reproduce observed storm intensities and synoptic features related to cyclogenesis (Camargo, 2013). The storms that~~ may be counted using ~~indirect~~ methods such as the TRACK algorithm ~~include~~(Hodges, 1995; Jones et al. 2017) that allow for feedbacks with the ~~whole~~ climate ~~condition~~system. Statistical methods (Moore et al., 2015) may also implicitly include feedbacks between regional storm and background global climate conditions, but dynamical downscaling methods (Emanuel, 2013) ~~cannot~~do not include them. The GPI and VI proxies we ~~apply~~utilize here are useful tools for relating storm activity to meteorological conditions but do not account for changes to TC tracks or intensity. Since they require ~~relatively little~~coarse temporal-resolution data to calculate (monthly means), compared with daily or 6 hourly data required for TRACK or the CHIPS tools, and they convey information from more than simply surface temperature fields, they may give reasonable insights into the complex changes to TC under ~~SRM geoengineering~~SAI schemes.

We evaluated the hurricane index over six TC ocean basins in ~~six~~five CMIP5 and GeoMIP models. We used G4 and RCP4.5 experiments to assess and compare the genesis potential and ventilation indices that ~~diagnose~~relate tropical ~~storms in climate models.~~storm activity to ambient meteorology. Based on the climatology of the years ~~2040~~2020-2069, GPI and VI both show small rising trends for TC genesis in all ~~six~~five models under both G4 and RCP4.5 scenarios. The TC season as measured by elevated monthly GPI values is almost a month earlier in G4 than RCP4.5, a result that is consistent across basins and models. There are fewer TC's expected globally under SAI G4 than under the purely GHG forcing of RCP4.5 as assessed by differences significant at the 95% level in both GPI and VI. All 5 ESM models show significantly reduced GPI under G4 in Northern Hemisphere basins (Tables 3, 4) but results are inconclusive for southern basins. Spatial patterns of TCs, show both GPI and VI predicting fewer TC in the North Atlantic and North Indian Ocean under G4 compared with RCP4.5, and more TC in the South Pacific for most models in the ensemble. Thus ~~stratospheric sulphate aerosol~~the G4 scenario of SAI based on equatorial lower stratosphere injection of SO2 could lead to fewer TCs in the North Atlantic and Indian Ocean but more TCs in the South Pacific region than under ~~greenhouse gas~~GHG induced global warming. There is, however, large inter-model variationsvariability across the six ocean basins. The impact of ENSO on TCs can be detected in the GPI and shows a rising tendency for GPI under El Niño conditions across the TC basins, especially in the Pacific Ocean.

Detailed statistical analysis of the two TC indices indicates that theDetailed statistical analysis of the two TC indices indicates that NorESM1-M and 5 out of 9 MIROC-ESM-CHEM ensemble members have lower dependencies on explanatory variables for GPI or VI. This suggests that using GPI and VI to elucidate TC activity in those particular ESM simulations is much less reliable. It is not obvious from simple correlations between GPI and VI, or between fields such as T_s or H which ESM runs have relatively poor relationships for GPI.

The thermodynamic variables potential intensity and relative humidity are the dominant ones affecting genesis potential, while the dynamic variables such as absolute vorticity and entropy deficit are much less important. Vertical wind shear is a dynamic variable and dominates the ventilation index. By examining the contributions of variables to differences in GPI and VI under geoengineeringSAI and greenhouse gasGHG forced climates, we show that relative humidity is the dominant factor for GPI differences in all models and all TC basins, except . Relative humidityMIROC-ESM-CHEM for which potential intensity is also usefully correlated with wind shear, though the dominant factor.North Atlantic displays a qualitatively different relationship than the other basins. The analysis suggests that a simplified representation of TCs depending on fewer variables ismay be possible, but does require analysis of particular model behavior before choosing those variables. Although wind shear is important and a dynamic variable, it in encouraging that the thermodynamic state of the system is of prime importance for the GPI~~, suggesting~~. This suggests that statistical methods of predicting changes in ~~hurricane and storm~~TC behavior are plausible~~. But, these indices cannot fully represent~~, although individual basin behavior depends on particular local forcing factors in addition the ~~actual TC variations due to~~accessible thermodynamic variables used in the ~~complexity of TC genesis~~GPI and ~~evolution~~VI.

Potential intensity is related to the difference between sea surface temperature and outflow temperature (~~the~~evaluated at 100 hPa~~ level~~). In fact we ~~note~~find that changes in SSTs alone provide a better correlation with both potential intensity and GPI changes. This result is similar with previous observational (Grinsted et al., 2013) and modeling (Wu and Lau, 1992) studies that suggest it is the geographical distribution of SST anomalies that are crucial for the development of TC. Recent analysis of GeoMIP results by Davis et al. (2016), on the extent of the tropical belt under G1 and ~~4~~abrupt4×CO2 experiments, demonstrates that tropical upper-tropospheric temperature changes are well-correlated with the change in global-mean surface temperature. This is because changes in the static stability characterized by upper troposphere and surface temperature differences scales with the moist adiabatic lapse rate and surface temperatures.

In contrast with the solar dimming G1 experiments analyzed by Davis et al., (2016), here we ~~analysis~~analyze G4 which is an aerosol injection ~~scheme~~protocol. The aerosol

~~heats~~is prescribed (Kravitz et al., 2011a), as injected into the equatorial stratosphere ~~mainly between the~~ at 16-25 km ~~elevation injection levels~~altitude, where most of the direct radiative heating takes place (Pitari et al., 2014). However, due to the large size of the geoengineering aerosol particles (effective radius of the order of 0.6 μm or more), a significant fraction of the stratospheric particles settle below the tropical tropopause (Niemeier et al., 2011; English et al., 2012; Cirisan et al, 2013), thus producing some diabatic heating a few kilometres immediately below the tropical tropopause. This is superimposed on the convectively-driven upper tropospheric cooling caused by surface cooling due to the SAI and reduced convection and weakened hydrological cycle (Bala et al., 2008). This may be expected to be the dominant process controlling the SAI-induced changes in atmospheric static stability. Furthermore, recent work (Visioni et al., 2018 ACP in discussion) explores the surface cooling impact on upper tropospheric cirrus cloud formation, and the concomitant impact on static stability. Surface cooling and lower stratospheric warming, together, tend to stabilize the atmosphere, thus decreasing turbulence and updraft velocities. The net effect is an induced cirrus thinning, which indirectly increases net global cooling due to the SAI. ~~Furthermore, recent work (Visioni et al., 2018 ACP in discussion) explores the secondary of surface cooling on the upper troposphere with the impact on cirrus clouds, and the concomitant impact on static stability. Surface cooling and lower stratospheric warming at the tropopause of about 0.6 °C, together, tend to stabilize the atmosphere, thus decreasing turbulence and water vapor updraft velocities. The net effect is an induced cirrus thinning, which serves to increase net global cooling due to the SAI.~~

Pitari et al. (2014) note a warming of the 100 hPa layer under G4 relative to RCP4.5 for the MIROC-ESM-CHEM model ~~(Pitari et al., 2014). This is about half~~in the 2040s for the tropics. Most models (Table 3) in the TC basins and seasons show a cooling of (ensemble mean of 0.14°C) with only HadGEM2-ES and BNU-ESM having warming at 100 hPa. Given the complexities of changes in the upper troposphere due to the process outlined in the previous paragraph the range ~~of the G4~~ in static stabilities represented by the model range in Ts-To differences relative to RCP4.5 ~~difference in static stability (Fig. 7). Hence,~~is probably not surprising. Therefore, although we ~~would~~might expect to see ~~a significant~~an improvement in correlation of potential intensity and GPI by using 100 hPa temperatures in addition to SSTs, ~~but we do not. Table 3 shows that the upper troposphere measured by T_0 does not warm with most models under G4, which is consistent with the impact of G1 on the troposphere.~~the ability of the models to capture all the processes varies. The result is that the models used here have a better relationship with sea surface temperatures than static stability, and suggests that the aerosol ~~heating~~ effects are not ~~influencing~~being simulated well enough to allow their impacts on TC genesis to be fully estimated.

The change in relative humidity on the tropical ocean basins in future is a key aspect of TC genesis according to our analysis. Models tend to agree on the sign of change in relative humidity as temperatures rise, but there are consistent differences in response strength ~~of response~~ across the ocean basins. ~~The differences in response (G4-RCP4.5) even indicate a difference in sign of North Atlantic response under~~

geoengineering from the other basins. This indicates that although relative humidity is important for most models, changes in TC genesis processes between basins affect its utility as a predictor variable. Here we used the widely utilized formulation of GPI given by Emanuel and Nolan (2004), which specified moisture in terms of relative humidity. More recently Emanuel (2010) reformulate GPI in terms of "saturation deficit" that is a measure of the moist entropy deficit of the middle troposphere, which becomes larger as the middle troposphere becomes drier. This parameter has the same denominator as χ_m in Eq (4), which is used in the calculation of VI, Eq (3), while the numerator varies only in the definition of the boundary layer. Our analysis of the dependence of the three terms that describe VI shows χ_m is moderately important in some models (Fig. S5), and more useful reduced regression models are (V_{pot}, χ_m), or (V_{shear}, χ_m) than (V_{pot}, V_{shear}). This consistent with analysis of 6 ESM models 21st century trends in GPI by Emanuel (2013), who also notes that vorticity does not contribute to trends.

The final variable, vertical wind shearV_{shear} , shows large scatter across the models, but consistent anti-correlation with T_s. However, there are also good but different relations between V_{shear} and surface temperature, and that relationship is somewhat stronger under G4 than RCP4.5. The changes in GPI over the Pacific Ocean under G4 compared with RCP4.5 are similar to previous results comparing patterns of TC genesis under 20th century H and V_{shear} in every basin suggesting that the state of this dynamic variable can be explained to a significant degree by the thermodynamic state driving H

and T_S. This is consistent with analysis (Li et al., 2010), showing that prescribed sea surface temperatures ~~relative to 21st patterns (Li et al., 2010).~~can account for some changes in TC in the Pacific basins as surface temperature gradients drive trade winds, which changes the wind shear. Overall our analysis of the driving parameters in GPI, suggests that despite large model differences, the simple dependence of GPI on surface temperatures is reasonably robust.

Smyth et al. (2017) report the seasonal migration of the Intertropical Convergence Zone (ITCZ) in G1, associated with preferential cooling of the summer hemisphere, and annual mean ITCZ shifts in some models that are correlated with the warming of one hemisphere relative to the other. ITCZ location is correlated with ~~tropical cyclone and season.~~TC and season. The timing of the TC season under G4 is about a month earlier in both hemispheres than under RCP4.5. This might also be a function of the reduced amplitude of ITCZ motion, though this effect has not yet been verified as occurring under SAI as prescribed by G4. It is plausible because reduced solar heating of the ocean basins mean that less sea water is heated and there will be reduced lag of those surface waters with solar zenith position. Our analysis of seasonality of TCs shows that there appears to be a difference in behavior between the Southern and Northern Hemispheres, with the southern one showing no consistent changes between models under RCP4.5 and G4 scenarios. Davis et al. (2016) show that there are differences in the evolution of the northern and southern Hadley cells under ~~greenhouse~~GHG forcing, with the expansion of the northern one scaling non-linearly with temperature. Differences seem to be driven fundamentally by the equator-pole temperature gradient, and therefore may be expected given the far greater fraction of land surface and larger polar amplification in the Northern~~ compared with Southern~~ Hemisphere.

~~Many models, owing to their low resolutions, produce much weaker and larger TCs (Camargo et al., 2005) than seen observationally.~~ Considering the ~~insufficient~~coarse spatio-temporal resolution of most ESM models, evaluating the GPI ~~and VI may~~is likely to remain a popular be a ~~better~~good diagnostic of TC ~~variations~~variability under different climates. The results presented here suggest that ~~SRM~~SAI produces reductions in TCs across most of the major storm basins, and ~~would be~~this is primarily due to reduced sea surface temperatures in the genesis regions.

Acknowledgements. ~~We thank~~We thank two anonymous referees for very constructive comments, the climate modeling groups for participating in the Geoengineering Model Intercomparison Project and their model development teams; the CLIVAR/WCRP Working Group on Coupled Modeling for endorsing the GeoMIP; and the scientists managing the earth system grid data nodes who have assisted with making GeoMIP output available. This research was funded by the National Basic Research Program of China (Grant 2015CB953600) and the Fundamental Research Funds for the Central Universities (312231103).

REFERENCES

Balaguru, K., Foltz, G. R., Leung, L. R., Asaro, E. D', ~~Emanuel~~Gabriel , K. A., ~~H.~~ Liu, H., and Zedler, S. E.: Dynamic Potential Intensity: An improved representation of the ocean's impact on tropical cyclones, Geophys. Res. Lett., 42, 6739-6746, 2015.

~~Bengtsson, L., Hodges, K. I. and Esch, M.: Tropical cyclones in a T159 resolution global climate model: comparison with observations and re-analyses, Tellus A, 59: 396–416, 2007.~~

Bala, G., Duffy, P. B., and Taylor, K. E.: Impact of geoengineering schemes on the global hydrological cycle, Proc. Natl. Acad. Sci., 105,7664–7669, doi:10.1073/pnas.0711648105, 2008.

Bentsen, M., Bethke, I., Debernard, J. B., Iversen, T., Kirkevåg, A., Seland, Ø., Drange, H., Roelandt, C., Seierstad, I. A., Hoose, C., and Kristjánsson, J. E.: The Norwegian Earth System Model, NorESM1-M – Part 1: Description and basic evaluation of the physical climate, Geosci. Model Dev., 6, 687–720, 2013.

Bister, M., and Emanuel, K. A.: The genesis of Hurricane Guillermo: TEXMEX analyses and a modeling study, Mon. Wea. Rev., 125, 2662–2682, 1997.

Bister, M., and Emanuel, K. A.: Dissipative heating and hurricane intensity, Meteor. Atmos. Phys., 65, 233–240, 1998.

~~Camargo, S. J., Barnston, A. G., and Zebiak, S. E.: A statistical assessment of tropical cyclone activity in atmospheric general circulation models, Tellus A, 57, 589-604, 2005.~~

~~Camargo, S. J.: Global and regional aspects of tropical cyclone activity in the CMIP5 models. J. Clim., 26, 9880–9902, 2013.~~

Chan, J. C. L.: Interannual and interdecadal variations of tropical cyclone activity over the western North Pacific, Meteor. Atmos. Phys., 89, 143-152, 2005.

~~Chylek, P., Li, J., Dubey, M. K., Wang, M., and Lesins, G.: Observed and model simulated 20th century Arctic temperature variability: Canadian Earth System Model CanESM2.Atmos,~~Cirisan, A., Spichtinger, P., Luo, B. P., Weisenstein, D. K., Wernli, H., Lohmann, U., and Peter, T.: Microphysical and radiative changes in cirrus clouds by geoengineering the stratosphere, J. Geophys. Res.-Atmos., 118, 4533–4548, doi:10.1002/jgrd.50388, 2013.

~~Chem. Phys. Discuss., 11, 22 893–22 907, 2011.~~

Crutzen, P. J.: Albedo enhancement by stratospheric sulfur injections: A contribution to resolve a policy dilemma?, Clim. Change, 77(3), 211–220, 2006.

Collins, W. J., Bellouin, N., Doutriaux-Boucher, M., Gedney, N., Halloran, P., Hinton, T., Hughes, J., Jones, C. D., Joshi, M., Liddicoat, S., Martin, G., O'Connor, F., Rae, J., Senior, C., Sitch, S., Totterdell, I., Wiltshire, A., and Woodward, S.: Development and evaluation of an Earth-System model – HadGEM2, Geosci. Model Dev., 4, 1051–1075, 2011.

Davis, N. A., Seidel, D. J., Birner, T., Davis, S. M., and Tilmes, S.: Changes in the width of the tropical belt due to simple radiative forcing changes in the GeoMIP simulations, Atmos. Chem. Phys., 16, 10083-10095, 2016.

Emanuel, K. A.: Tropical cyclone activity downscaled from NOAA-CIRES reanalysis, Journal of Advances in Modeling Earth Systems, 2:1–12, 1908-1958, 2010.

Emanuel, K. A.: Downscaling CMIP5 climate models shows increased tropical cyclone activity over the 21st century, PNAS, 110(30), 12219-12224, 2013.

Emanuel, K. A.: A statistical analysis of tropical cyclone intensity, Mon. Wea. Rev., 128, 1139–1152, 2000.

Emanuel, K. A.: Atmospheric Convection, Oxford University Press, 580 pp, 1994.

Emanuel, K. A., Nolan, D.: Tropical cyclone activity and global climate system, Am. Meteorol. Soc., 26, 240–241, 2004.

Emanuel, K. A., Sundararajan, R., and Williams, J.: Hurricanes and global warming: Results from downscaling IPCC AR4 simulations, Bull. Amer. Meteor. Soc., 89, 347-367, 2008.

Emanuel, K. A.: Climate and tropical cyclone activity: A new model downscaling approach, J. Climate, 19, 4797-4802, 2006.

~~Gabriel, C.~~English, J. M., Toon, O. B., and ~~Robock, A.: Stratospheric~~Mills, M. J.: Microphysical simulations of sulfur burdens from stratospheric sulfur geoengineering ~~impacts on El Niño/Southern Oscillation~~, Atmos. Chem. Phys., ~~15, 11949-11966, 2015~~12, 4775-4793, https://doi.org/10.5194/acp-12-4775-2012, 2012.

Gray, W. M.: Hurricanes: Their formation, structure, and likely role in the tropical circulation, Roy. Meteor. Soc., 155-218, 1979.

~~Gray, W. M.: Atlantic seasonal hurricane frequency: Part I: El Niño and 30 mb quasi-biennial oscillation influences, Mon. Wea. Rev., 112, 1649-1668, 1984.~~

Grinsted, A., Moore, J. C., Jevrejeva, S.: A homogeneous record of Atlantic hurricane surge threat since 1923, PNAS, 109(48):19601-19605, 2012.

Grinsted, A., Moore, J. C., Jevrejeva, S.: Projected Atlantic tropical cyclone threat from rising temperatures, PNAS, 110(14), 5369-5373, 2013.

Huneeus, N., Boucher, O., Alterskj, K., Cole, J. N. S., Curry, C. L., Ji, D., Jones, A., Kravitz, B., Kristjánsson, J. E., Moore, J. C., Muri, H., Niemeier, U., Rasch, P., Robock, A., Singh, B., Schmidt, H., Schulz, M., Tilmes, S., Watanabe, S., and Yoon, J.-H.: Forcings and feedbacks in the GeoMIP ensemble for a reduction in solar irradiance and increase in CO2, J. Geophys. Res. Atmos., 119, 5226–5239, 2014.

Hodges, K.: Feature tracking on a unit sphere, Mon. Wea. Rev., 123, 3458–3465,1995.

IPCC: Climate Change 2007: Synthesis Report. Contribution of Working Groups I, II and III to the Fourth Assessment Report of the Intergovernmental Panel on Climate Change, edited by Core Writing Team, R. K. Pachauri, and A. Reisinger, 104 pp., IPCC, Geneva, Switzerland, 2007.

Ji, D., Wang, L., Feng, J., Wu, Q., Cheng, H., Zhang, Q., Yang, J., Dong, W., Dai, Y., Gong, D., Zhang, R.-H., Wang, X., Liu, J., Moore, J. C., Chen, D., and Zhou, M.: Description and basic evaluation of Beijing Normal University Earth System Model(BNU-ESM) version 1, Geosci. Model Dev., 7, 2039–2064, 2014.

Jones, A. C., Haywood, J. M., Dunstone, N., Emanuel, K., Hawcroft, M. K., Hodges, K. I., Jones, A.: Impacts of hemispheric solar geoengineering on tropical cyclone frequency, Nat. Commun., 8 (1382), 1-10, 2017.

Kashimura, H., Abe, M., Watanabe, S., Sekiya, T., Ji, D., Moore, J.C., Cole, J.N.S. and Kravitz, B.: Shortwave radiative forcing, rapid adjustment, and feedback to the surface by sulfate geoengineering: analysis of the Geoengineering Model Intercomparison Project G4 scenario, Atmospheric Chemistry and Physics 17, 3339-3356, doi:10.5194/acp-17-3339-2017, 2017.

Knutson, T. R., Mcbride, J.L., Chan, J., Emanuel, K., Holland, G., Landsea, C., Held, I., Kossin,J.P., Srivastava, A.K., and Sugi, M.: Tropical cyclones and climate change. Nat. Geosci., 3, 157–163, doi:10.1038/ngeo779, 2010.

Knutson, T. R., Sirutis, J., Zhao, M., Tuleya, R., Bender, M., Vecchi, G., Villarini, G., and Chavas, D.: Global projections of intense tropical cyclone activity for the late twenty-first century from dynamical downscaling of CMIP5/RCP4.5 scenarios, J. Climate, 28, 7203–7224, 2015.

Kravitz, B., Robock, A., Boucher, O., Schmidt, H., Taylor, K. E., Stenchikov, G., and Schulz, M.: The Geoengineering Model Intercomparison Project (GeoMIP), Atmos. Sci. Lett., 12, 162-167, 2011a.

Kravitz, B., Robock, A., Tilmes, S., Boucher, O., English, J. M., Irvine, P. J., Jones, A., Lawrence, M. G., MacCracken, M., Muri, H., Moore, J. C., Niemeier, U., Phipps, S. J., Sillmann, J., Storelvmo, T., Wang, H., and Watanabe, S.: The Geoengineering Model Intercomparison Project Phase 6 (GeoMIP6): simulation design and preliminary results, Geosci. Model Dev., 8, 3379-3392, 2015.

Kang, N. and Elsner, J. B.: Consensus on Climate Trends in Western North Pacific Tropical Cyclones, J. Climate, 25, 7564–7573, 2012.

Knutson, T. R., Sirutis, J., Zhao, M., Tuleya, R., Bender, M., Vecchi, G., Villarini, G., and Chavas, D.: Global projections of intense tropical cyclone activity for the late twenty-first century from dynamical downscaling of CMIP5/RCP4.5 scenarios, J. Climate, 28, 7203–7224, 2015.

Landsea, C. W.: Hurricanes and global warming, Nature, 438, E11-E12, 2005.

Landsea, C. W., Franklin, J. L.: Atlantic hurricane database uncertainty and presentation of a new database format, Mon. Weather Rev., 141, 3576–3592, 2013.

Li, T., Kwon, M., Zhao, M., Kug, J. - S., Luo, J. - J, and Yu, W.: Global warming shifts Pacific tropical cyclone location, Geophys. Res. Lett., 37, L21804, 2010.

Li, Z., Yu, W., Li, T., Murty, V.S. and Tangang F.: Bimodal Character of Cyclone Climatology in the Bay of Bengal Modulated by Monsoon Seasonal Cycle, J. Climate, 26, 1033–1046, 2013.

Moore, J. C., Kekonen, T., Grinsted, A., and Isaksson, E.: Sulfate source inventories from a Svalbard ice core record spanning the Industrial Revolution, J. Geophys. Res., 111, D15307, 2006.

Moore, J. C., Grinsted, A., Guo, X., Yu, X., Jevrejeva, S., Rinke, A., Cui, X., Kravitz, B., Lenton, A., Watanabe, S., Ji, D.: Atlantic hurricane surge response to geoengineering, PNAS, 112 (45), 13794-13799, 2015.

Niemeier, U., Schmidt, H. and Timmreck, C.: The dependency of geoengineered sulfate aerosol on the emission strategy. Atmos. Sci. Lett., 12: 189-194. doi:10.1002/asl.304, 2011

Nolan, D. S.: What is the trigger for tropical cyclogenesis?, Aust. Meteorol. Mag., 56, 241-266, 2007.

Pitari, G., Aquila, V., Kravitz, B., Robock, A., Watanabe, S., Cionni, I., Luca N. D., Genova, G.D., Mancini, E., and Tilmes, S.: Stratospheric ozone response to sulfate geoengineering: Results from the Geoengineering Model Intercomparison Project (GeoMIP), J. Geophys. Res. Atmos., 119, 2629–2653, 2014.

Rappin, E. D., Nolan, D. S., and Emanuel, K. A.: Thermodynamic control of tropical cyclogenesis in environments of radiative convective equilibrium with shear, Q. J. R. Meteorol. Soc., 136, 1954-1971, 2010.

Riehl, H.: A model for hurricane formation. J Appl Phys, 21, 917–925, 1950.

Rogelj, J., Luderer, G., Pietzcker, R.C., Kriegler, E., Schaeffer, M., Krey, V., Riahi, K.: Energy system transformations for limiting end-of-century warming to below 1.5°

C, Nature Climate Change, 5, 519-527, 2015.

Russotto, R. D. and Ackerman, T. P.: Energy transport, polar amplification, and ITCZ shifts in the GeoMIP G1 ensemble, Atmospheric Chemistry and Physics, 18, 2287–2305, doi:10.5194/acp-18-2287-2018, 2018.

Smyth, J. E., Russotto, R. D., and Storelvmo, T.: Thermodynamic and dynamic responses of the hydrological cycle to solar dimming, Atmos, Chem. Phys., 17, 6439-6453, 2017.

Song, Y. J., Wang, L., Lei, X. Y., and Wang, X. D.: Tropical cyclone genesis potential index over the western North Pacific simulated by CMIP5 models, Adv. Atmos. Sci., 32(11), 1539-1550, 2015.

Tang, B., and Emanuel, K. A.: A ventilation index for tropical cyclones, Bull. Am. Meteorol. Soc., 93, 1901-1912, 2012a.

Tang, B., and Camargo, S. J.: Environmental control of tropical cyclones in CMIP5: A ventilation perspective, J. Adv. Model. Earth Syst., 6, 115-128, 2014.

Taylor, K. E., Stouffer, R. J., and Meehl, G. A.: An overview of CMIP5 and the experiment design, Bull. Amer. Meteor. Soc., 93, 485-498, 2012.

Tippett, M. K., Camargo, S. J., and Sobel, A. H.: A Poisson regression index for tropical cyclone genesis and the role of large-scale vorticity in genesis, J. Climate, 24, 2335–2357, 2011.

Tory, K. J., Chand, S. S., McBride, J.L., Ye, H., and Dare, R.A.: Projected Changes in Late-Twenty-First-Century Tropical Cyclone Frequency in 13 Coupled Climate Models from Phase 5 of the Coupled Model Intercomparison Project, J. Climate, 26, 9946–9959, 2013.

Vecchi, G. A., and Soden, B. J.: Increased tropical Atlantic wind shear in model projections of global warming, Geophys. Res. Lett., 34, L08702, 2007.

Visioni, D., Pitari, G., and Aquila, V.: Sulfate geoengineering: a review of the factors controlling the needed injection of sulfur dioxide, Atmos. Chem. Phys., 17, 3879-3889, https://doi.org/10.5194/acp-17-3879-2017, 2017.

Visioni, D., Pitari, G., and di Genova, G.: Upper tropospheric ice sensitivity to sulfate geoengineering, Atmos. Chem. Phys. Discuss., ~~Wang, B. and Chan, J. C.: How Strong ENSO Events Affect Tropical Storm Activity over the Western North Pacific, J. Climate, 15, 1643–1658, 2002.~~

~~Wang, X., Zhou, W., Li, C. Y., and Wang, D. X.: Effects of the East Asian summer monsoon on tropical cyclone genesis over the South China Sea on an interdecadal timescales, Adv~~https://doi.org/10.5194/acp-2018-107, under review, 2018.

: Atmos. Sci., 29, 249-262, 2012.

Watanabe, S., Hajima, T., Sudo, K., Nagashima, T., Takemura, T., Okajima, H., Nozawa, T., Kawase, H., Abe, M., Yokohata, T., Ise, T., Sato, H., Kato, E., Takata, K., Emori, S., and Kawamiya, M.: MIROC-ESM 2010: model description and basic results of CMIP5-20c3m experiments, Geosci. Model Dev., 4, 845-872, 2011.

Wigley, T. M. L.: A combined mitigation/geoengineering approach to climate stabilization, Science, 314(5798), 452-454, 2006.

Wing, A. A., Emanuel, K. and Solomon, S.: On the factors affecting trends and variability in tropical cyclone potential intensity, Geophys. Res. Lett., 42, 8669–8677, doi:10.1002/2015GL066145, 2015.

Wu, G., and Lau, N.-C.: A GCM simulation of the relationship between tropical-storm formation and ENSO, Mon.Wea.Rev.,120,958-977, 1992.

Yu, X., Moore, J. C., Cui, X., Rinke, A., Ji, D., Kravitz, B., Yoon, J.-H.: Impacts, effectiveness and regional inequalities of the GeoMIP G1 to G4 solar radiation management scenarios, Global Planet Change, 129, 10-22, 2015.

Zhi, L., Yu, W., Li, T., Murty, V.S. and Tangang F.: Bimodal Character of Cyclone Climatology in the Bay of Bengal Modulated by Monsoon Seasonal Cycle, J. Climate, 26, 1033–1046, 2013.

~~**Tables and**~~

Figures and tables

Table 1. Climate models used in this study

~~Model~~	~~Reference~~	~~Resolution (Lon×Lat)~~	~~ensemble members~~
~~BNU-ESM~~	~~Ji et al. (2014)~~	~~128×64~~	~~1~~
~~CanESM2~~	~~Chylek et al. (2011)~~	~~128×64~~	~~3~~
~~HadGEM2-ES~~	~~Collins et al.(2011)~~	~~192×144~~	~~3~~
~~MIROC-ESM~~	~~Watanabe et al. (2011)~~	~~128×64~~	~~1~~
~~MIROC-ESM-CHEM~~	~~Watanabe et al. (2011)~~	~~128×64~~	~~9~~
~~NorESM1-M~~	~~Bentsen et al. (2013)~~	~~144×96~~	~~1~~

Model	Reference	Resolution (Lon×Lat)	ensemble members
BNU-ESM	Ji et al. (2014)	128×64	1
HadGEM2-ES	Collins et al.(2011)	192×144	3
MIROC-ESM	Watanabe et al. (2011)	128×64	1
MIROC-ESM-CHEM	Watanabe et al. (2011)	128×64	9
NorESM1-M	Bentsen et al. (2013)	144×96	1

Table 2. Definitions of ~~Regions~~regions and numbers of observed TC

Region	*Latitudes*	*Longitudes*	*Annual Mean Numbers and percentages (1980-2008)*
North Atlantic (NA)	6-18°N	20-60°W	12 (15%)
Eastern North Pacific (ENP)	5-16°N	90-170°W	15 (19%)
Western North Pacific (WNP)	5-20°N	110-150°E	25 (32%)
North Indian (NI)	5-20°N	50-110°E	4 (5%)
South Indian (SI)	5-20°S	50-100°E	23 (29%)
South Pacific (SP)	5-20°S	160E-130°W	

Table 3. Differences (G4-RCP4.5) in TC basins and season during ~~2040~~2020-2069 year calculated point-by-point. Northern Hemisphere numbers are above and Southern Hemisphere below. GPI and VI are expressed as percentages (G4-RCP4.5)/RCP4.5. Bold fonts are significant at 95% level~~. The ensemble means are not normalized~~ according to the Wilcoxon signed-rank test.

Models	*Ts* (°C)	*To* (°C)	*Ts-To* (°C)	GPI (%)	V_{pot} (ms^{-1})	*H* (%)	V_{shear} (ms^{-1})	η ($\times 10^{-8}$ s^{-1})	VI ~~(×10³)~~ (%)	χm (×~~10³~~10^{-3})
BNU-ESM	**-0.5150** **-0.4342**	**0.023** **-12** 0.04411	**-0.5362** **-0.3853**	**-3.8** 0.62 0.05737	**-0.59** **-45** 0.040070	-0.26071 0.7320	0.012 014 **-0.07627**	-0.63 -1.2 0.83	20 7.2.2 -1.5	17 1916 15
MIROC-ESM	**-0.3234** **-0.2430**	**-0.5258** **-0.5256**	**0.2024** **0.2826**	-6.7 -0.50 0.002786	**-1.0.94** **-0.2850**	**-0.28** 36 -0.1219	0.28 -13 0.1613	1.3 -0.322.3	15 1.62.5 2.3	-4.9 3.7 6.8.6
MIROC-ESM-CHEM	**-0.2925** **-0.2421**	**-0.5045** **-0.4843**	**0.2721** **0.2922**	-2.6 0.194.8 -11	**6.629** **6.345**	**4.68** **3.56**	**1.98** **2.32**	-0.56054 -0.76027	8.7 -5.81.9 1.3	-11 1.27.9 3.6
NorESM1-MCanESM2	**-0.5023** **-0.4621**	**-0.13087** -0.086071	**-0.3715** **-0.3714**	4.8 -0.017 -0.04473	**-0.8652** **-0.4462**	**-0.1751** -0.2110	-0.045 029 -0.02612	-3.4 -0.08 -5.383	13 **-2.70** 2.5	19 -4.98 3.3
HadGEM2-ESNorESM1-M	**-0.2765** **-0.2461**	**-0.13** **-16** **0.1415**	**-0.1580** **-0.09576**	-2.7 3.1.9 0.39	**-1.0** **-0.6571**	-0.2417 -0.52088	0.33 041 -0.085079	-3.7 **-1.9** 1.0	19 -213.8 1.1	2.8 -9.835 30
HadGEM2-ESEnsemble	**-0.7540** **-0.7035**	**-0.14** **-0.13** 0.075	**-0.8826** **-0.7323**	-0.30 0.0532.7 -2.5	-1.2 **-0.6680** **0.95**	**0.43** -80 **0.01868**	**0.083** -40 **0.02837**	5.8 1-0.2 -0.7	23 3.41.9 1.0	52 377.0 11.8
~~Ensemble~~	~~-0.44~~ ~~-0.38~~	~~-0.17~~ ~~-0.20~~	~~-0.24~~ ~~-0.17~~	~~-1.1~~ ~~0.38~~	~~0.33~~ ~~0.71~~	~~0.73~~ ~~0.60~~	~~0.43~~ ~~0.38~~	~~0.44~~ ~~-0.98~~	~~16~~ ~~-3.0~~	~~12~~ ~~10~~

Table 4. Mean TC frequency Across basin differences in Northern Hemisphere basins fromGPI –and VI calculated as (G4-RCP4.5)/RCP4.5 as percentages for averaged over the 3-member ensemble of periodHadGEM2-ES using TRACK (4.5, 3.5, 4) during August, September, October 2020-2069. GPI are written above VI in each cell. Bold

Models	WNP	ENP	NA	NI	SI	SP	all
BNU-ESMRegion	Mean G42.8	Mean RCP4. -4.0	St.Dev RCP4.5 **-3.7**	**-8.7**	0.9	2.1	**-3.3**
	3.0	5.6	3.0	1.9	-0.7	-1.7	0.7
WNPMIROC-ESM	-4.2	**-5.06**	**-8.4**	**-4.6**	2.02	8.5	**-6.1**
	8.1	2.4	1.9	1.9	**2.2**	0.1.8	**2.3**
MIROC-ESM-CHEM ENP	3.-**4.1**	11.-**7.7**	**-10.2**	**-12.2**	**-14.0**	-3.0	**-8.6**
	-1.7	-0.9	**3.9**	**8.0**	**1.2**	0.3	**2.0**
NANorESM1-M	0.4	**137.0**	**9.1**	**11.2**	-0.83	3.1	0.9
	-1.27	**-8.1**	-1.3	**6.0**	**4.7**	1.3	-0.8
HadGEM2-ES	3.2	**-6.8**	**-5.2**	**-4.2**	-0.7	2.1	**-2.3**
	4.0	**6.0**	0.9	**7.1**	**2.5**	0.1	**3.0**
Ensemble**NI**	-0.4	3.3	**-3.7**	**-3.7**	-2.4	2.6	**-3.9**
	2.3.5	1.0	**1.7**	**5.0**	**2.0**	0.5	**1.5**

indicates regions with significantly more TC under G4 than RCP4.5means the difference is significant at the 955% level according to the Wilcoxon signed-rank test.

Models	WNP	ENP	NA	NI	SI	SP	all
BNU-ESM	2.8	-4.0	**-3.7**	**-8.7**	0.9	2.1	**-3.3**
	3.0	5.6	3.0	1.9	-0.7	-1.7	0.7
MIROC-ESM	-4.2	**-5.6**	**-8.4**	**-4.6**	2.2	8.5	**-6.1**
	8.1	2.4	1.9	1.9	**2.2**	0.1	**2.3**
MIROC-ESM-CHEM	**-4.1**	**-7.7**	**-10.2**	**-12.2**	**-14.0**	-3.0	**-8.6**
	-1.7	-0.9	**3.9**	**8.0**	**1.2**	0.3	**2.0**
NorESM1-M	0.4	**37.0**	**9.1**	**11.2**	-0.3	3.1	0.9
	-1.7	**-8.1**	-1.3	**6.0**	**4.7**	1.3	-0.8
HadGEM2-ES	3.2	**-6.8**	**-5.2**	**-4.2**	-0.7	2.1	**-2.3**
	4.0	**6.0**	0.9	**7.1**	**2.5**	0.1	**3.0**
Ensemble	-0.4	3.3	**-3.7**	**-3.7**	-2.4	2.6	**-3.9**
	2.3	1.0	**1.7**	**5.0**	**2.0**	0.5	**1.5**

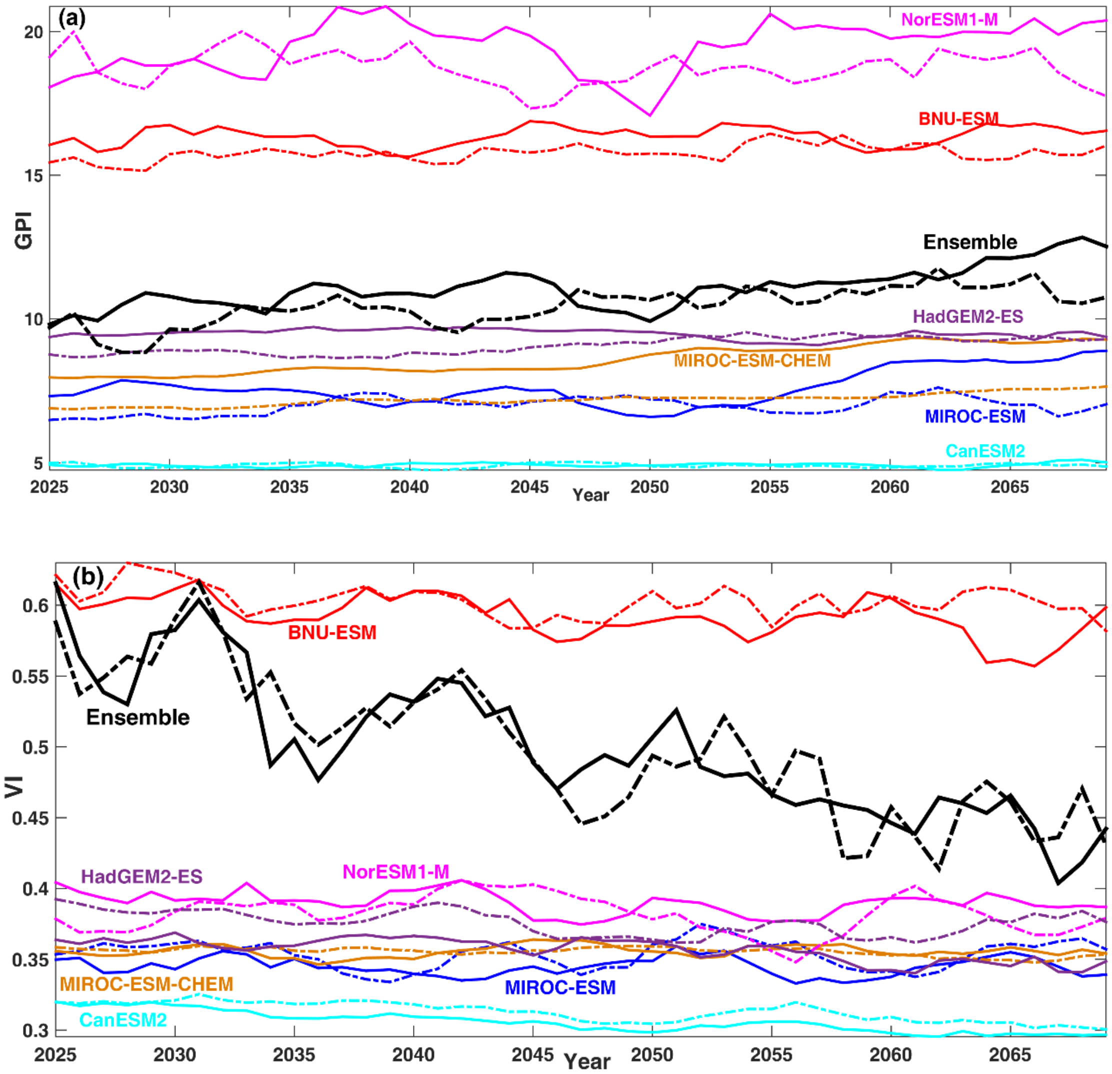
(a)
NorESM1-M
BNU-ESM
GPI
Ensemble
HadGEM2-ES
MIROC-ESM-CHEM
MIROC-ESM
CanESM2
Year
(b)
BNU-ESM
Ensemble
VI
HadGEM2-ES
NorESM1-M
MIROC-ESM-CHEM
MIROC-ESM
CanESM2
Year

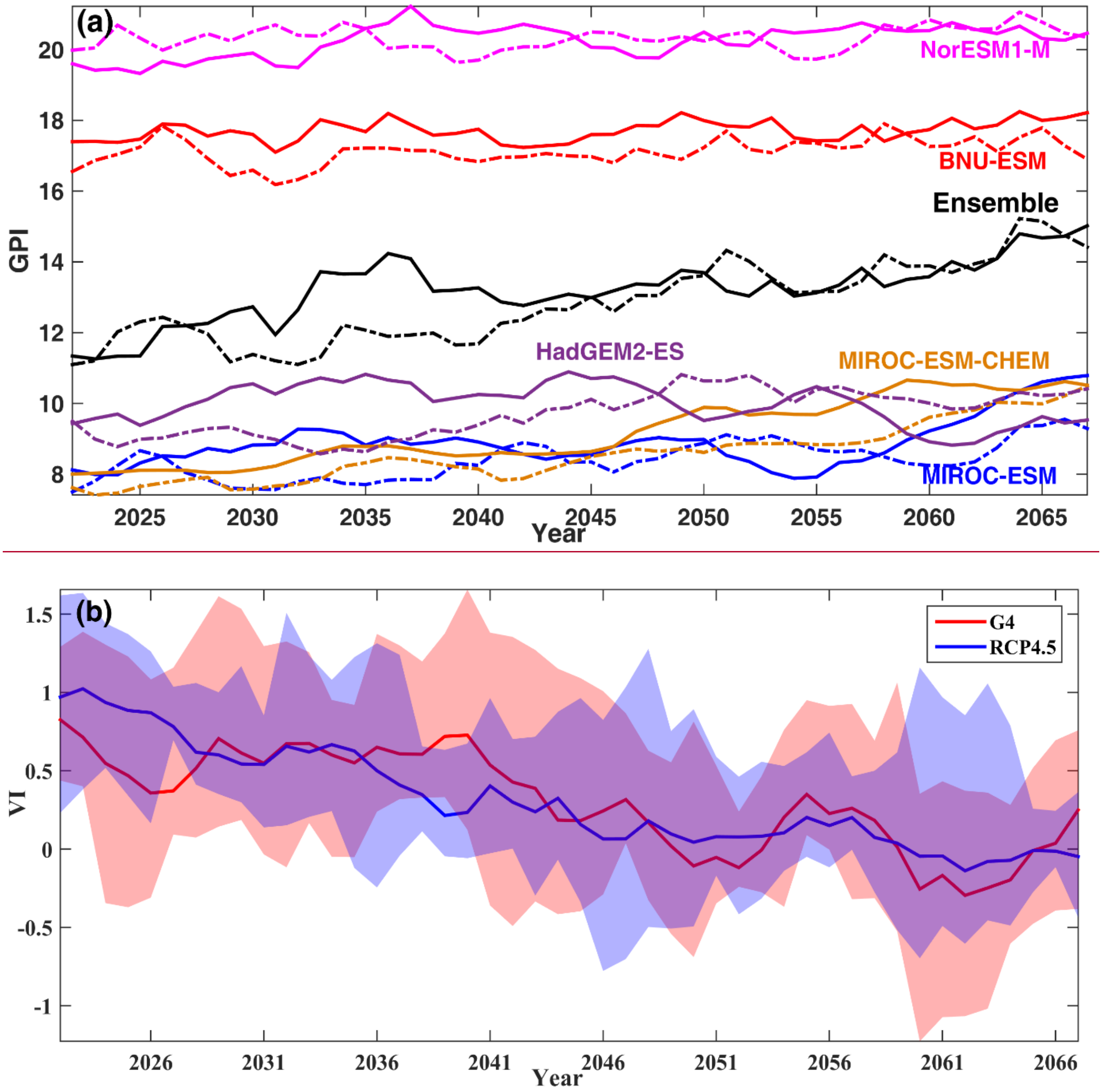

Figure 1. Five yearly moving annual averages~~, of (a) GPI index and (b) ventilation index in~~ across the 6 TC ~~season~~basins and TC ~~basin. Solid~~season, of (a) normalized GPI shifted by the each model's mean over 2020-2069, solid lines denote forcing under RCP4.5 and dotted lines values under G4. The ~~Ensemble mean series were calculate using normalized time series, shifted by the~~ ensemble was calculated as the mean of normalized models then offset by the mean across-model GPI. (b) VI with solid lines denoting model ensemble means and shading indicating the range across the five models.

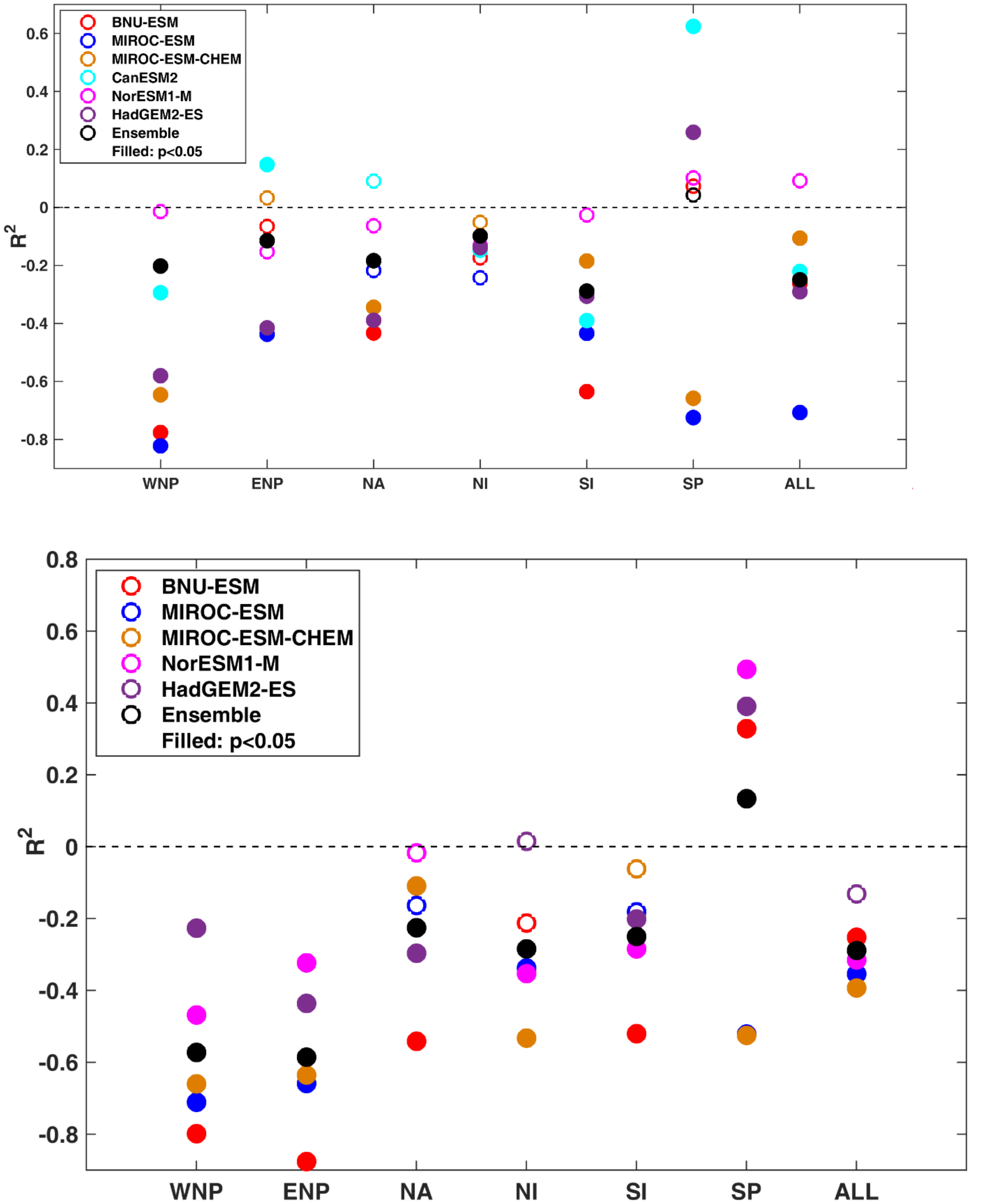

Figure 2. The correlation coefficients (R^2) between annual GPI and VI anomalies (G4-RCP4.5) during TC season and six ocean TC basins. The MIROC-ESM-CHEM model has ~~9~~4 ensemble members, the ~~CanESM2~~HadGEM2-ES model has 3 ensemble members, and other models have one member. Each model is weighted equally and normalized for the ensemble regardless of the number of separate realizations. Dashed line represent R^2=0.

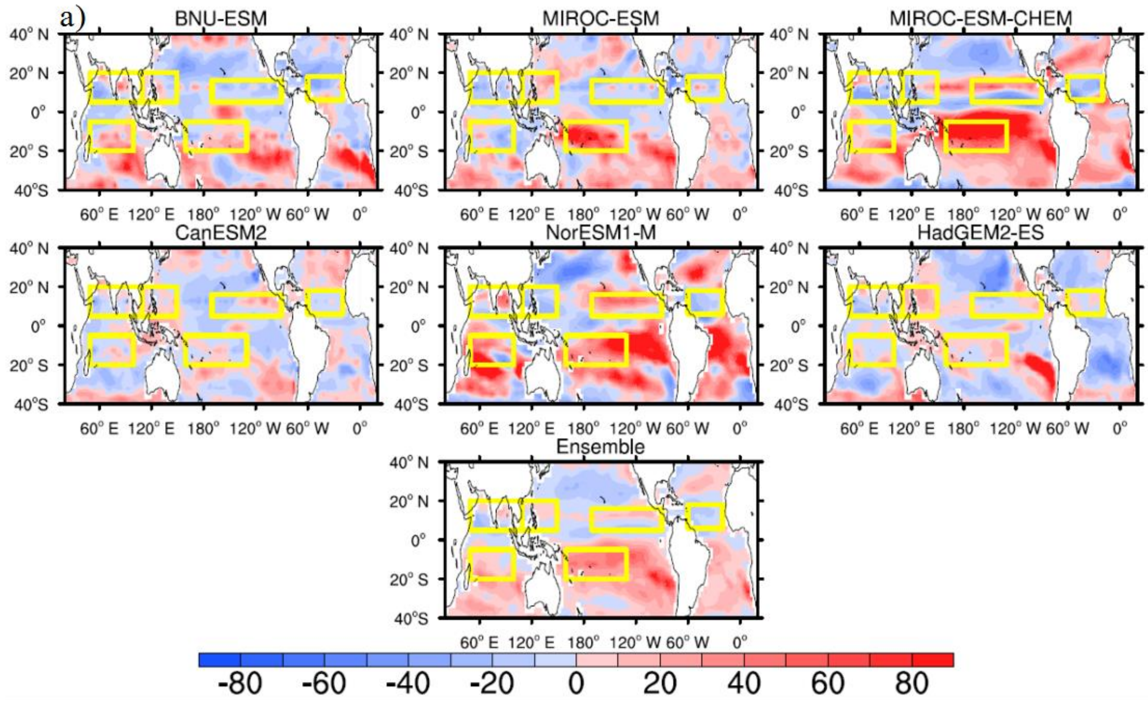
a)
BNU-ESM
MIROC-ESM
MIROC-ESM-CHEM
CanESM2
NorESM1-M
HadGEM2-ES
Ensemble
40° N
20° N
0°
20° S
40°S
60° E 120° E 180° 120° W 60° W 0°
-80 -60 -40 -20 0 20 40 60 80

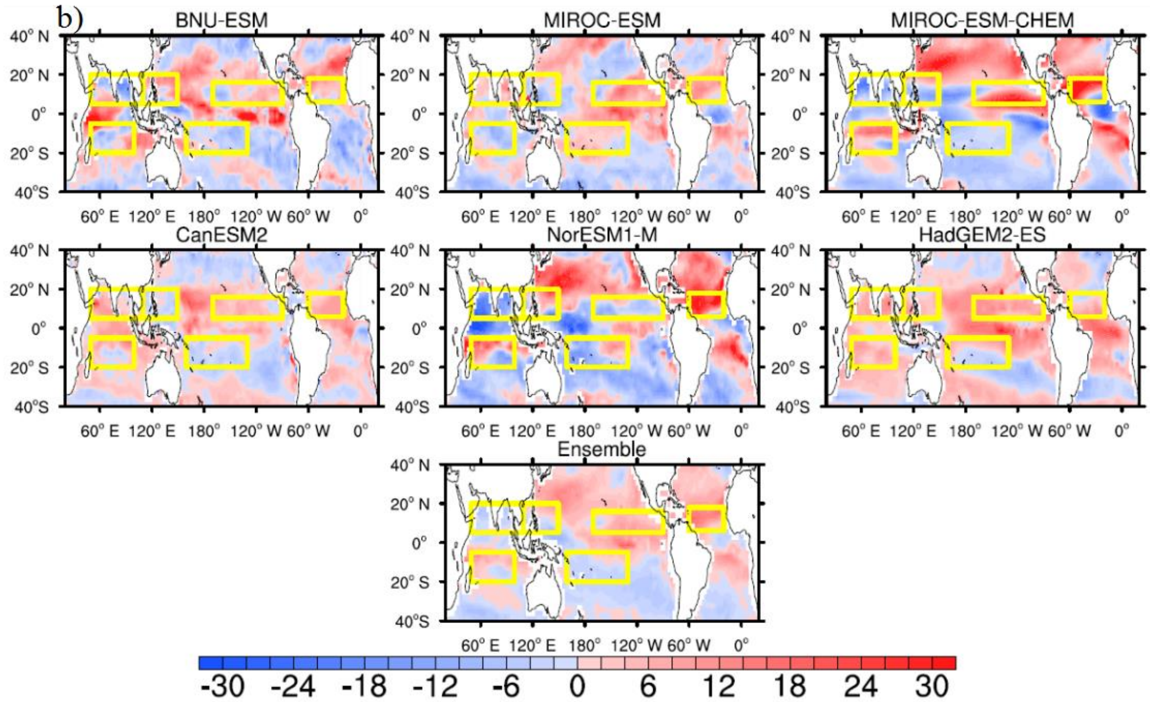
b)
BNU-ESM
MIROC-ESM
MIROC-ESM-CHEM
CanESM2
NorESM1-M
HadGEM2-ES
Ensemble
40° N
20° N
0°
20° S
40°S
60° E 120° E 180° 120° W 60° W 0°
-30 -24 -18 -12 -6 0 6 12 18 24 30

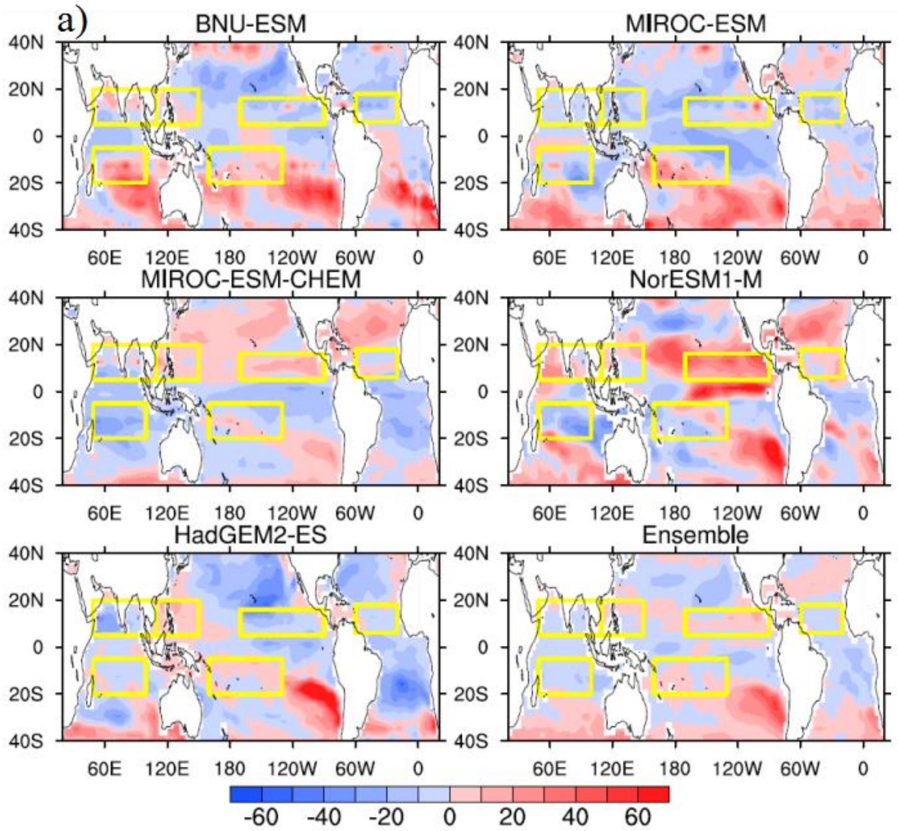
a)
BNU-ESM
MIROC-ESM
MIROC-ESM-CHEM
NorESM1-M
HadGEM2-ES
Ensemble
40N
20N
0
20S
40S
60E
120E
180
120W
60W
0
-60
-40
-20
0
20
40
60

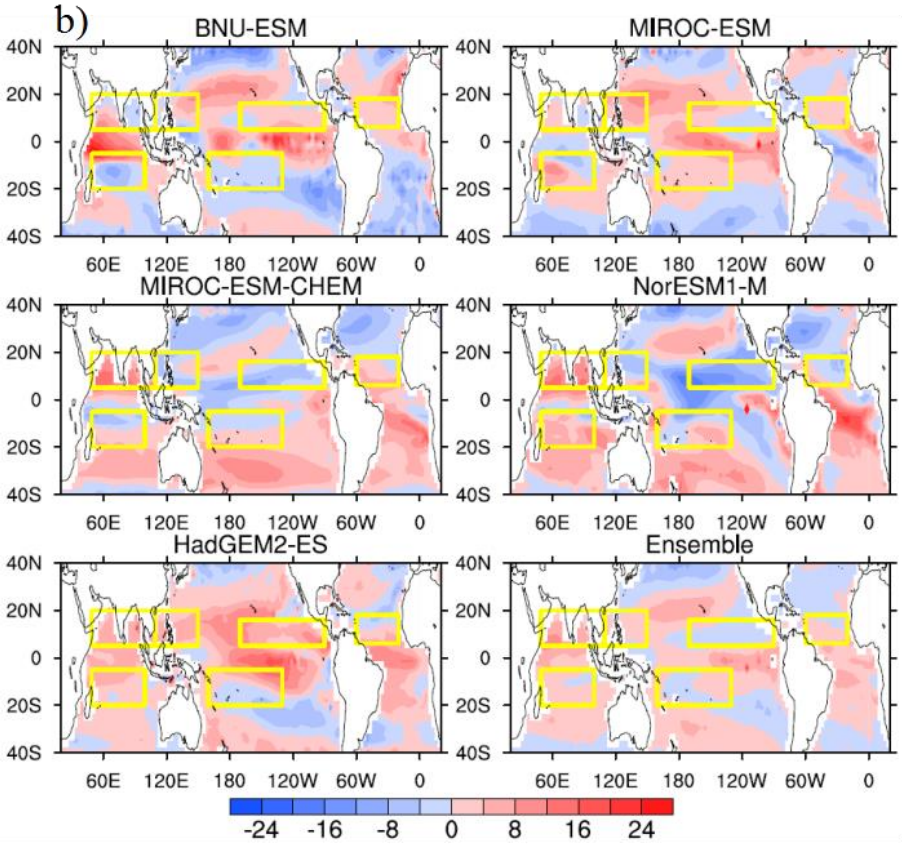

Figure 3. Spatial distribution at each grid point during the appropriate TC season between ~~2040~~2020-2069 of the anomaly (GPI_{G4}-$GPI_{RCP4.5}$)/$GPI_{RCP4.5}$ as a percentage, for a) GPI and b) VI. Yellow rectangles delimit the six TC ocean basins. The Northern Hemisphere ~~peak~~ TC season is defined ~~to be August~~as June through ~~October~~November, and the Southern Hemisphere season is defined to be January through ~~March.~~ June.

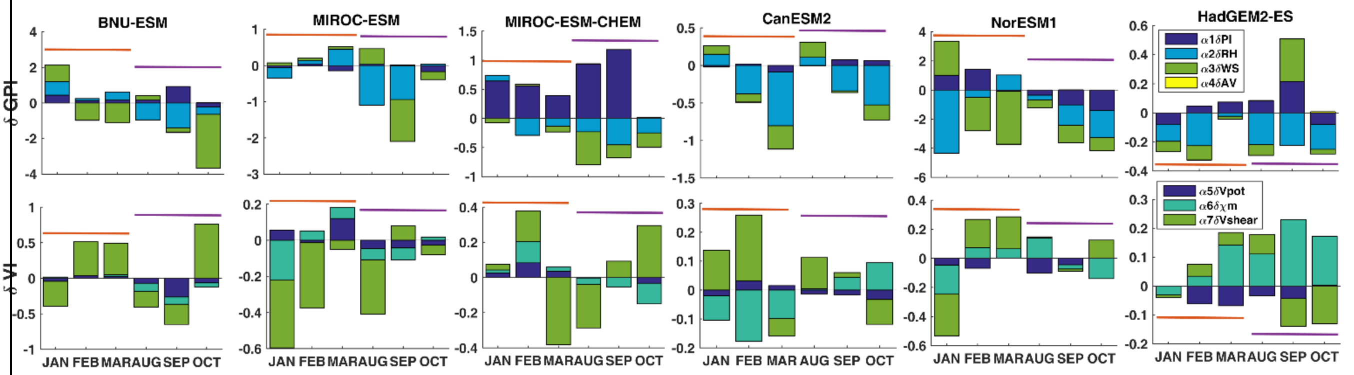

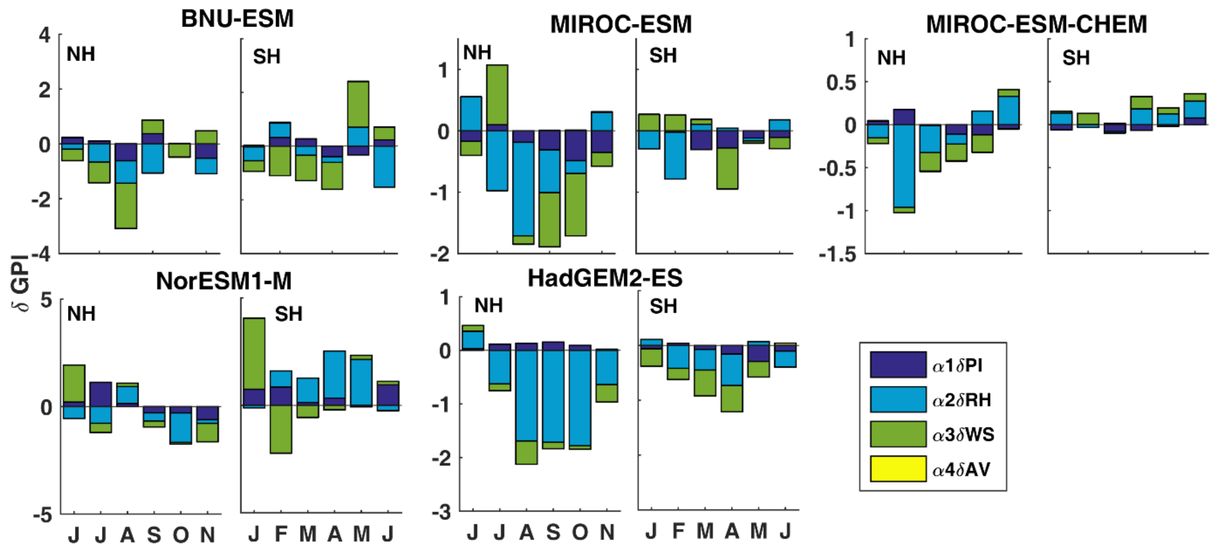

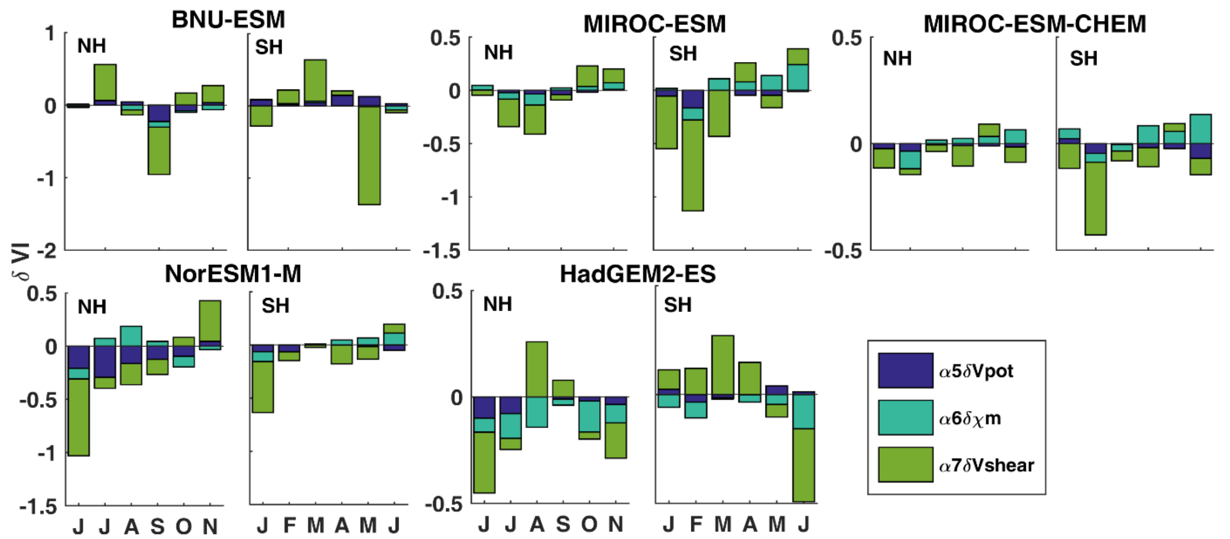

Figure 4 The mean month contribution of each variable to the difference (G4-RCP4.5) for the years ~~2040~~2020-2069 in TC basins and TC season in GPI and VI~~. Brown lines represent Southern Hemisphere and purple lines represent Northern Hemisphere TC seasons~~.

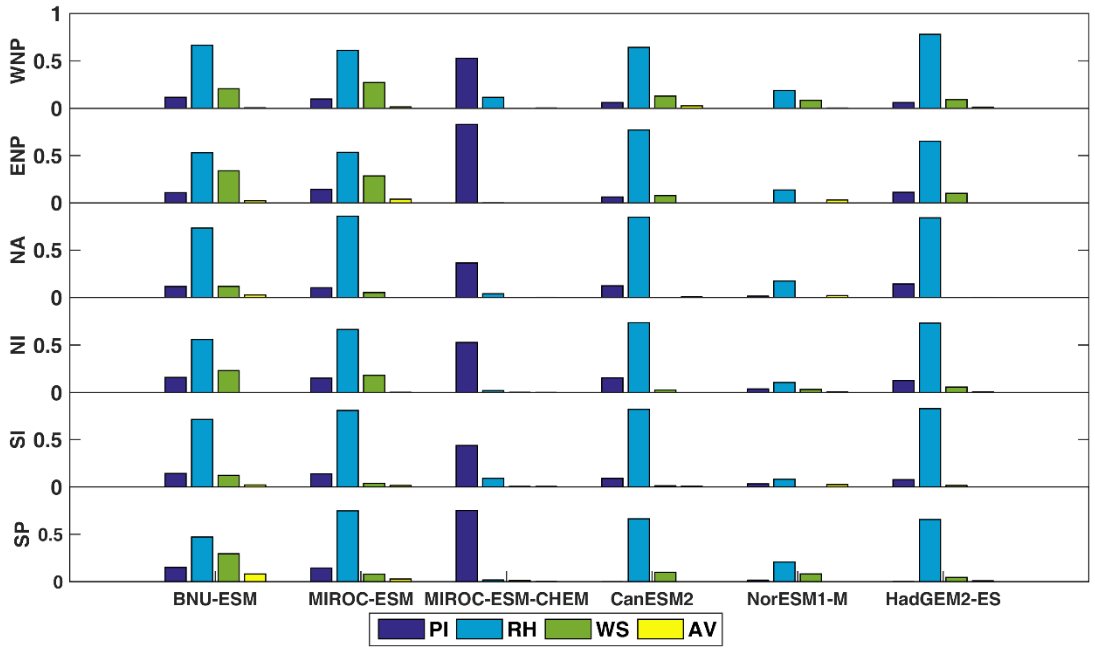

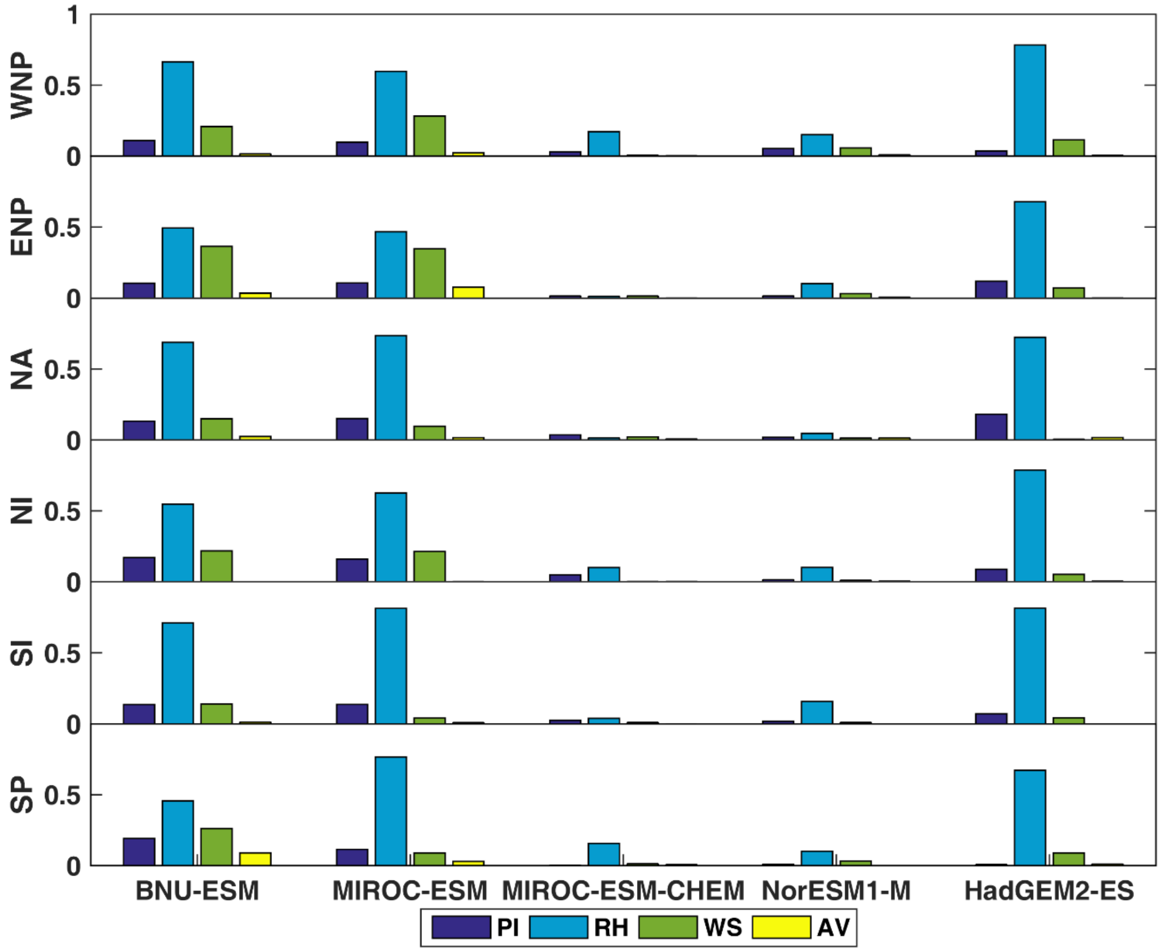

Figure 5. The fractional variance contribution of components of GPI during the TC season and within the six TC basins during ~~2040~~2020-2069.

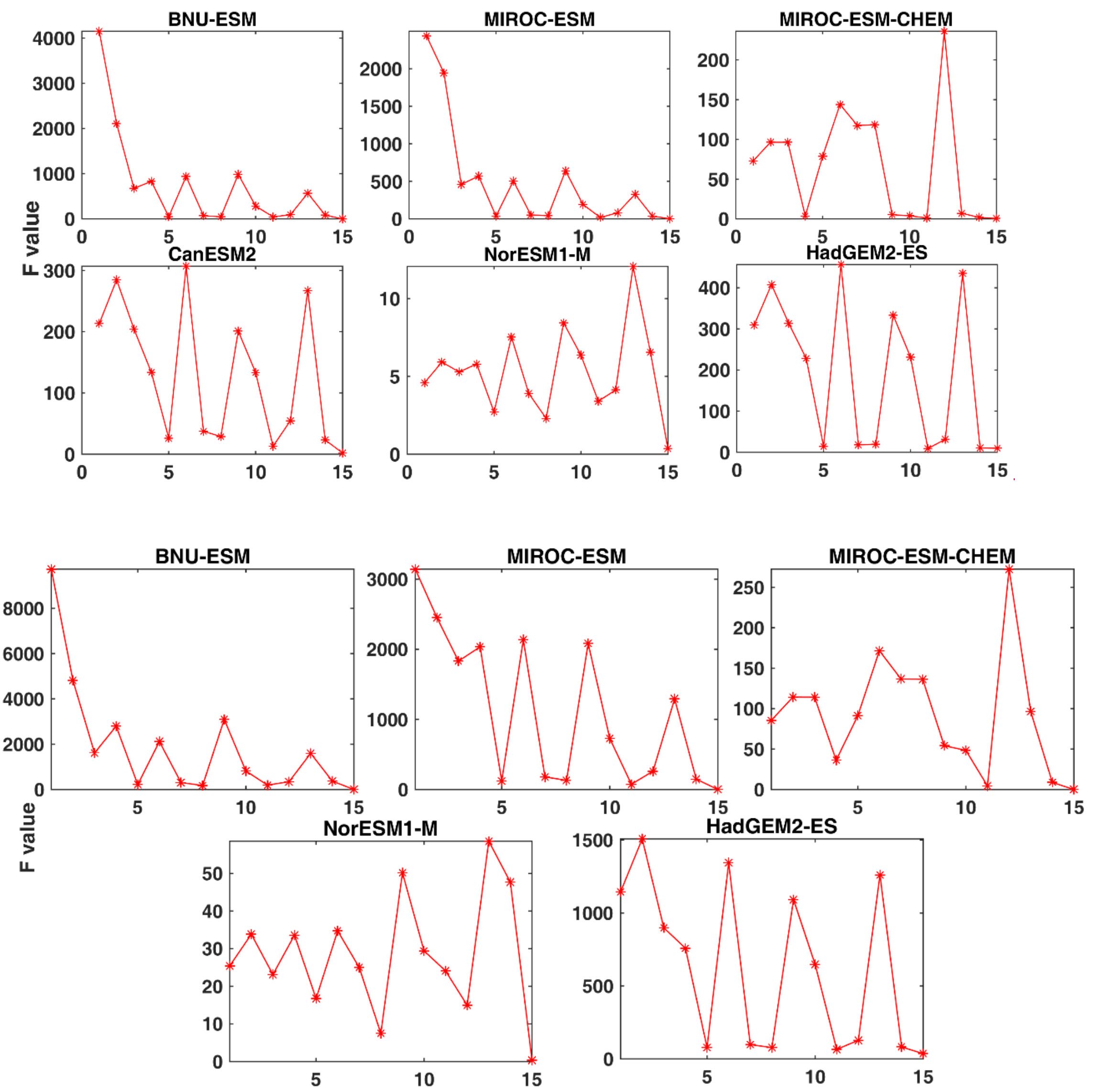

Figure 6. The F-statistic of the 15 different combinations of regression variables for GPI differences between G4 and RCP4.5. The x-axis on each panel represents the combination of components used as predictors in each regression equation: 1:*(PI,RH,WS,AV)*, 2:*(PI,RH,WS)*, 3:*(PI,RH,AV)*, 4:*(AV,RH,WS)*, 5:*(PI,AV,WS)*, 6:*(PI,RH)*, 7:*(PI,WS)*, 8:*(PI,AV)*, 9:*(RH,WS)*, 10:*(RH,AV)*, 11:*(AV,WS)*, 12:*(PI)*, 13:*(RH)*, 14:*(WS)*, 15:*(AV)*.

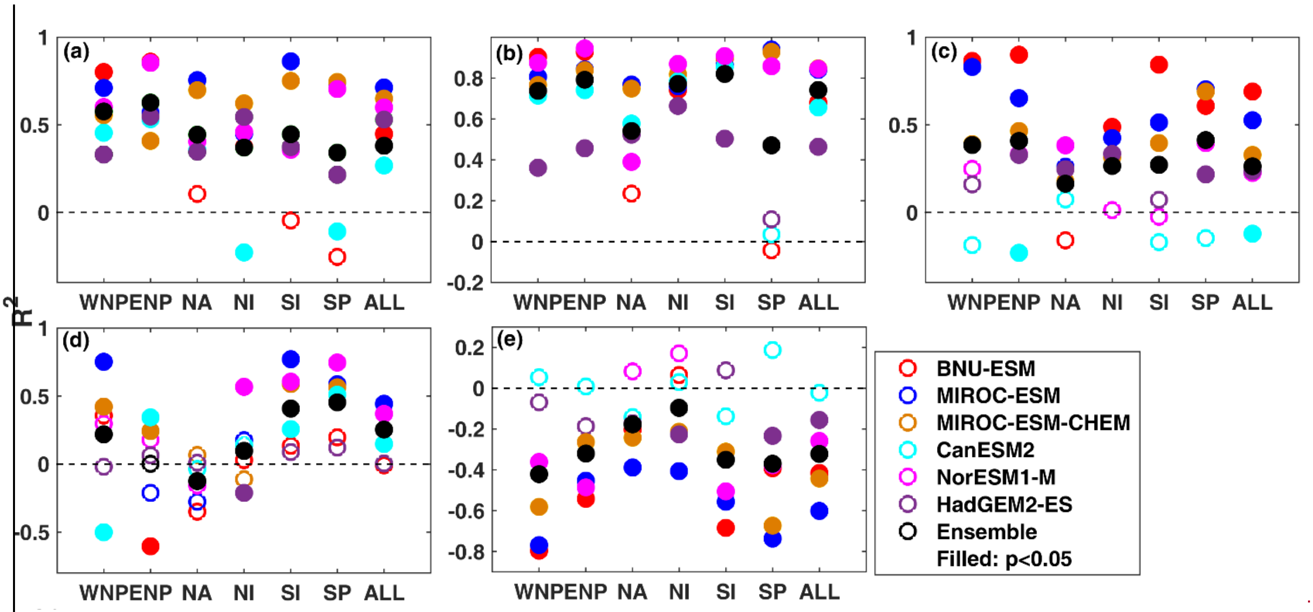

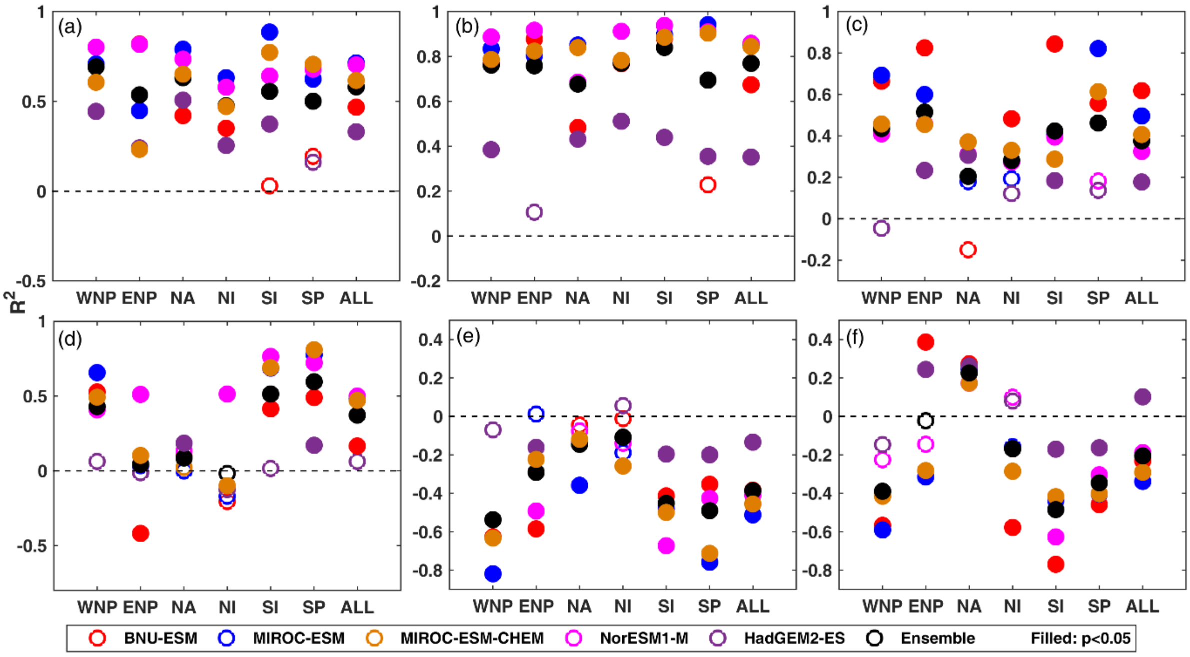

Figure 7. The correlations (R^2) between differences (G4-RCP4.5) during TC season and across the six TC basins for the years ~~2040~~2020-2069 for (a) ~~V_{pot}~~ V_{pot} anomalies as a function static stability ~~$T_S - T_O$~~ T_s-T_o. Panels b-e show R^2 coefficients for anomalies with sea surface temperature differences (T_s) and: (b) ~~V_{pot},~~ V_{pot}, (c) GPI , (d) relative humidity, (e) vertical wind shear. Each model is weighted equally in the ensembles regardless of number of observations.

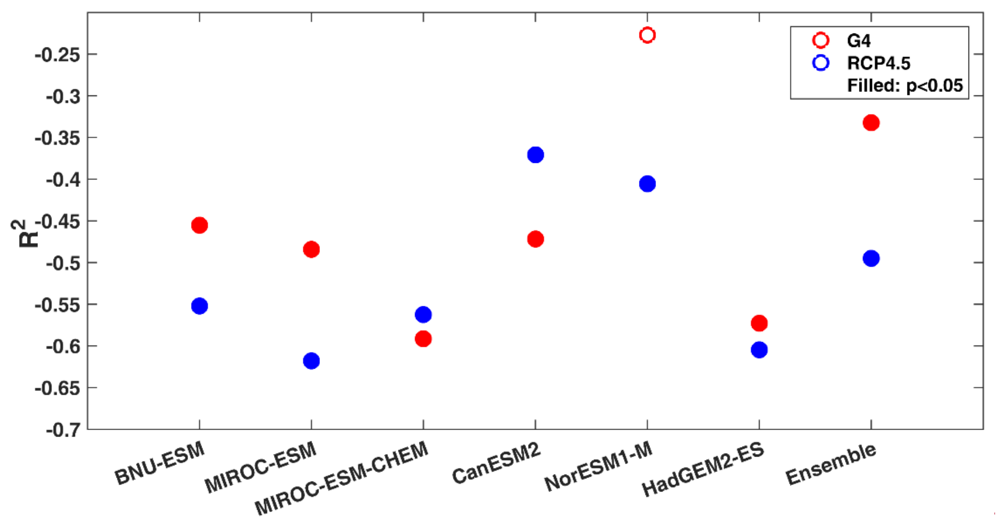

Figure 8. The model correlation coefficients between annual Niño3.4 index and SOI during TC season for 2040-2069.

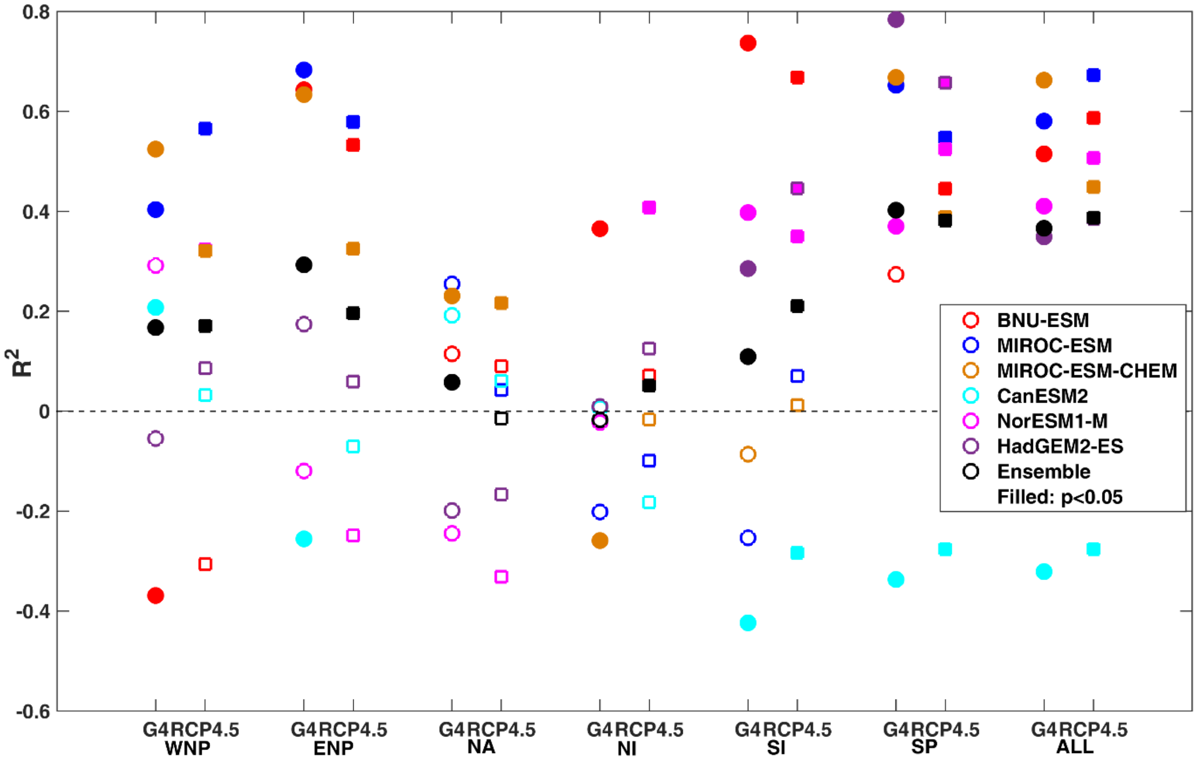

Figure 9. The correlation of GPI as a function of (Niño3.4-SOI)/2 during TC season and six TC basins and all TC basins for the G4 and RCP4.5 experiments.

Supplementary Material

Table S1: see Excel spreadsheet "gpi_basin_month.xls", where data can be found by model, month, basin and experiment. Sheet "GPI" contains the GPI results for RCP4.5, G4, the t-test and Wilcoxon signed-rank test results for their difference over the years 2020-2069. Sheet "VI" contains the VI analogous results.

Table S2 Monthly GPI and VI as a fraction of the annual totals. Note that in the TC season VI is relatively low. The TC seasons defined by 10% anomaly in GPI months are highlighted in yellow.

GPI	NH		SH		Anomalies	
Month	RCP4.5	G4	RCP4.5	G4	NH mean	SH mean
1	0.07	0.05	0.08	0.10	0.69	1.10
2	0.04	0.03	0.10	0.11	0.40	1.25
3	0.03	0.03	0.12	0.12	0.32	1.43
4	0.04	0.05	0.13	0.14	0.52	1.59
5	0.07	0.09	0.13	0.13	0.92	1.52
6	0.10	0.11	0.11	0.08	1.27	1.16
7	0.11	0.12	0.07	0.06	1.38	0.77
8	0.11	0.11	0.05	0.04	1.35	0.52
9	0.11	0.12	0.04	0.04	1.39	0.49
10	0.12	0.11	0.05	0.05	1.39	0.57
11	0.11	0.11	0.06	0.06	1.29	0.71
12	0.10	0.09	0.07	0.08	1.09	0.89

VI	NH		NH		Anomalies	
Month	RCP4.5	G4	RCP4.5	G4	NH mean	SH mean
1	0.09	0.10	0.07	0.06	1.17	0.78
2	0.11	0.11	0.06	0.06	1.32	0.60
3	0.11	0.11	0.05	0.05	1.34	0.63
4	0.10	0.10	0.05	0.06	1.20	0.67
5	0.09	0.08	0.07	0.07	0.99	0.81
6	0.07	0.07	0.09	0.09	0.85	1.04
7	0.07	0.08	0.10	0.10	0.92	1.21
8	0.08	0.08	0.11	0.11	0.96	1.33
9	0.08	0.07	0.11	0.12	0.89	1.37
10	0.06	0.06	0.11	0.11	0.71	1.32
11	0.06	0.06	0.10	0.09	0.73	1.15
12	0.07	0.08	0.08	0.08	0.92	0.93

Table S3: The fraction of total annual GPI and VI accounted for by the 6 month TC seasons chosen in each hemisphere across the 6 TC basins. Note that in the TC season VI is relatively low.

	GPI		VI	
Basin	RCP4.5	G4	RCP4.5	G4
WNP	0.62	0.64	0.43	0.43
ENP	0.70	0.71	0.35	0.33
NA	0.75	0.71	0.34	0.34
NI	0.58	0.60	0.60	0.61
SI	0.67	0.66	0.40	0.42
SP	0.74	0.76	0.38	0.38
mean	0.68	0.68	0.42	0.42

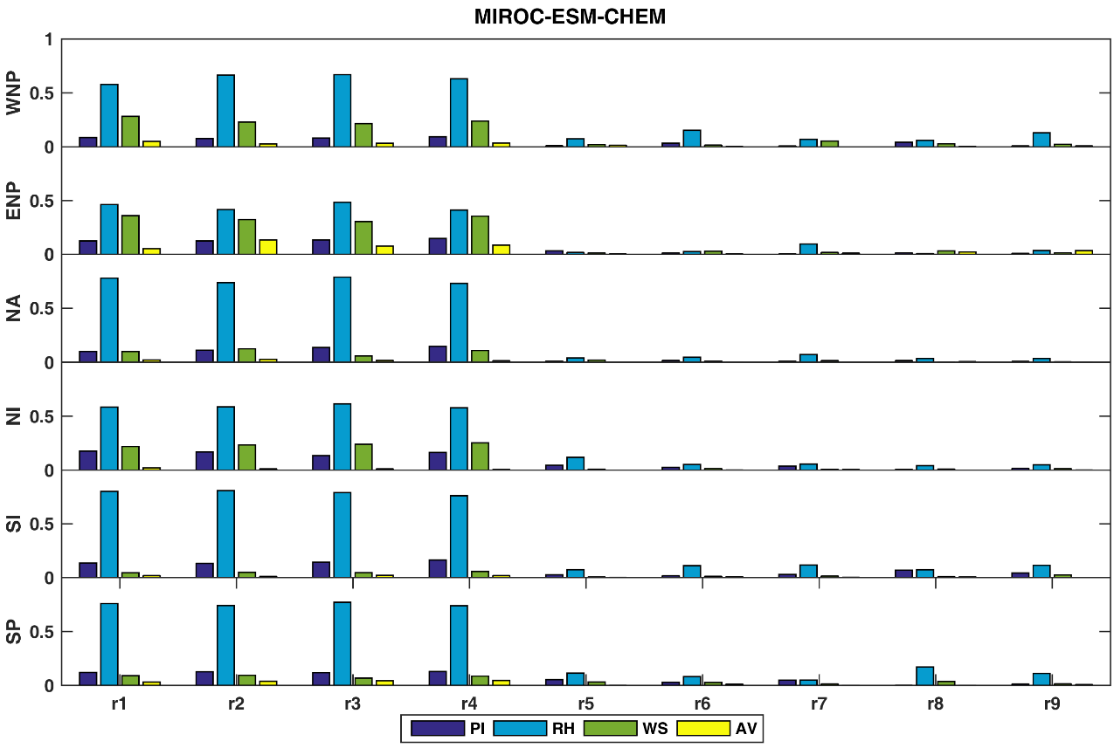

Figure S1. As Fig. 5 but for the 9 realizations of MIROC-ESM-CHEM: The fractional variance contribution of components of GPI during the TC season and within the six TC basins during 2020-2069.

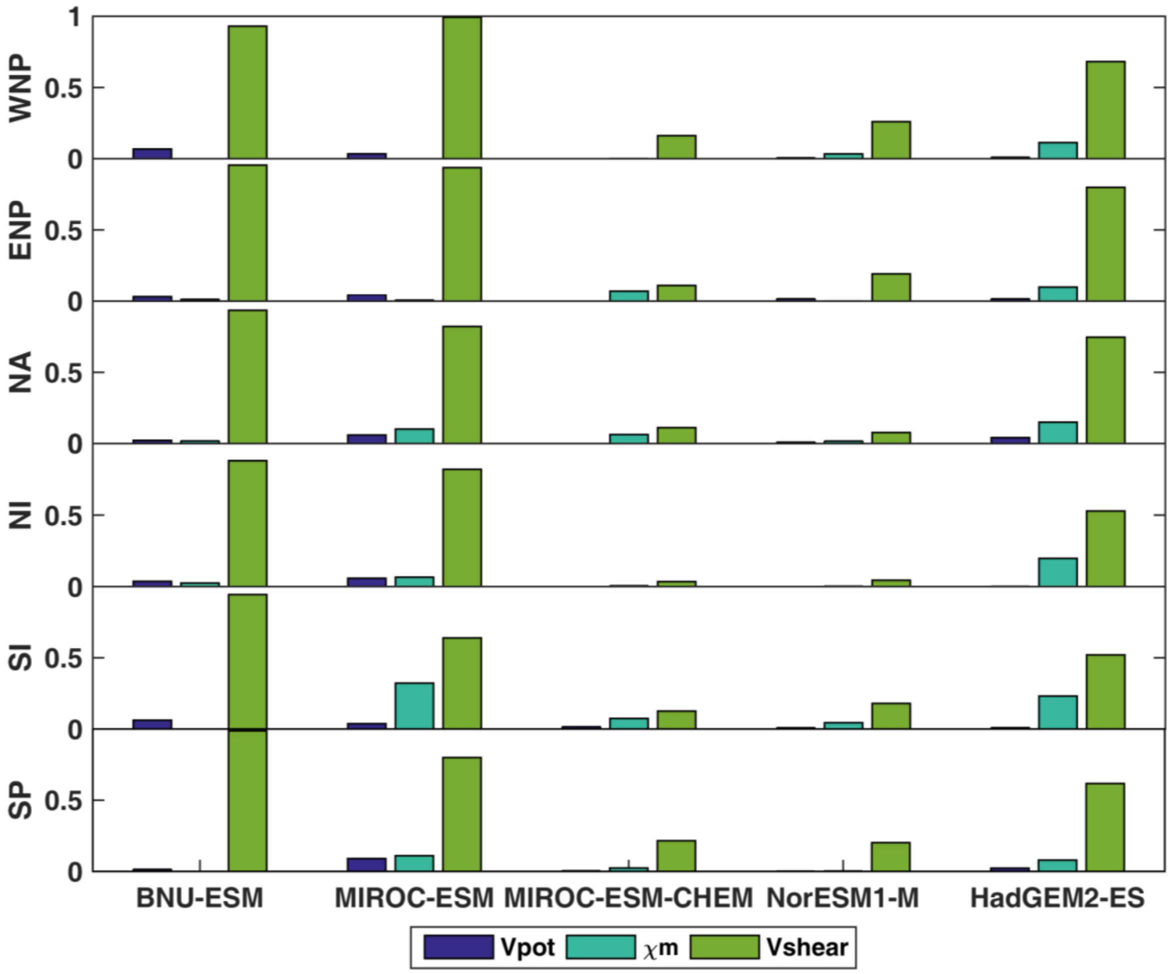

Figure S2. The fractional variance contribution of components of VI during the TC season and within the six TC basins during 2020-2069.

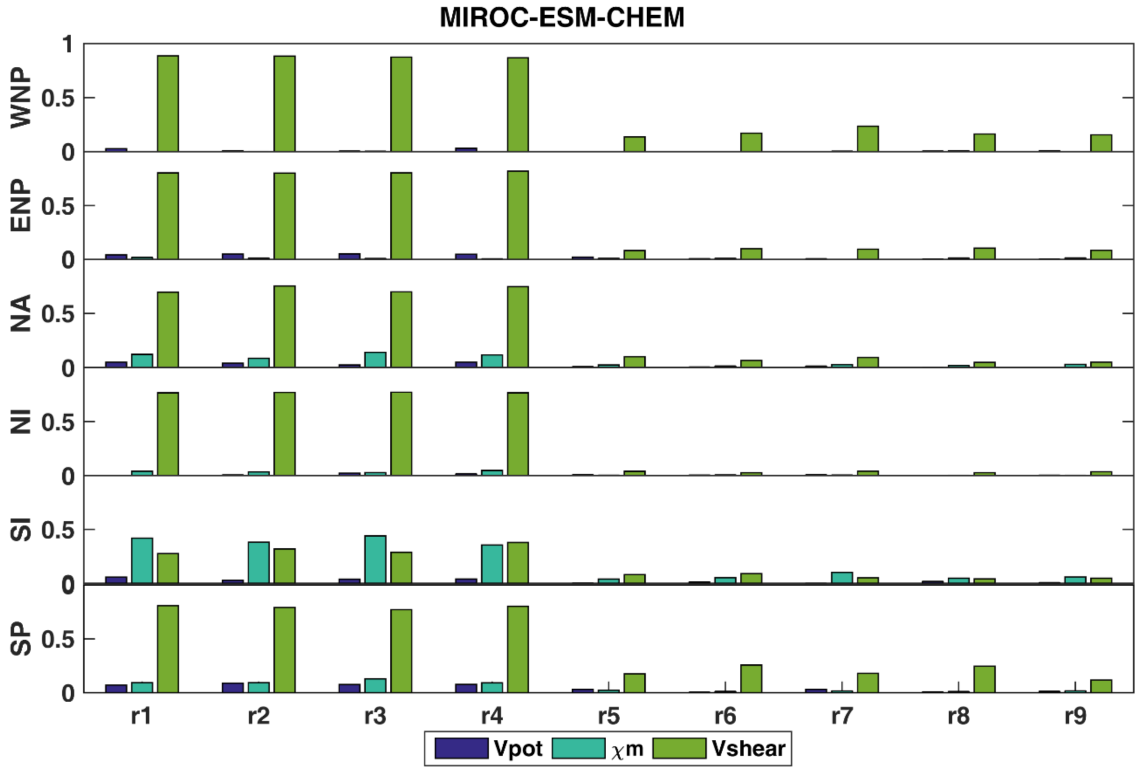

Figure S3. As S2 but for the 9 realizations of MIROC-ESM-CHEM: The fractional variance contribution of components of VI during the TC season and within the six TC basins during 2020-2069.

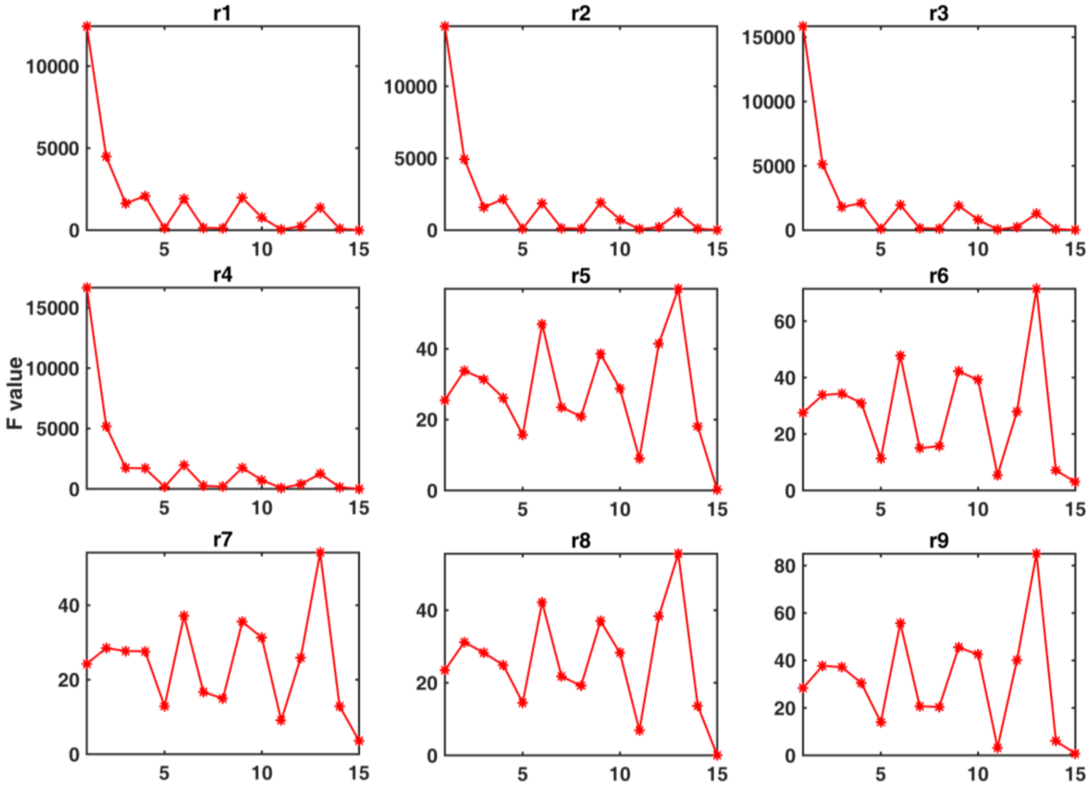

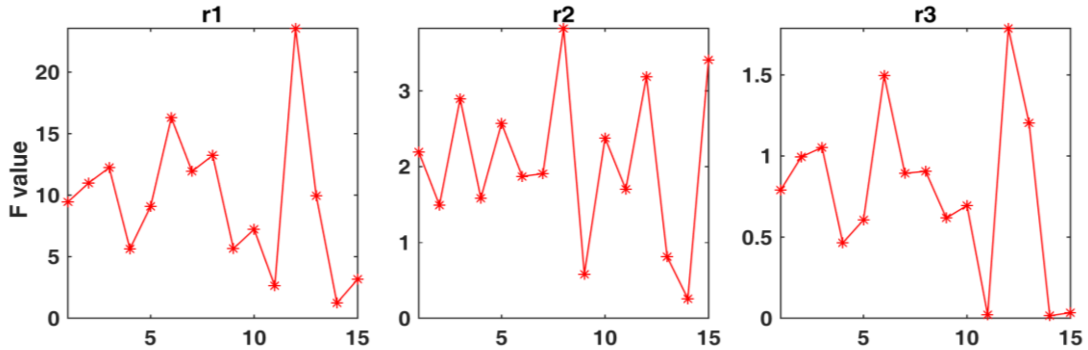

Fig. S4 As Fig6: The F-statistic of the 15 different combinations of regression variables for GPI differences between G4 and RCP4.5, but for each of realizations 1-9 of MIROC-ESM-CHEM, (top 3 rows), and for the 3 realizations of CanESM2 (bottom row). The x-axis on each panel represents the combination of components used as predictors in each regression equation: 1:*(PI,RH,WS,AV)*, 2:*(PI,RH,WS)*, 3:*(PI,RH,AV)*, 4:*(AV,RH,WS)*, 5:*(PI,AV,WS)*, 6:*(PI,RH)*, 7:*(PI,WS)*, 8:*(PI,AV)*, 9:*(RH,WS)*, 10:*(RH,AV)*, 11:*(AV,WS)*, 12:*(PI)*, 13:*(RH)*, 14:*(WS)*, 15:*(AV)*.

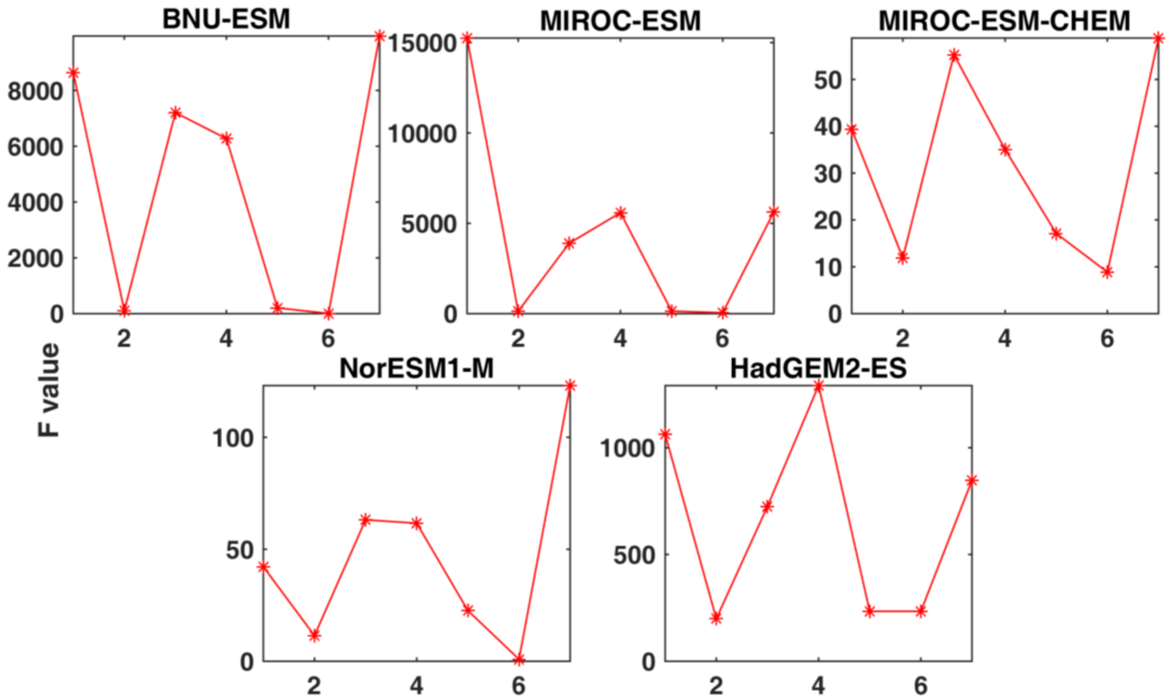

Figure S5. The F-statistic of the 7 different combinations of regression variables for VI differences between G4 and RCP4.5. The x-axis on each panel represents the combination of components used as predictors in each regression equation: 1:(V_{pot}, V_{shear}, χ_m), 2:(V_{pot}, V_{shear}), 3:(V_{pot}, χ_m), 4:(V_{shear}, χ_m), 5:(V_{pot}), 6:(χ_m), 7:(V_{shear}).

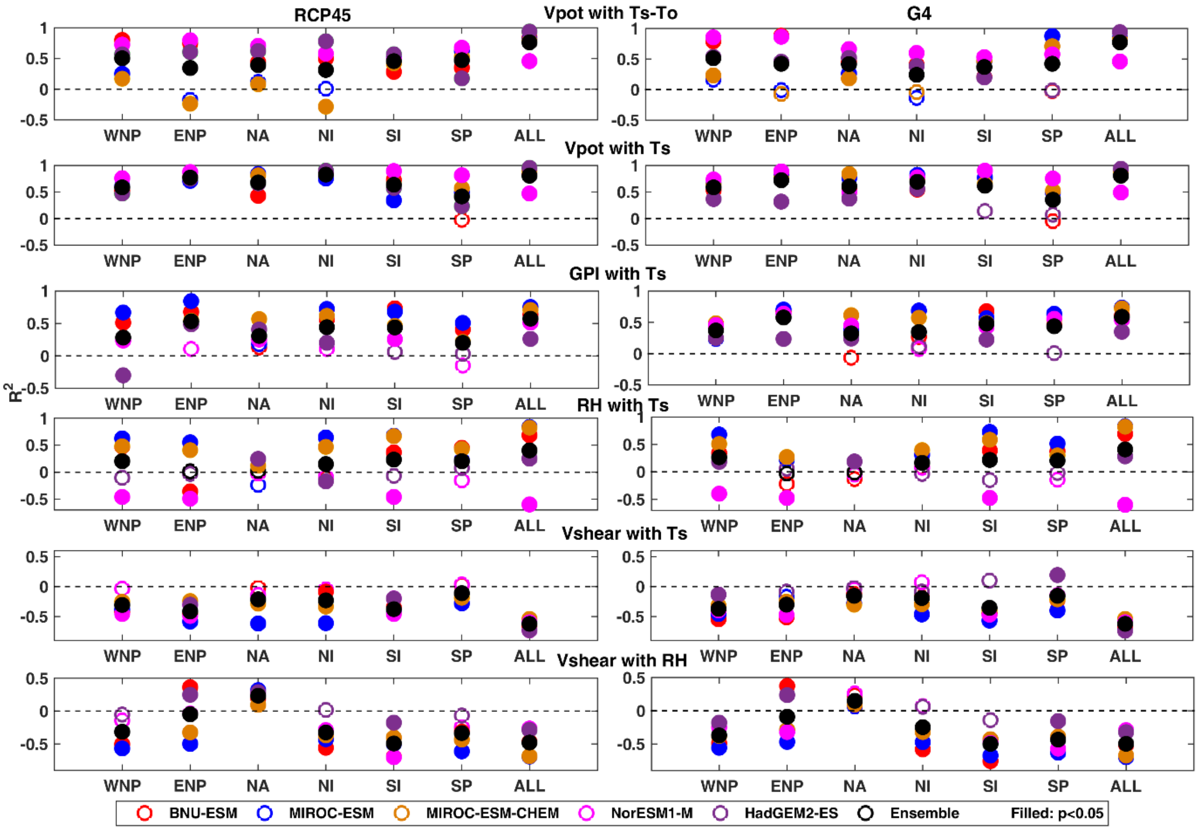

Figure S6. The correlations (R^2) between variable fields in RCP4.5 (left column), and G4 (right column) separately for comparison with Fig. 7. Top to bottom V_{pot} anomalies as a function static stability T_s-T_o; sea surface temperature differences (T_s) and: V_{pot} , GPI, relative humidity, and vertical wind shear. Data is during TC season and across the six TC basins for the years 2020-2069. Each model is weighted equally in the ensembles regardless of number of observations.

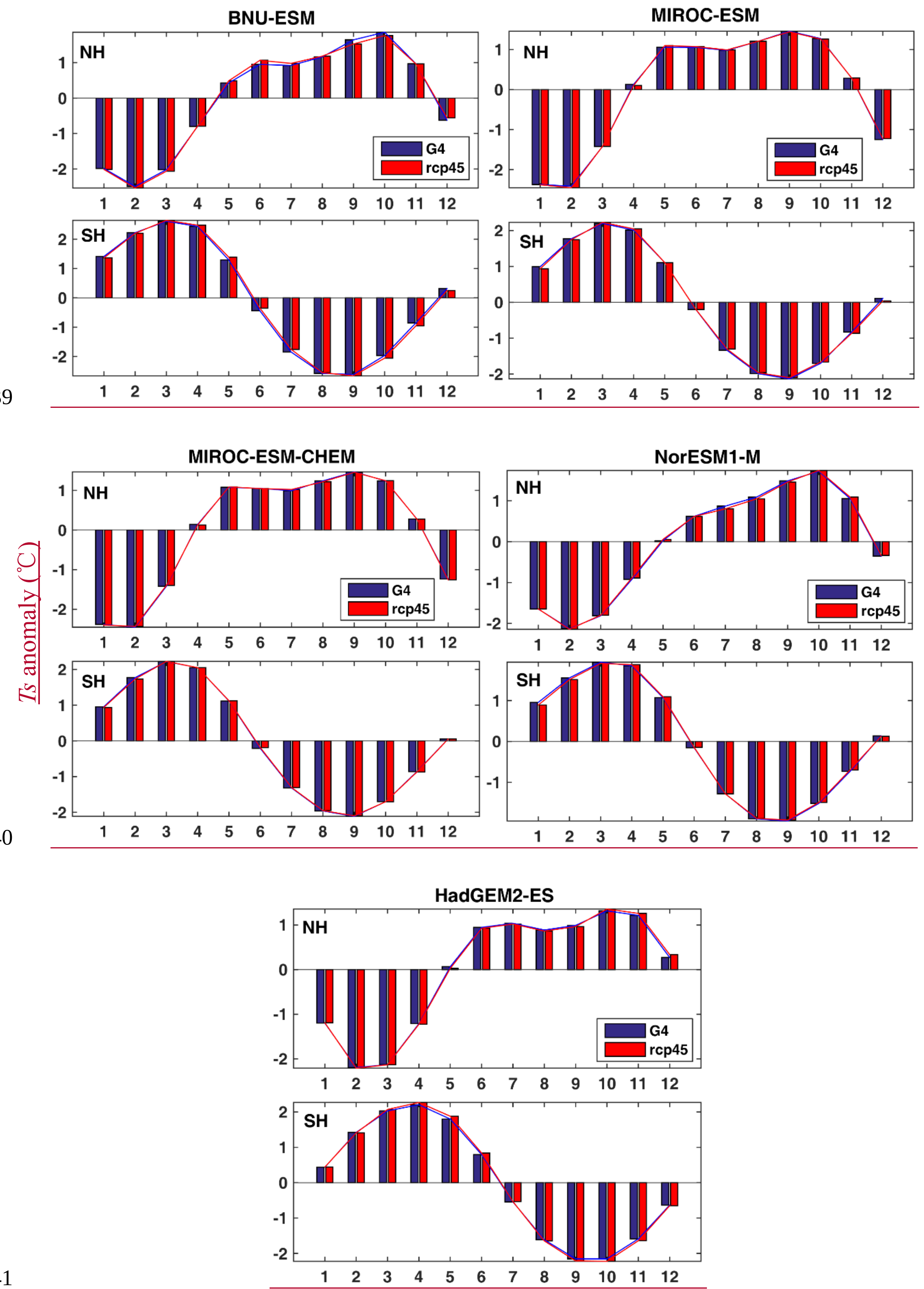

Figure S7.The seasonal cycle of T_s during 2020-2069 in Northern and Southern Hemisphere TC basins.

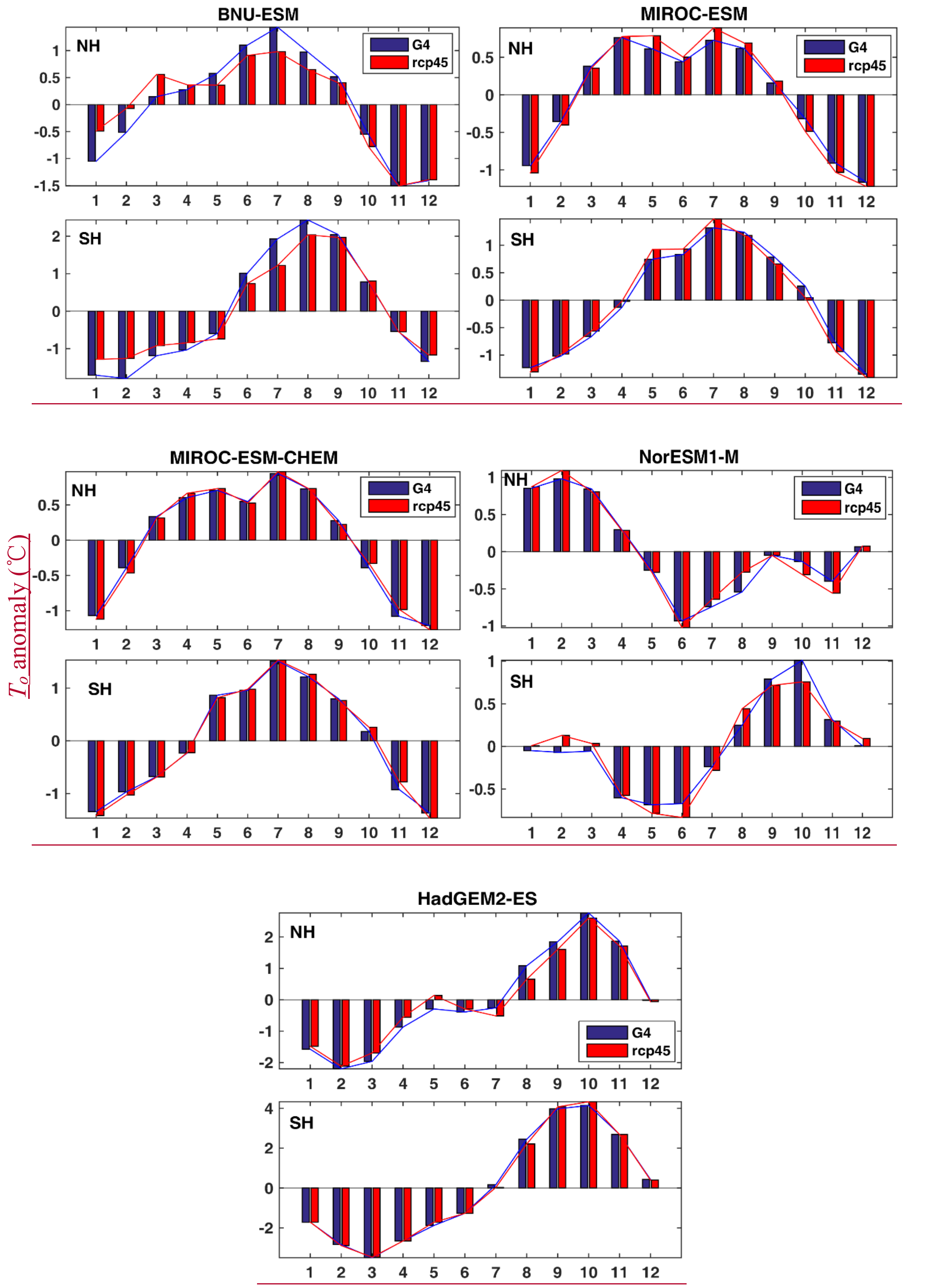

Figure S8. The seasonal cycle of T_o (100hPa) during 2020-2069 in Northern and Southern Hemisphere TC basins.

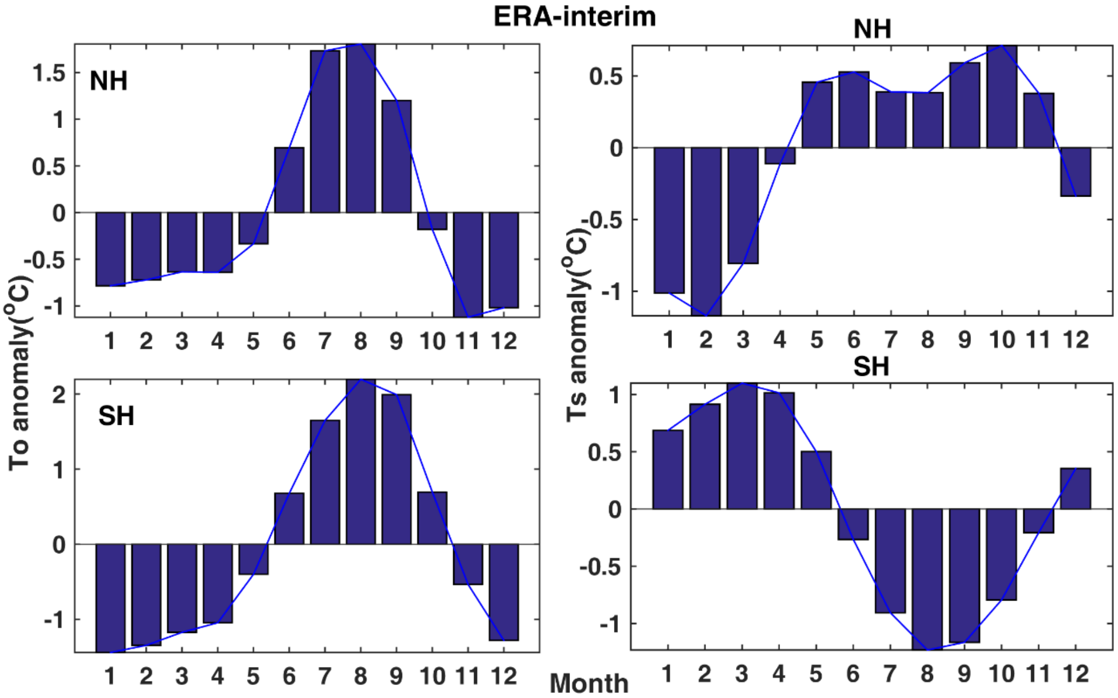

Figure S9. The seasonal cycle of T_o (100hPa) and T_s in Northern and Southern Hemisphere TC basins from ERA-interim for 1987-2016.